R O S E T T A

FLIGHT REPORTS
of RPC–MAG

RO–IGEP–TR–0033

Issue: 2 Revision: 1

February 14, 2019

Report of the

LUTETIA Flyby

Time period: July 07 - 13, 2010

Ingo Richter
Karl-Heinz Glassmeier

Institut für Geophysik und extraterrestrische Physik
Technische Universität Braunschweig
Mendelssohnstraße 3, 38106 Braunschweig
Germany

Contents

1 Introduction

ROSETTA's Flyby at asteroid 21 LUTETIA happened on July 10, 2010. RPC-MAG was switched on in the time between 2010-07-07T15:42 and 2010-07-13T16:15. The Closest Approach (C/A) took place at 2010-07-10T15:44:56.6 ±7.2 s. The C/A distance (ROSETTA - LUTETIA) was 3160 km. The Asteroid Sun distance was 2.72 AU, the distance to the Earth 3.05 AU. The Flyby velocity was about 15 km/s. Spacecraft flips occurred at C/A-04:19h and C/A+3:41h. The instrument performance was flawlessly. There were no problems from the instrument side.

This document gives a brief description of the executed activities and show the obtained data. Housekeeping data (Temperature of the OB & IB sensor, Filter Stages A & B, Filter configuration register, Reference voltage, negative and positive 5V supply voltage, and the coarse HK sampled magnetic field data of the OB sensor) are presented as well as magnetic field science data of the OB and IB sensor in the activated modes. Magnetic field data are plotted in s/c coordinates and ECLIPJ2000 coordinates if not otherwise stated. They are calibrated according to the results of the ground calibration and the results of the inflight temperature model 009 using the the magnetic field data of the complete ROSETTA mission until 2016. Sensitivity, Misalignment, and Temperature effects are taken into account. The s/c residual field is not subtracted.

The spectra of the magnetic field data measured by the OB sensor are plotted in section 5. As usual an influence of ROSETTAs reaction wheels (refer to section 6) can be seen in Burstmode.

From time to time there are also horizontal lines in the dynamic spectrum to be seen. These lines represent constant frequencies and are caused by the LAP instrument. This behavior was investigated and proofed during the PC10 campaign in November 2010. See RO-IGEP-TR0030 for further details.

The data quality and a comparison between OB,IB sensor and ROMAP is presented in section 4.

The Rotation Angles of the Solar Arrays and the High Gain Antenna have been plotted in section 7 for the assessment of their influence to the magnetic field data.

A temperature profile for the whole Fly–By is shown in section 8.

The results and assessment of the very flyby are presented in section 10.

2 The Fly–By Geometry

This section gives an overview about the trajectory during the Fly–By.

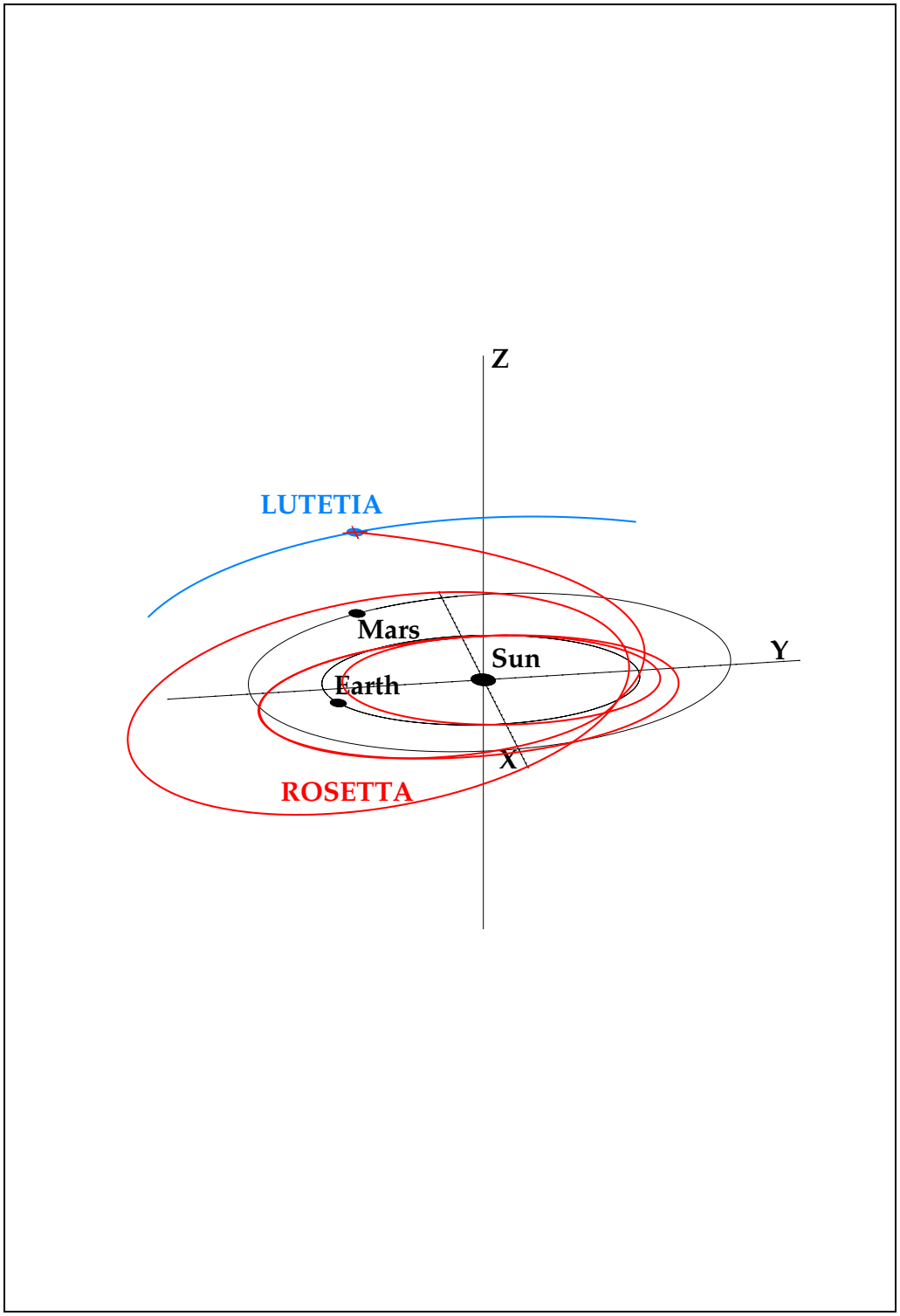

Figure 1: The Celestial Situation. ECLIPJ2000 Coordinates

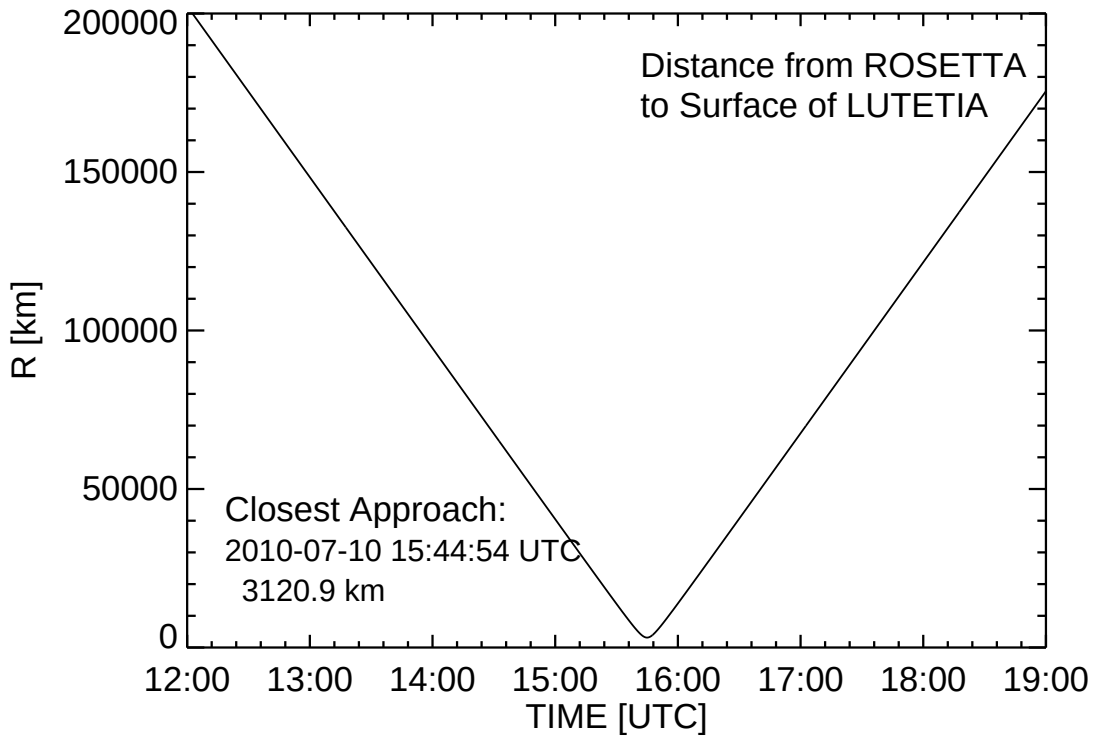

Figure 2: ROSETTA'S Distance to the LUTETIA Surface - Overview

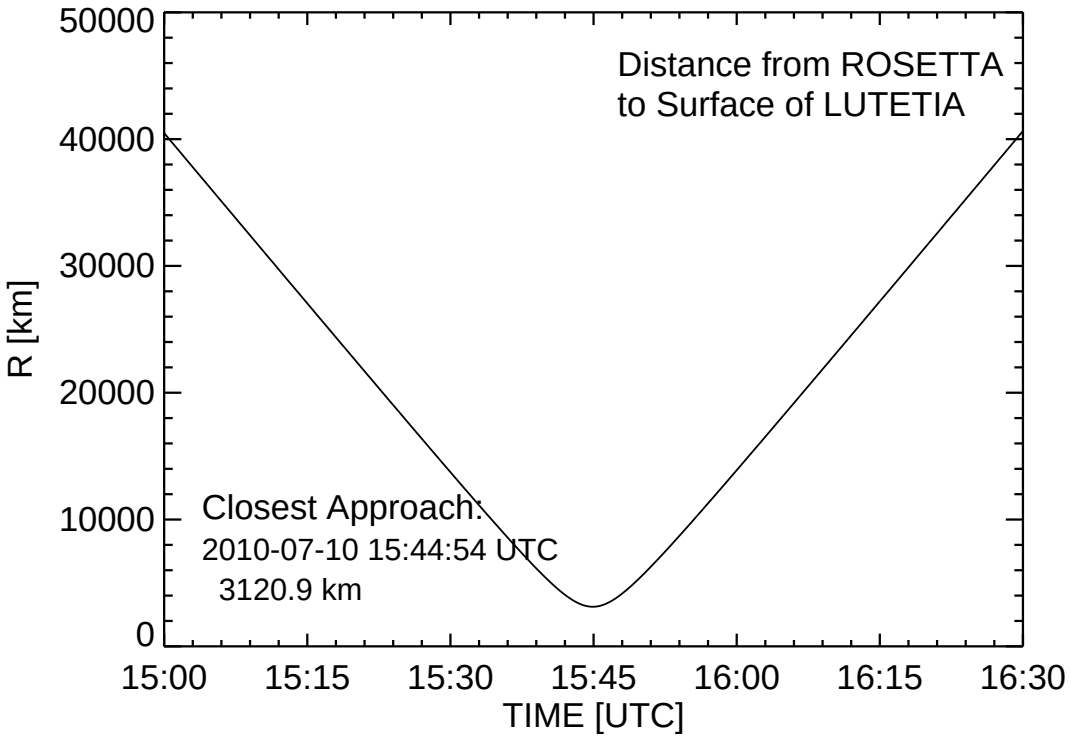

Figure 3: ROSETTA'S Distance to the LUTETIA Surface - Zoomed View

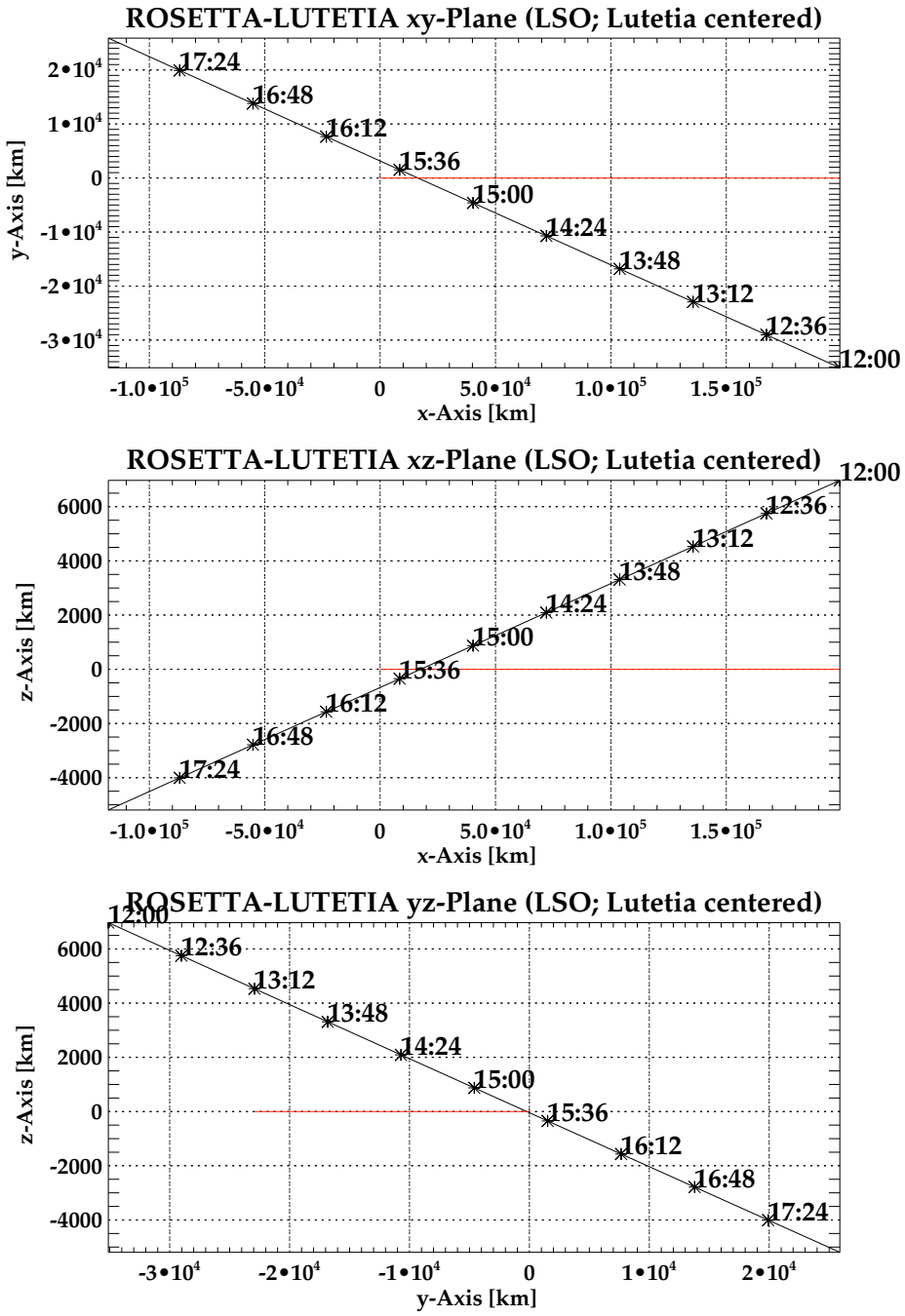

Figure 4: ROSETTA'S Fly-By Trajectory in LSO coordinates. Red Line: SUN Direction

3 Activities and data plots of the LUTETIA Fly By

This chapter presents all relevant data /data types measured by RPCMAG day by day:

- Housekeeping data (HK).
- Calibrated LEVEL_B data (s/c coordinates) of the IB and OB sensor with the original sampling frequency.
- Calibrated LEVEL_C data (ECLIPJ2000 coordinates) of the IB and OB sensor with the original sampling frequency.

3.1 July 07, 2010:

3.1.1 Actions

MAG was switched on immediately after PIU and set to HK mode at 15:42:19. The normal mode SID 2 was set at 16:10:34. All commands passed smoothly and the instrument followed in the expected way. Then there were normal mode data until 17:00 only, although no mode change happened. Probably the science packets got lost in the ESA DDS or already on the s/c. As this phase was only used for warming up the sensor, the loss does not be a problem.

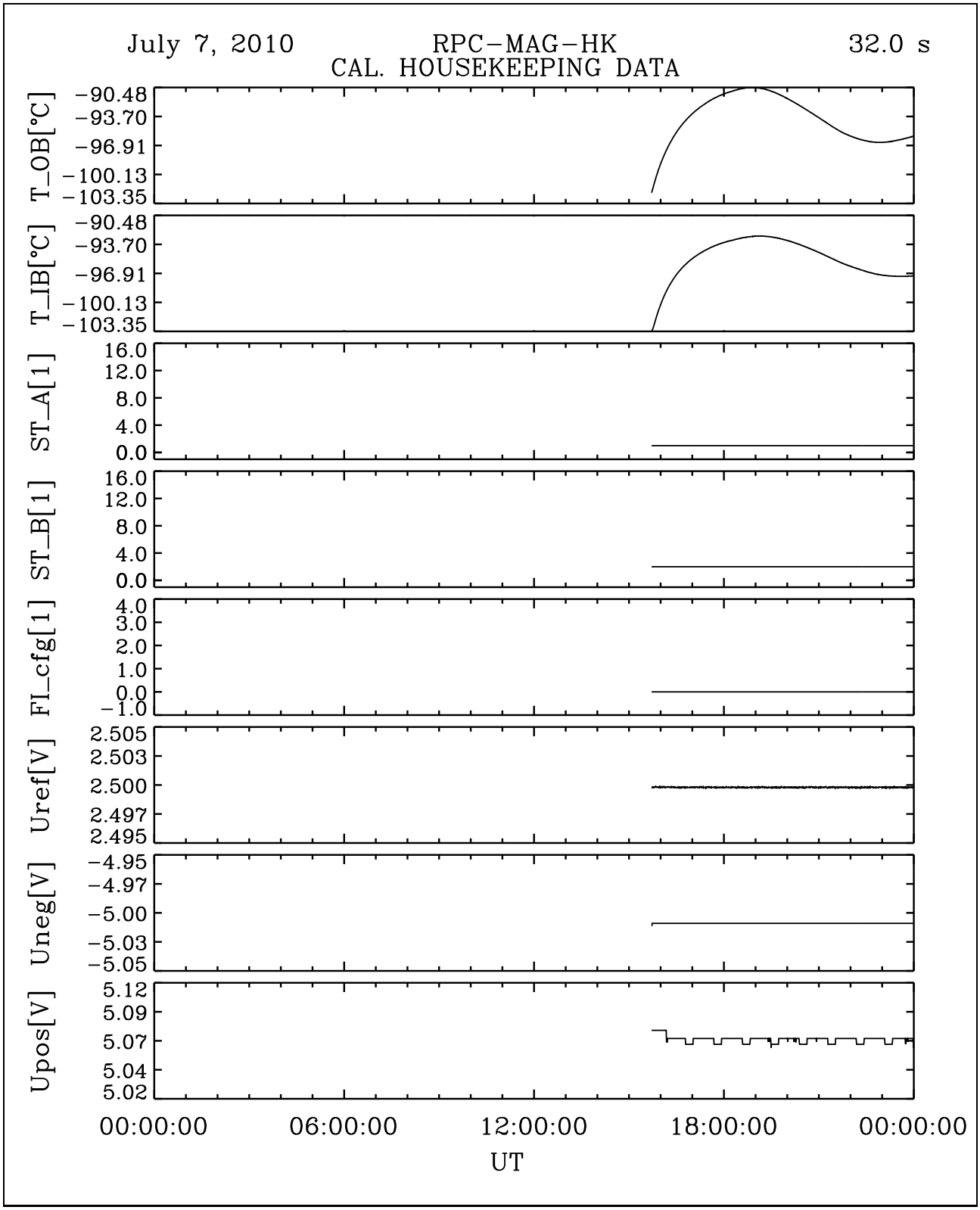

Figure 5: File: RPCMAG100707T1542_CLA_HK_P0000_2400

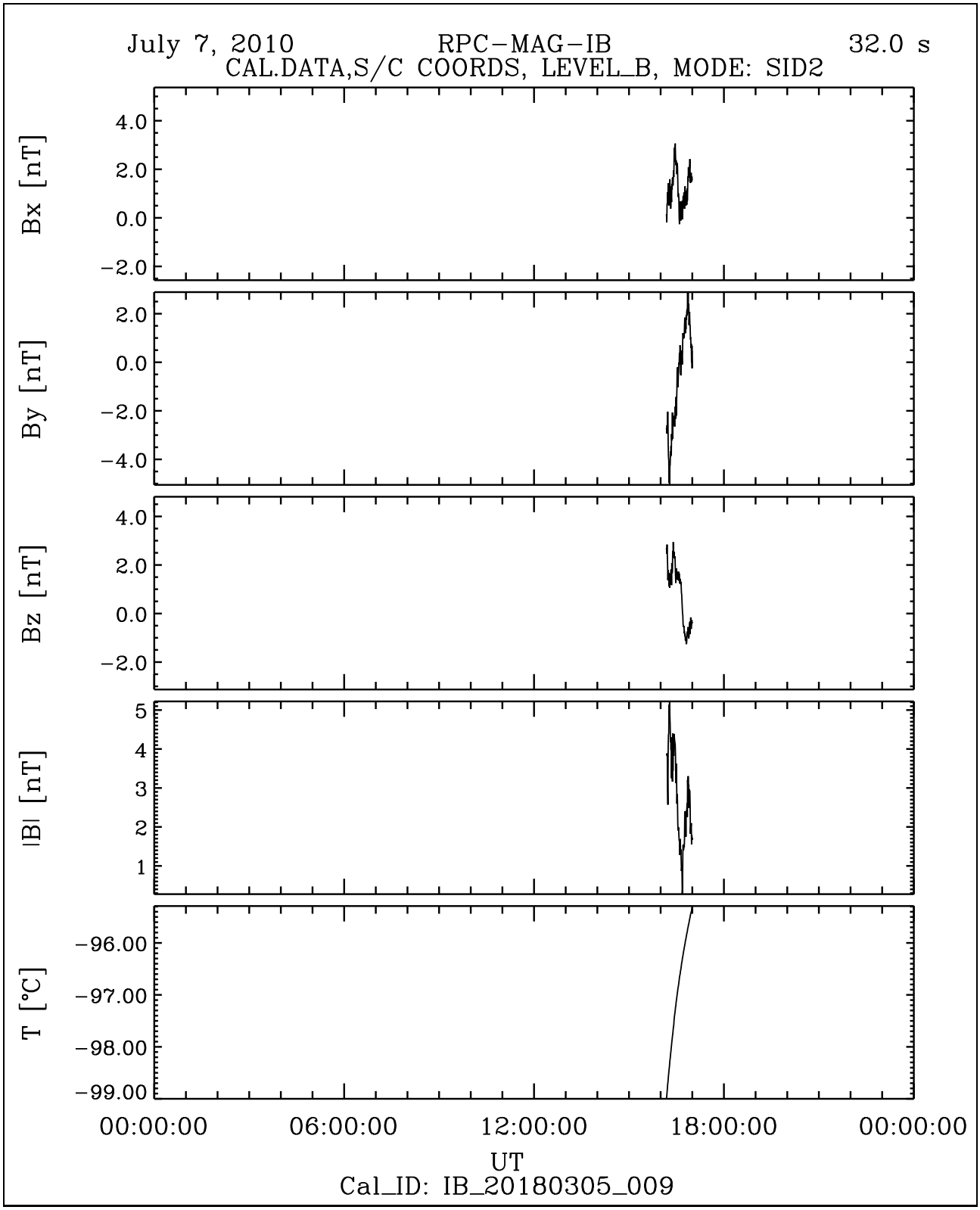

Figure 6: File: RPCMAG100707T1610_CLB_IB_M2_T0000_2400_009

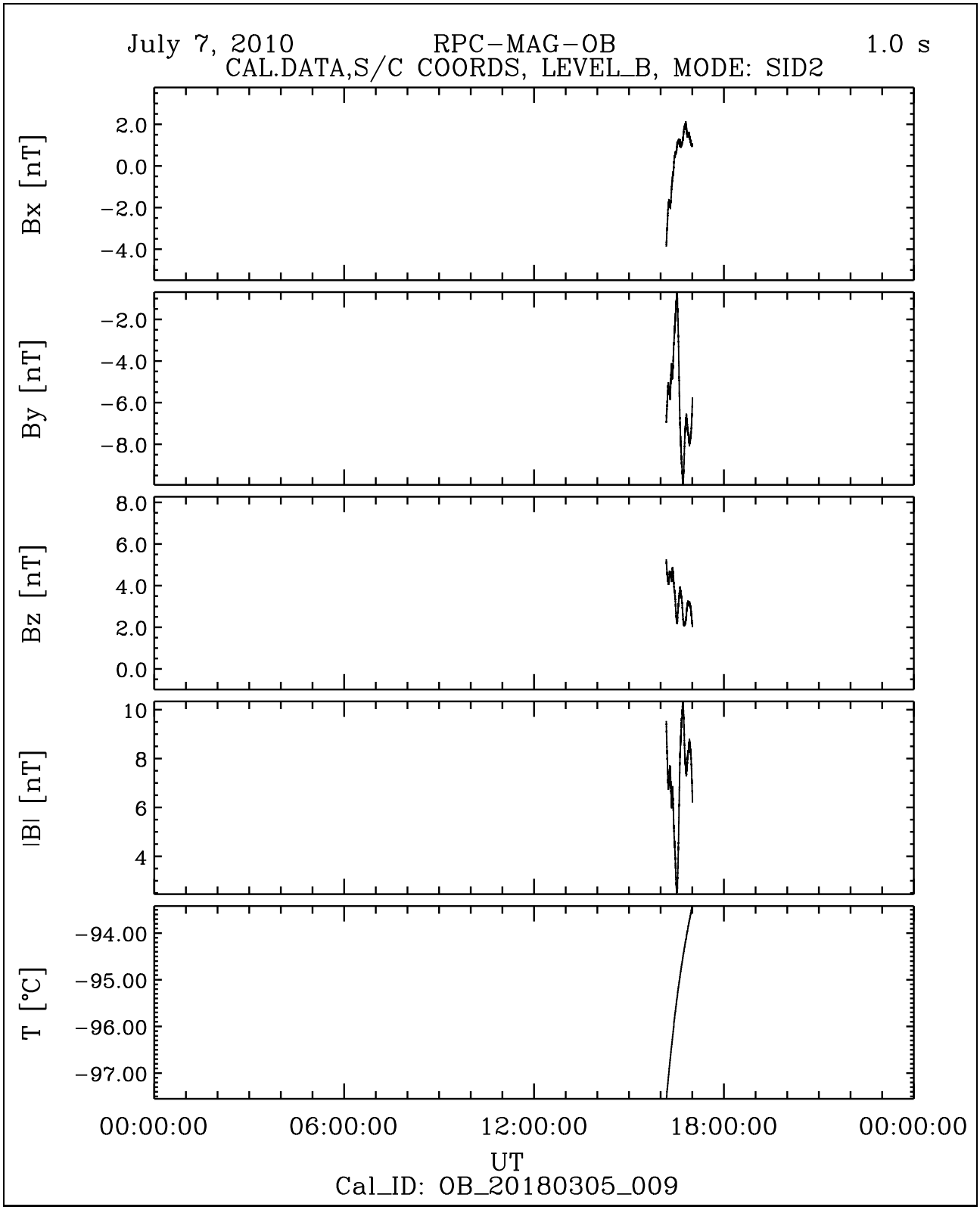

Figure 7: File: RPCMAG100707T1610_CLB_OB_M2_T0000_2400_009

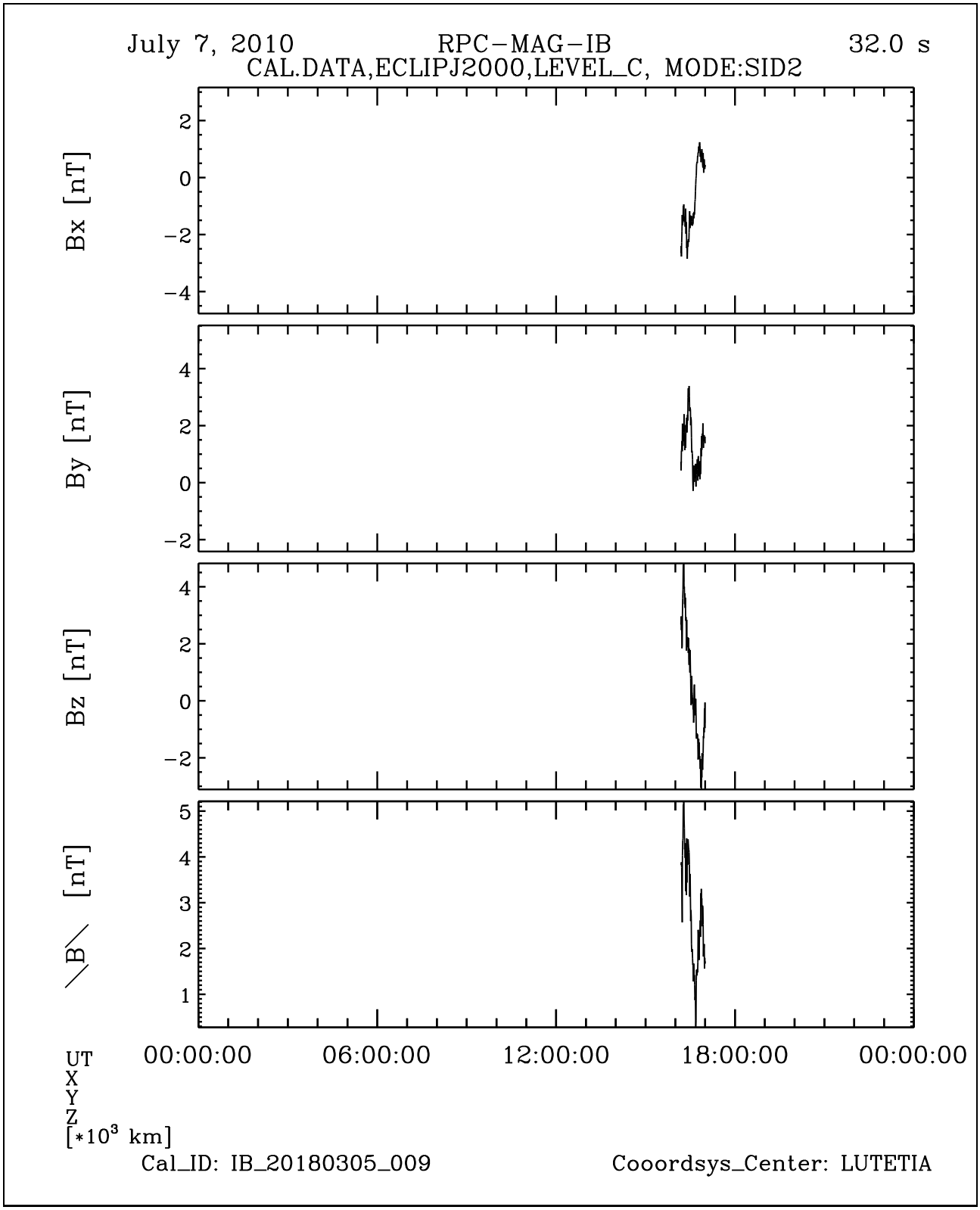

Figure 8: File: RPCMAG100707T1610_CLC_IB_M2_T0000_2400_009

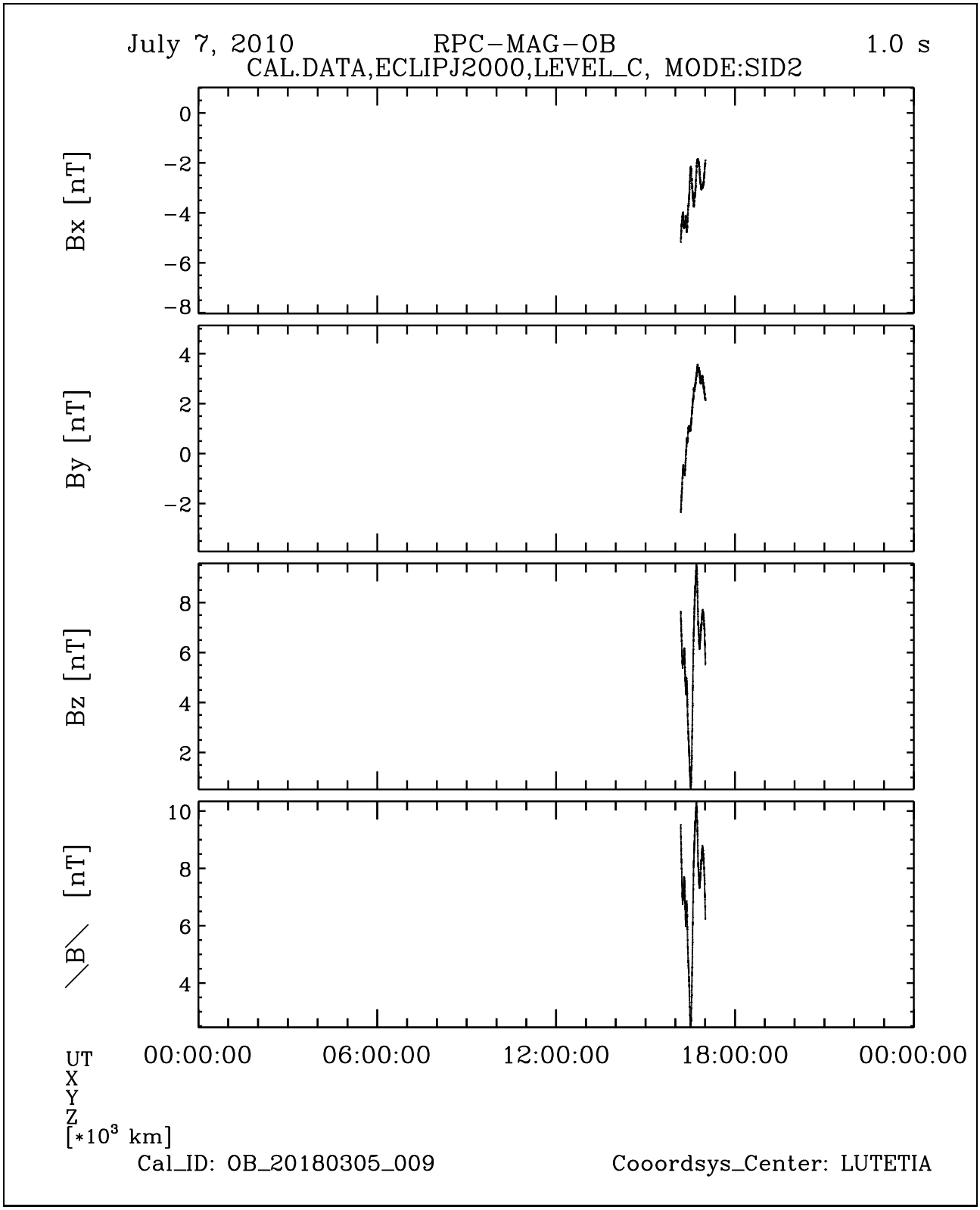

Figure 9: File: RPCMAG100707T1610_CLC_OB_M2_T0000_2400_009

3.2 July 08, 2010:

3.2.1 Actions

MAG stayed in SID 2. No problems occurred.

3.2.2 Plots of Calibrated Data

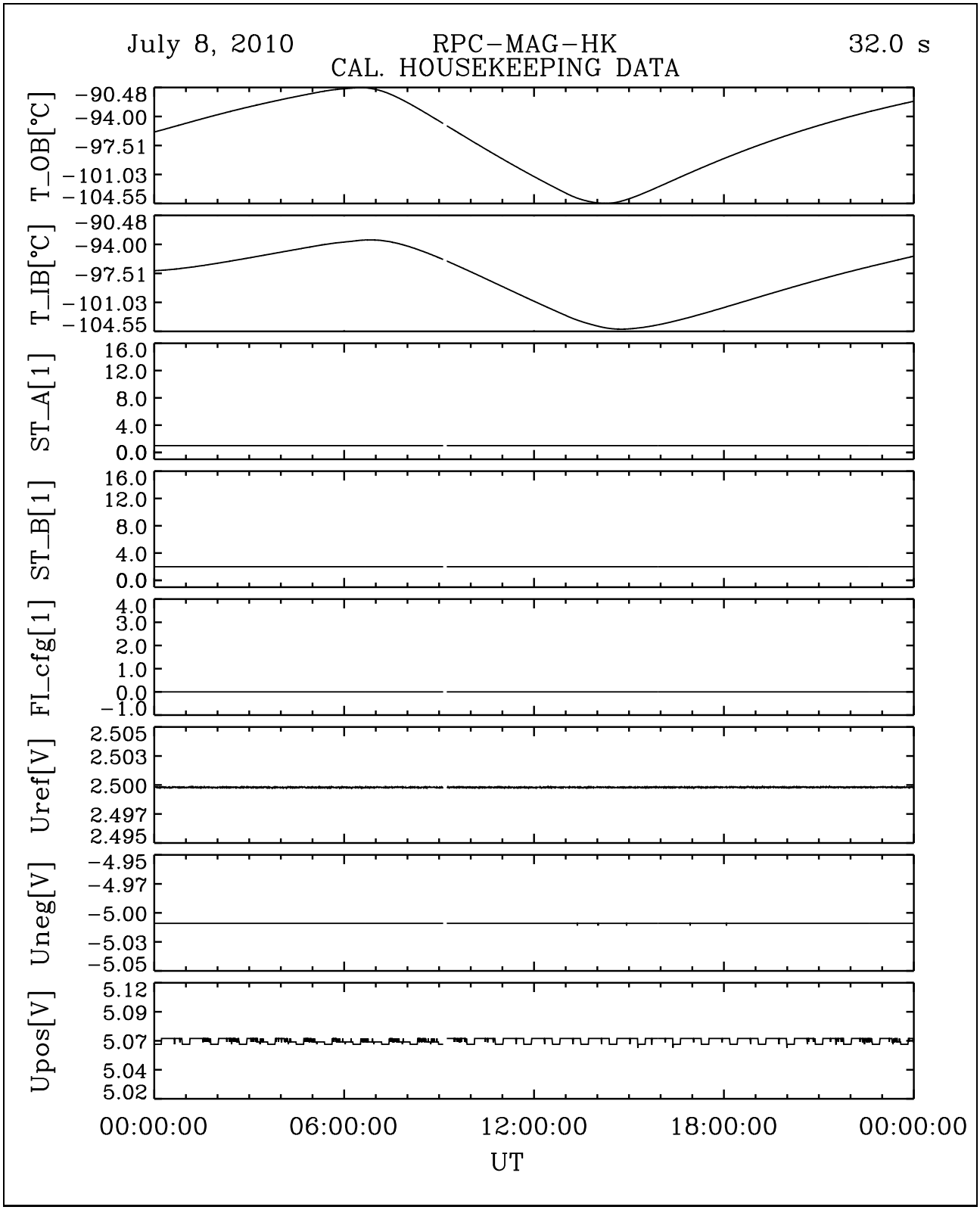

Figure 10: File: RPCMAG100708T0000_CLA_HK_P0000_2400

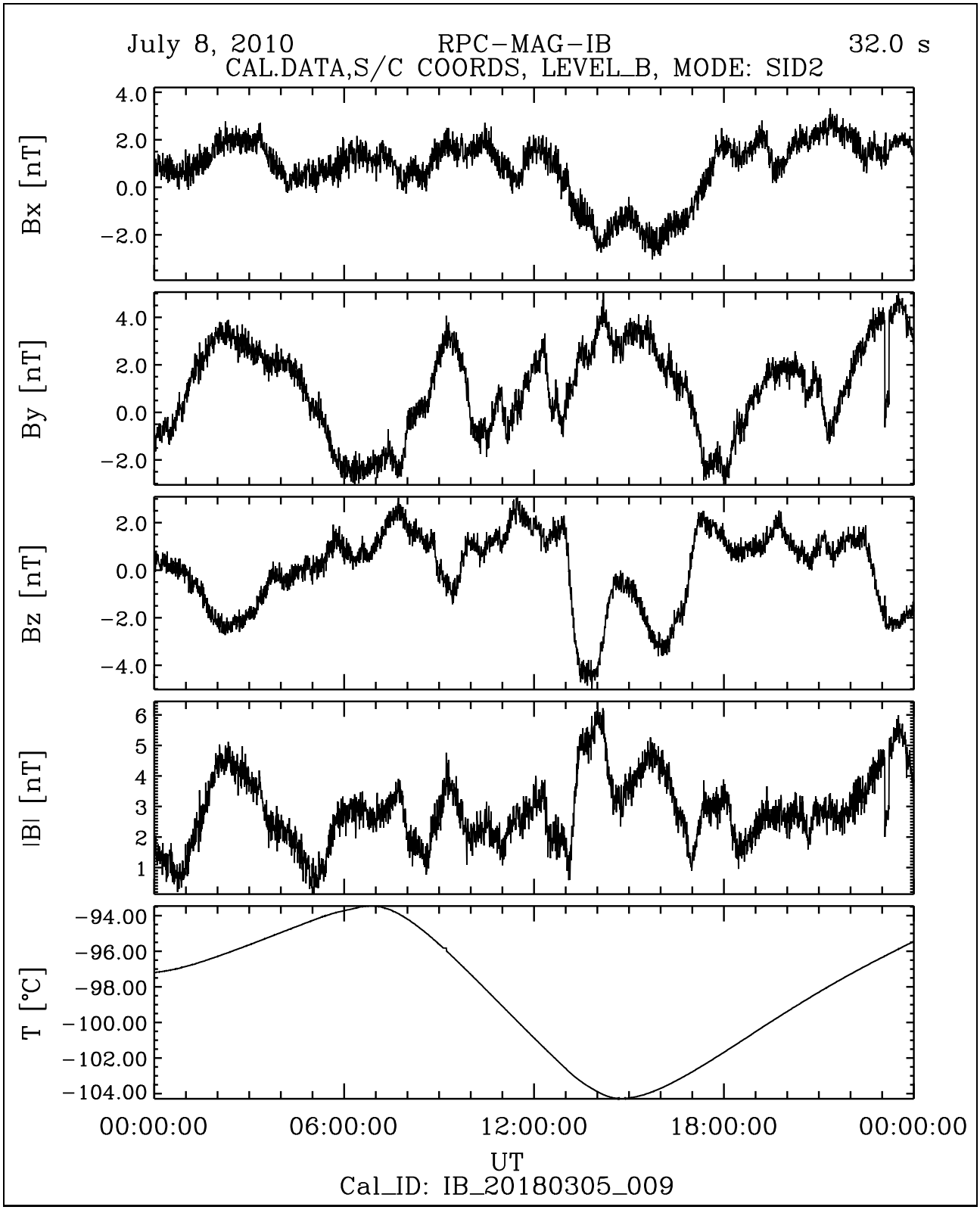

Figure 11: File: RPCMAG100708T0000_CLB_IB_M2_T0000_2400_009

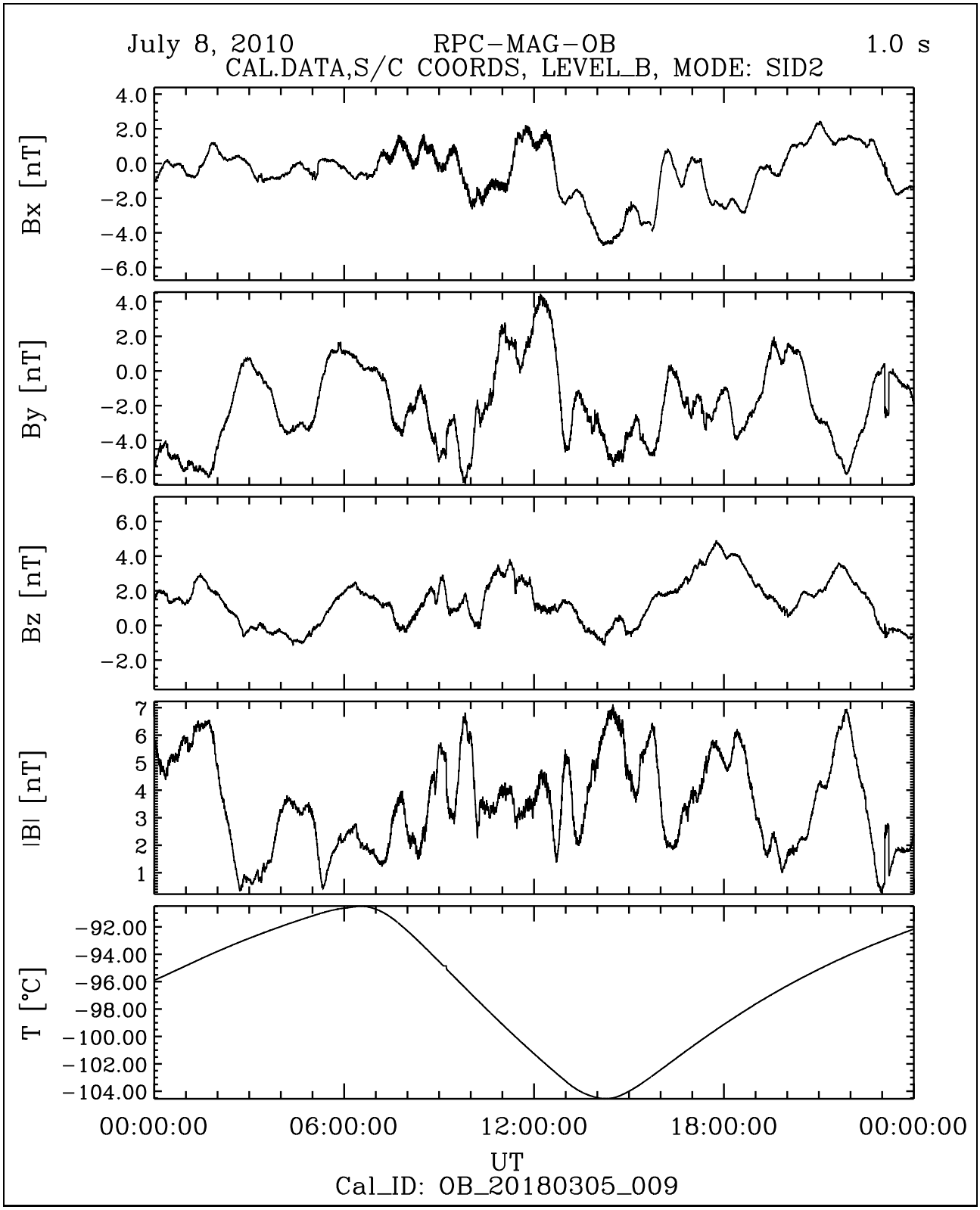

Figure 12: File: RPCMAG100708T0000_CLB_OB_M2_T0000_2400_009

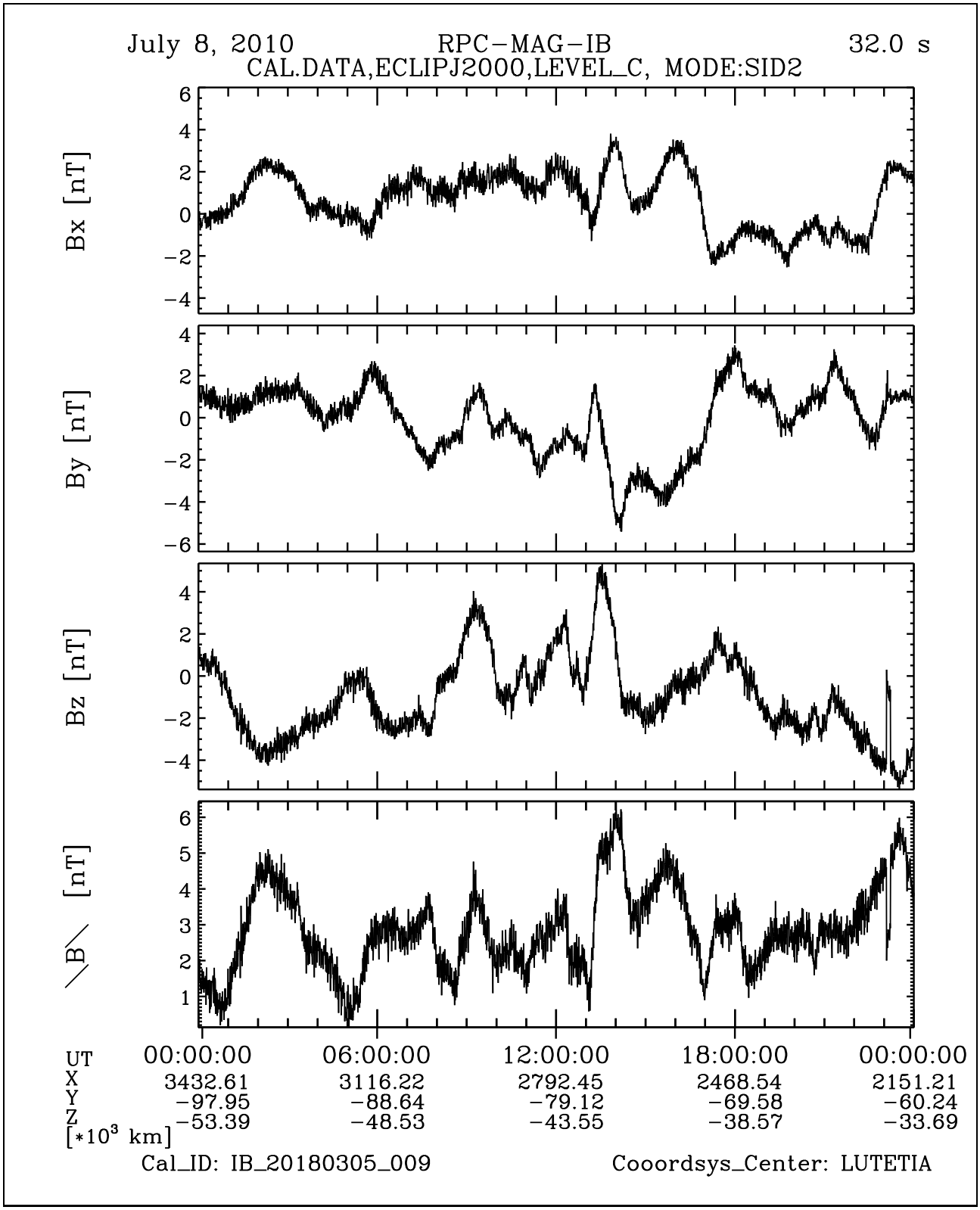

Figure 13: File: RPCMAG100708T0000_CLC_IB_M2_T0000_2400_009

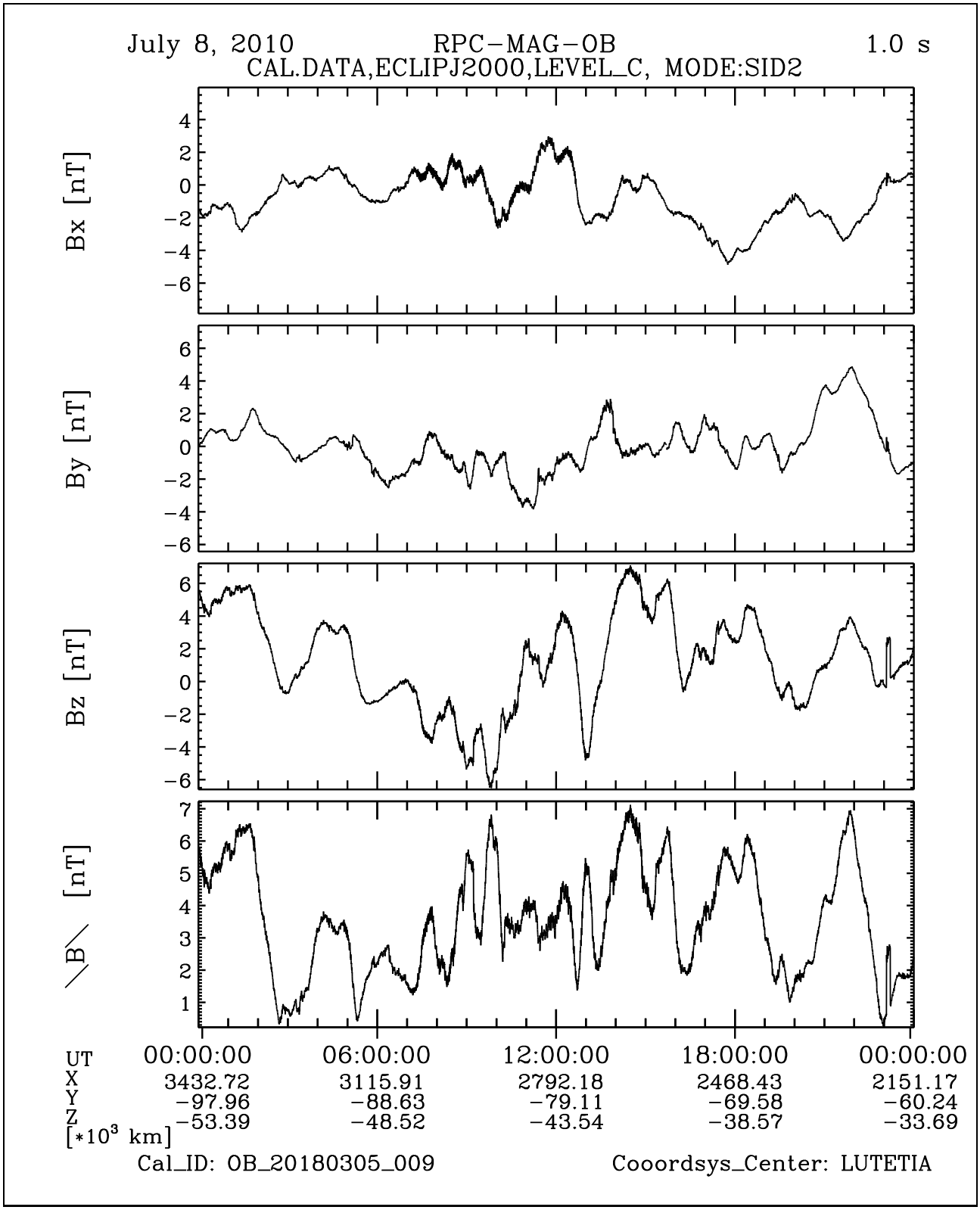

Figure 14: File: RPCMAG100708T0000_CLC_OB_M2_T0000_2400_009

3.3 July 09, 2010:

3.3.1 Actions

MAG stayed in SID 2. No problems occurred.

3.3.2 Plots of Calibrated Data

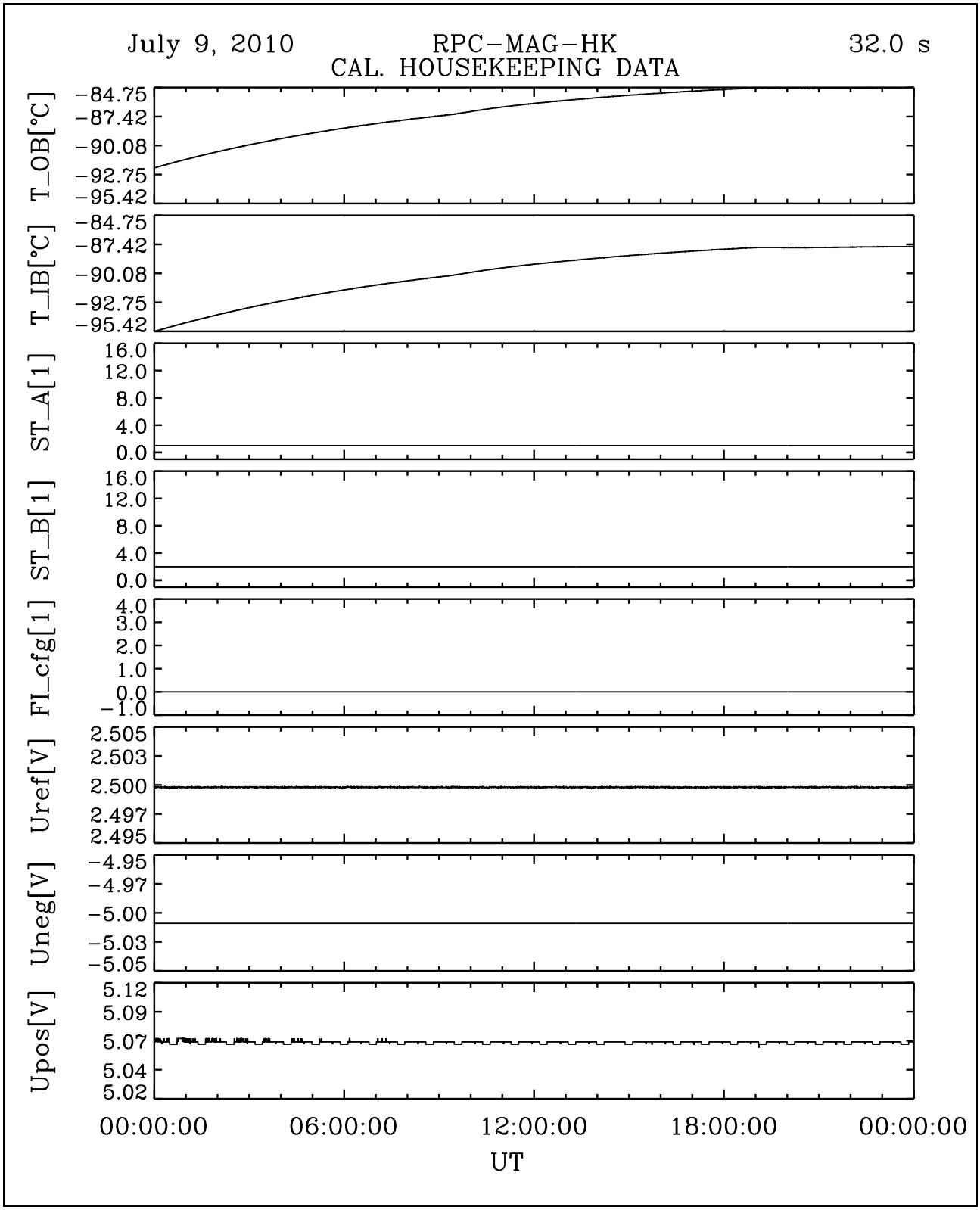

Figure 15: File: RPCMAG100709T0000_CLA_HK_P0000_2400

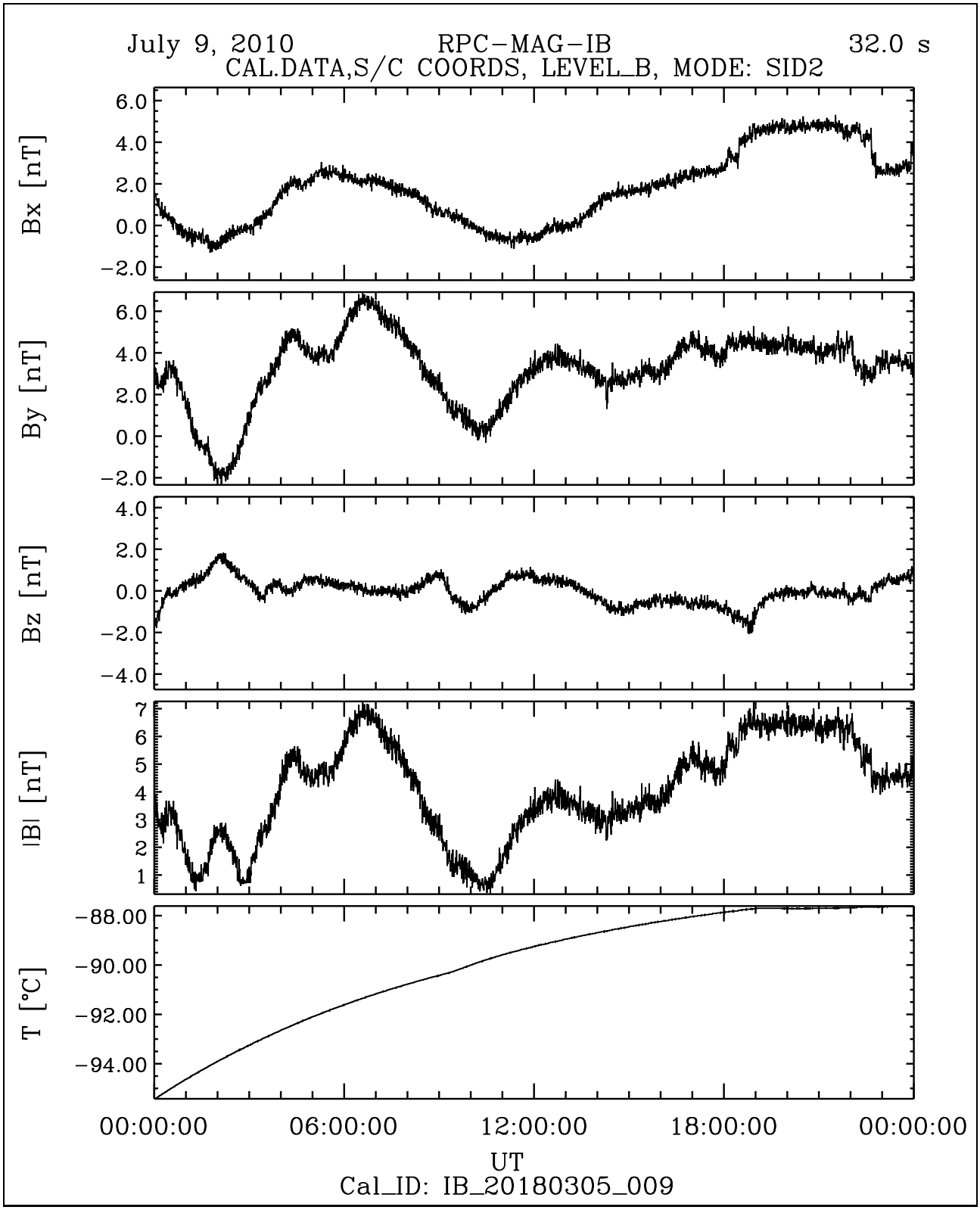

Figure 16: File: RPCMAG100709T0000_CLB_IB_M2_T0000_2400_009

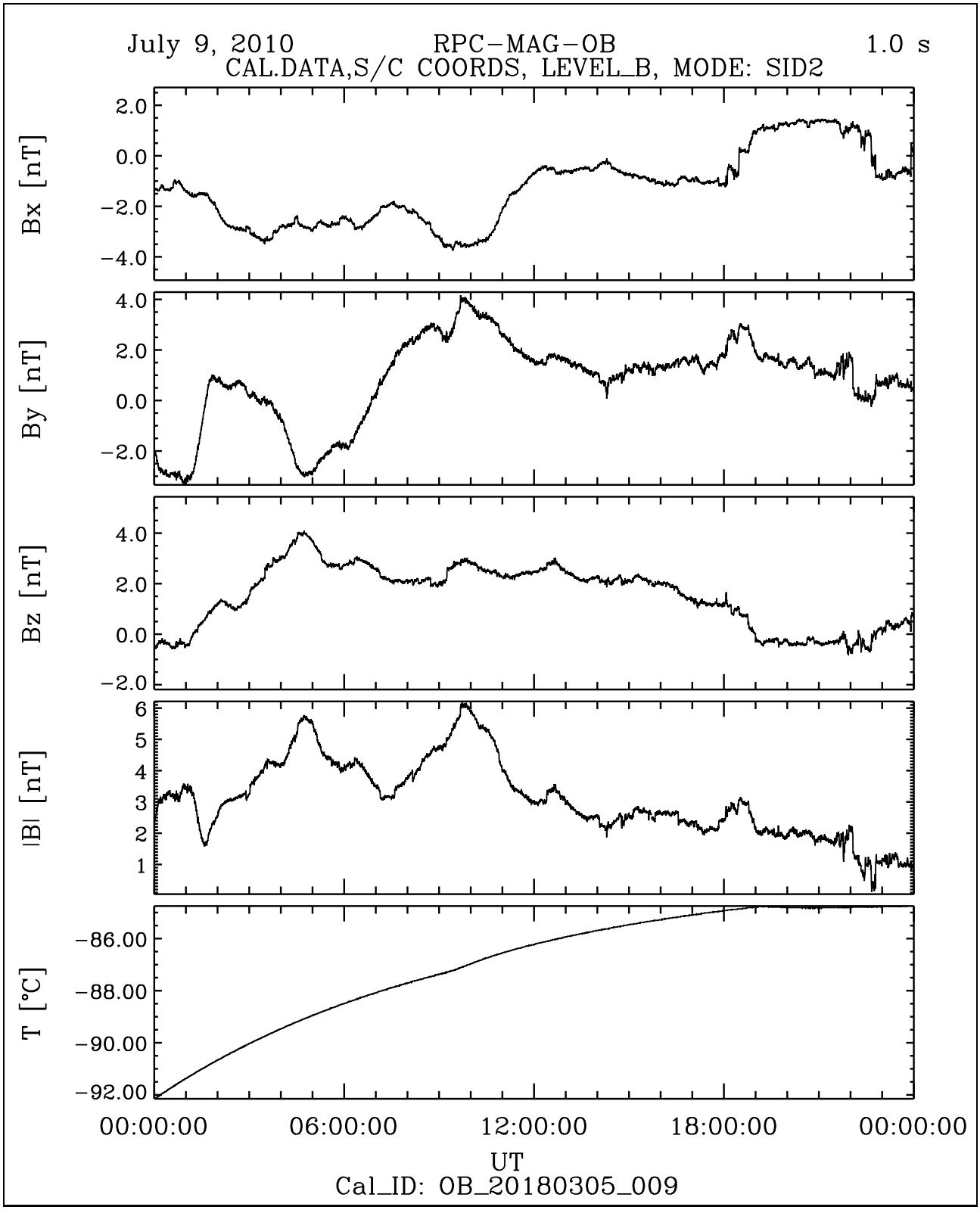

Figure 17: File: RPCMAG100709T0000_CLB_OB_M2_T0000_2400_009

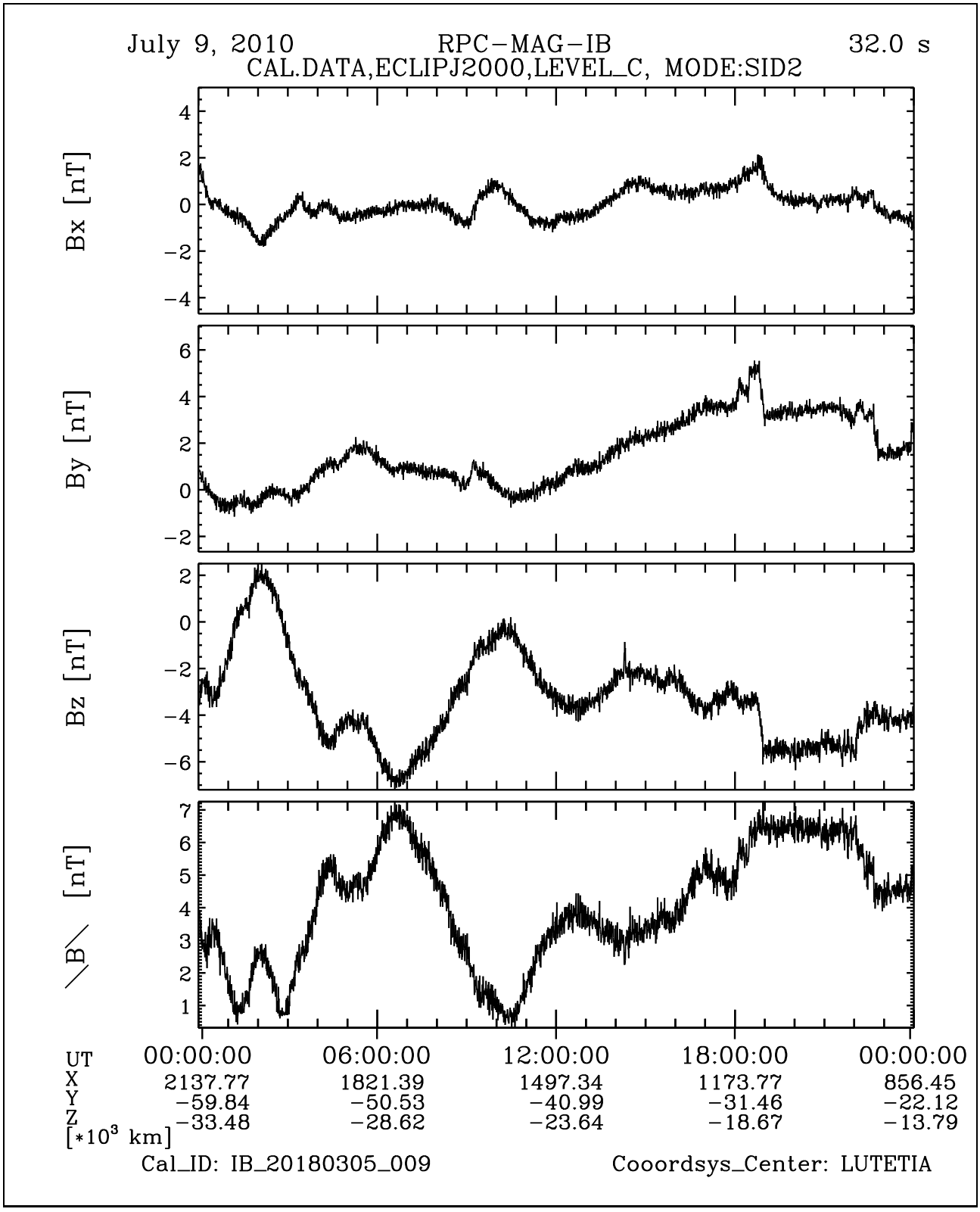

Figure 18: File: RPCMAG100709T0000_CLC_IB_M2_T0000_2400_009

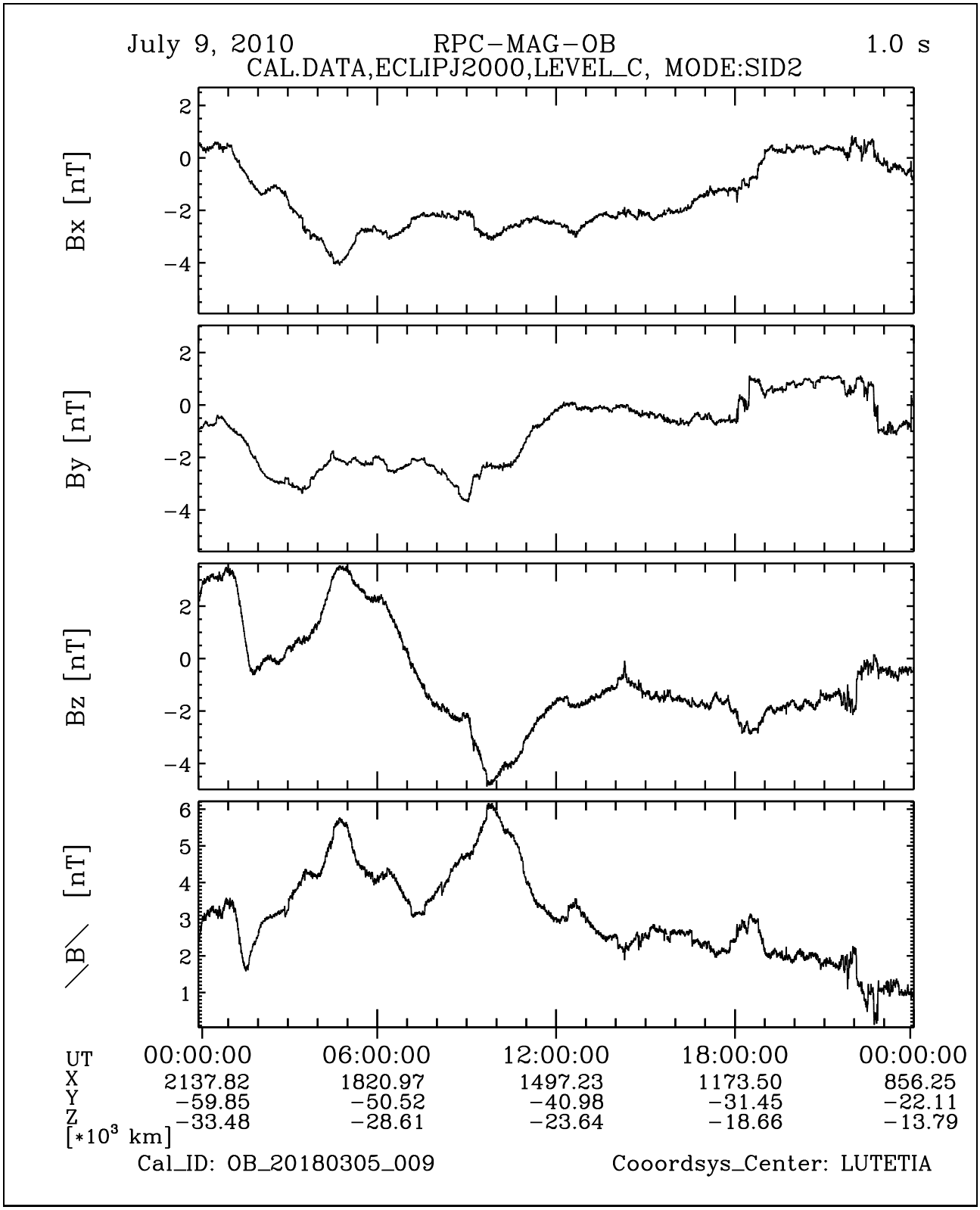

Figure 19: File: RPCMAG100709T0000_CLC_OB_M2_T0000_2400_009

3.4 July 10, 2010:

3.4.1 Actions

Today the real flyby at LUTETIA happened. MAG stayed in SID 2 until 12:55. Then Burst mode SID3 was activated. at 18:54 the mode was switched back to normal mode SID2. The very flyby happened at 15:44:56.6.

No problems occurred.

3.4.2 Plots of Calibrated Data

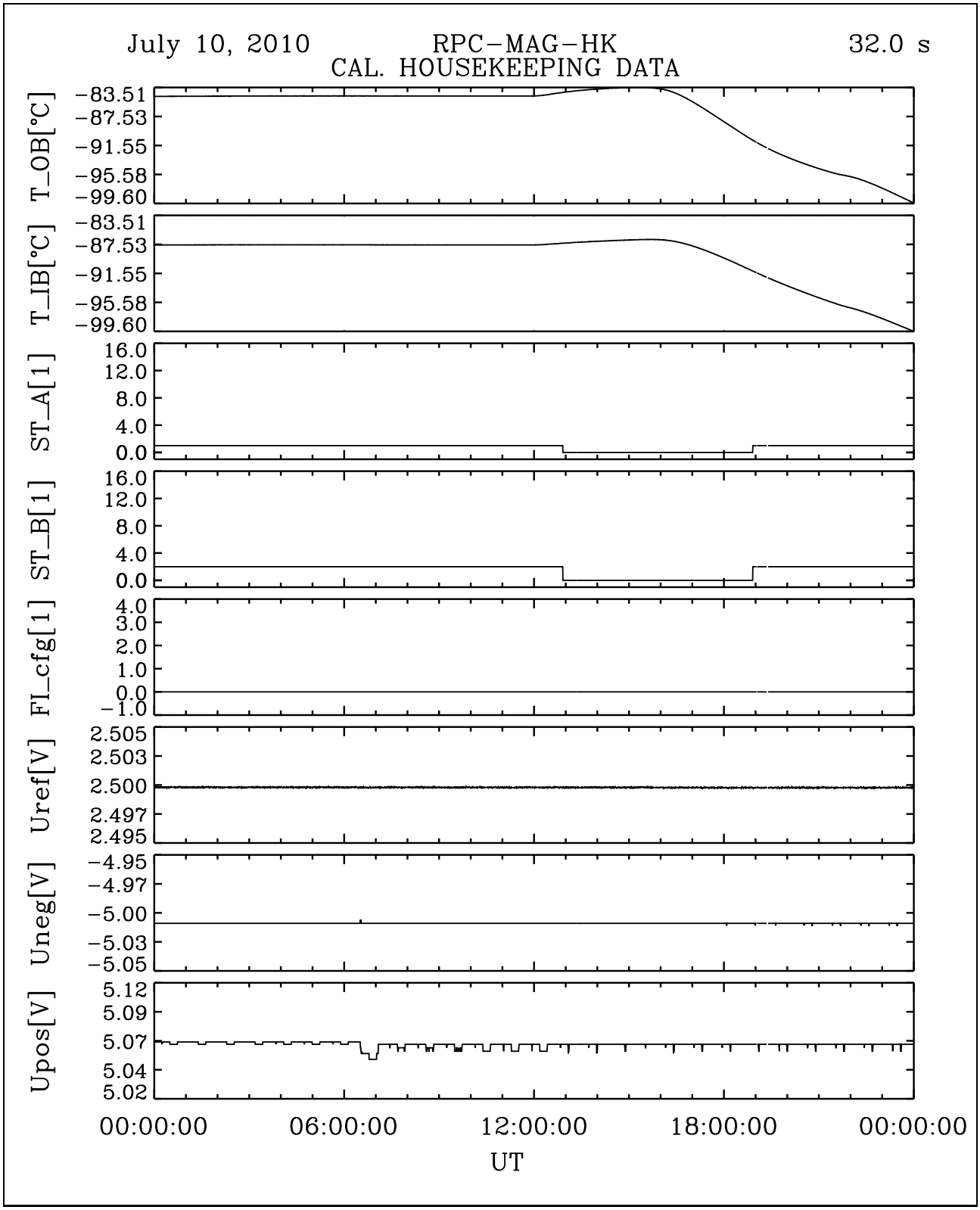

Figure 20: File: RPCMAG100710T0000_CLA_HK_P0000_2400

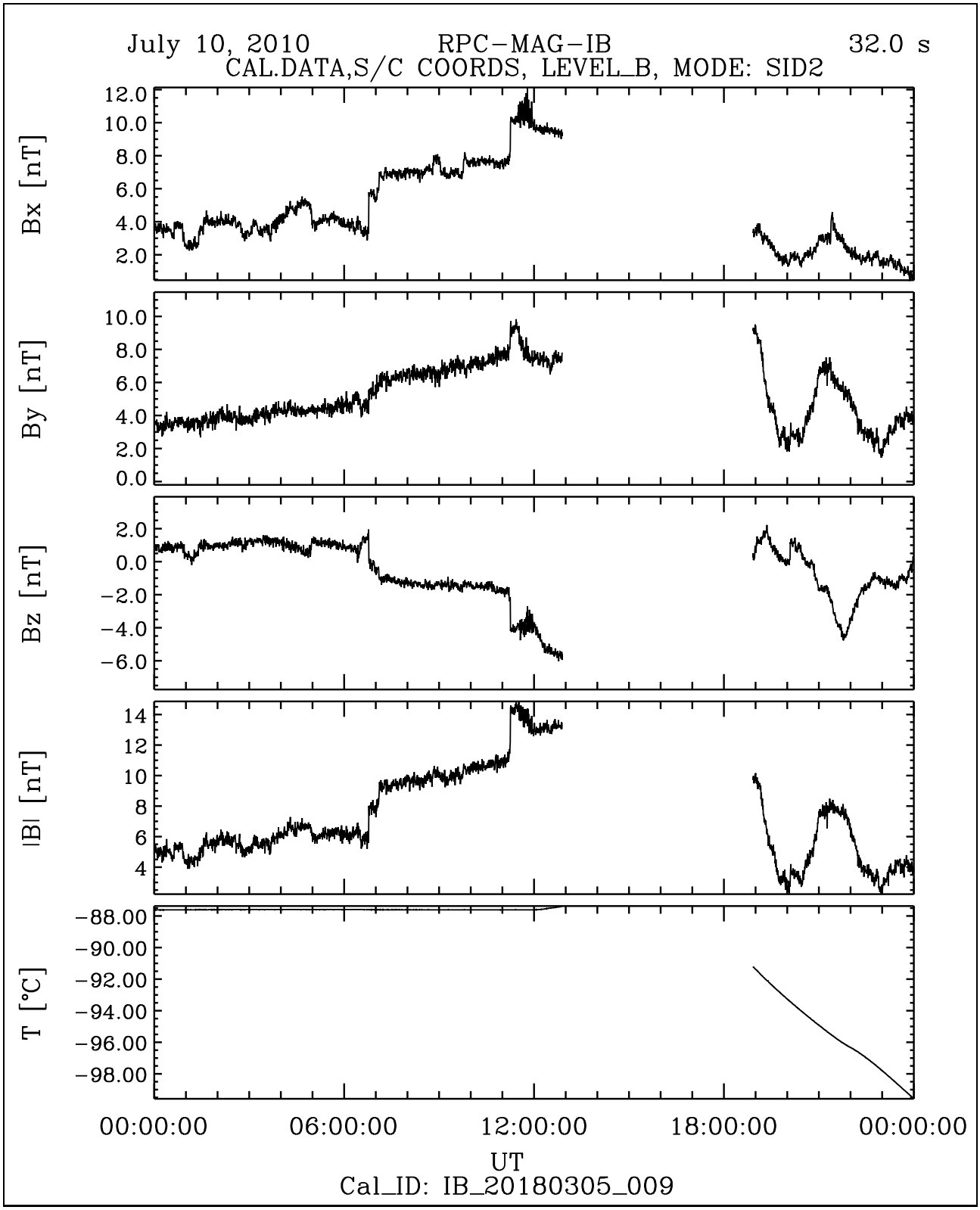

Figure 21: File: RPCMAG100710T0000_CLB_IB_M2_T0000_2400_009

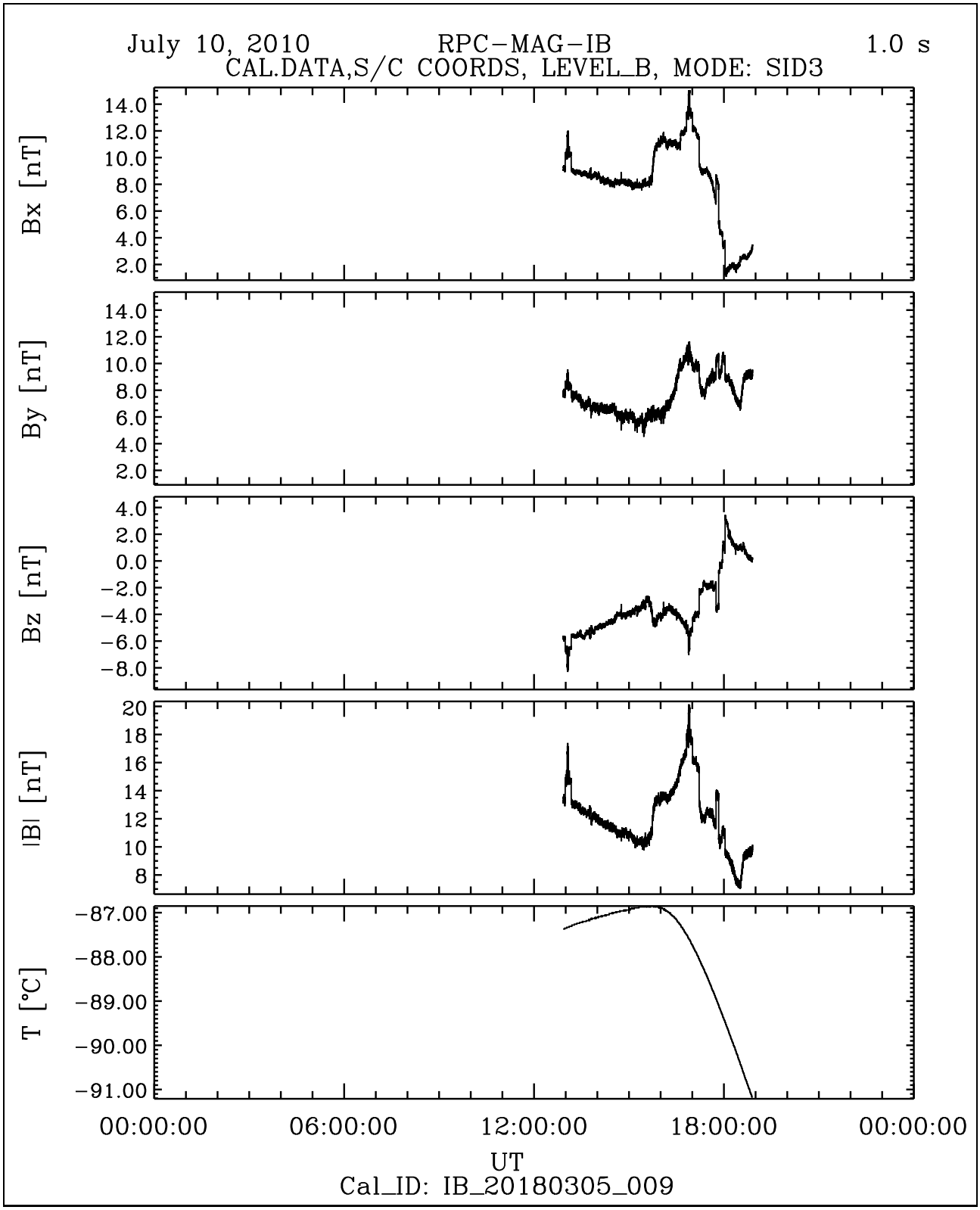

Figure 22: File: RPCMAG100710T1255_CLB_IB_M3_T0000_2400_009

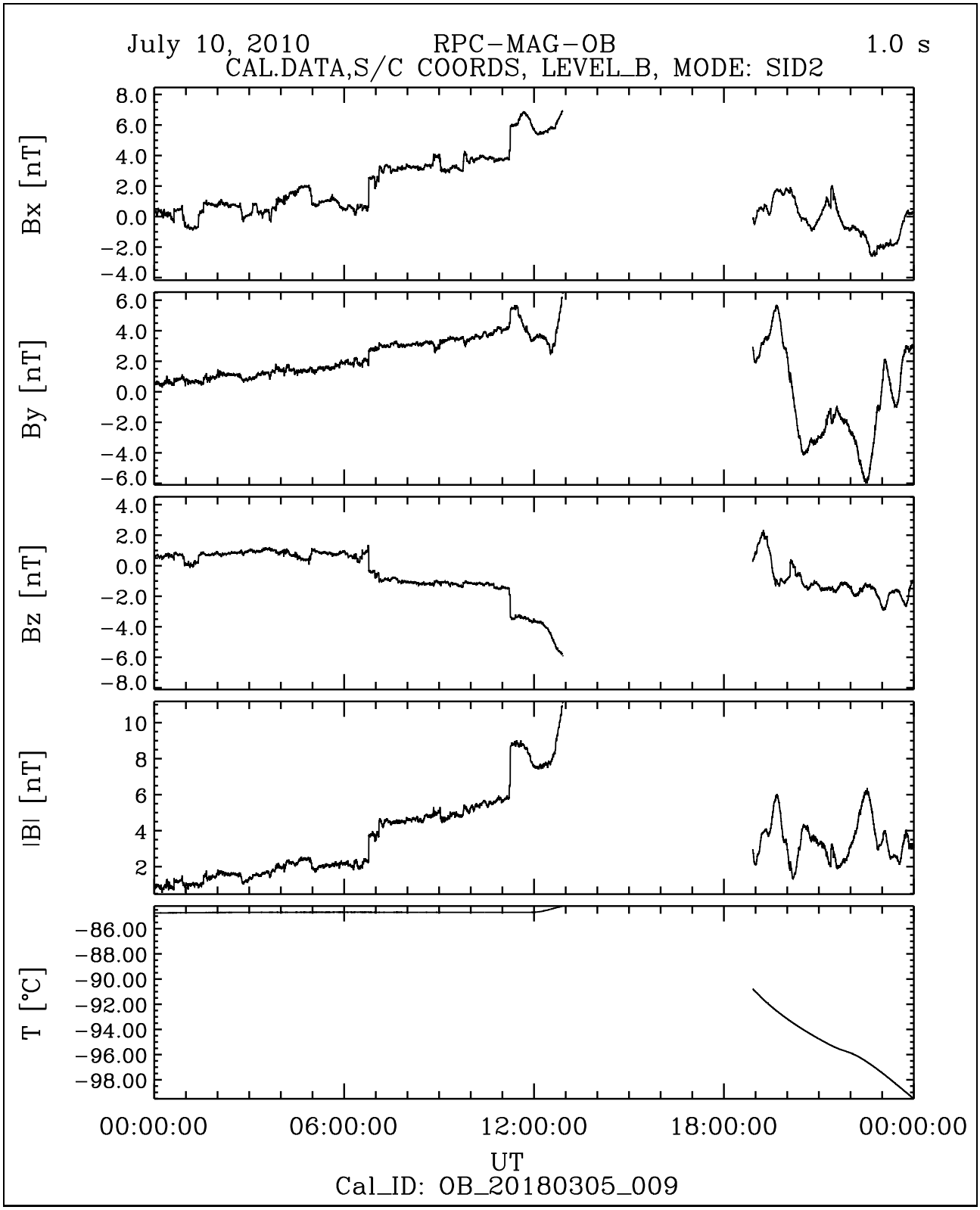

Figure 23: File: RPCMAG100710T0000_CLB_OB_M2_T0000_2400_009

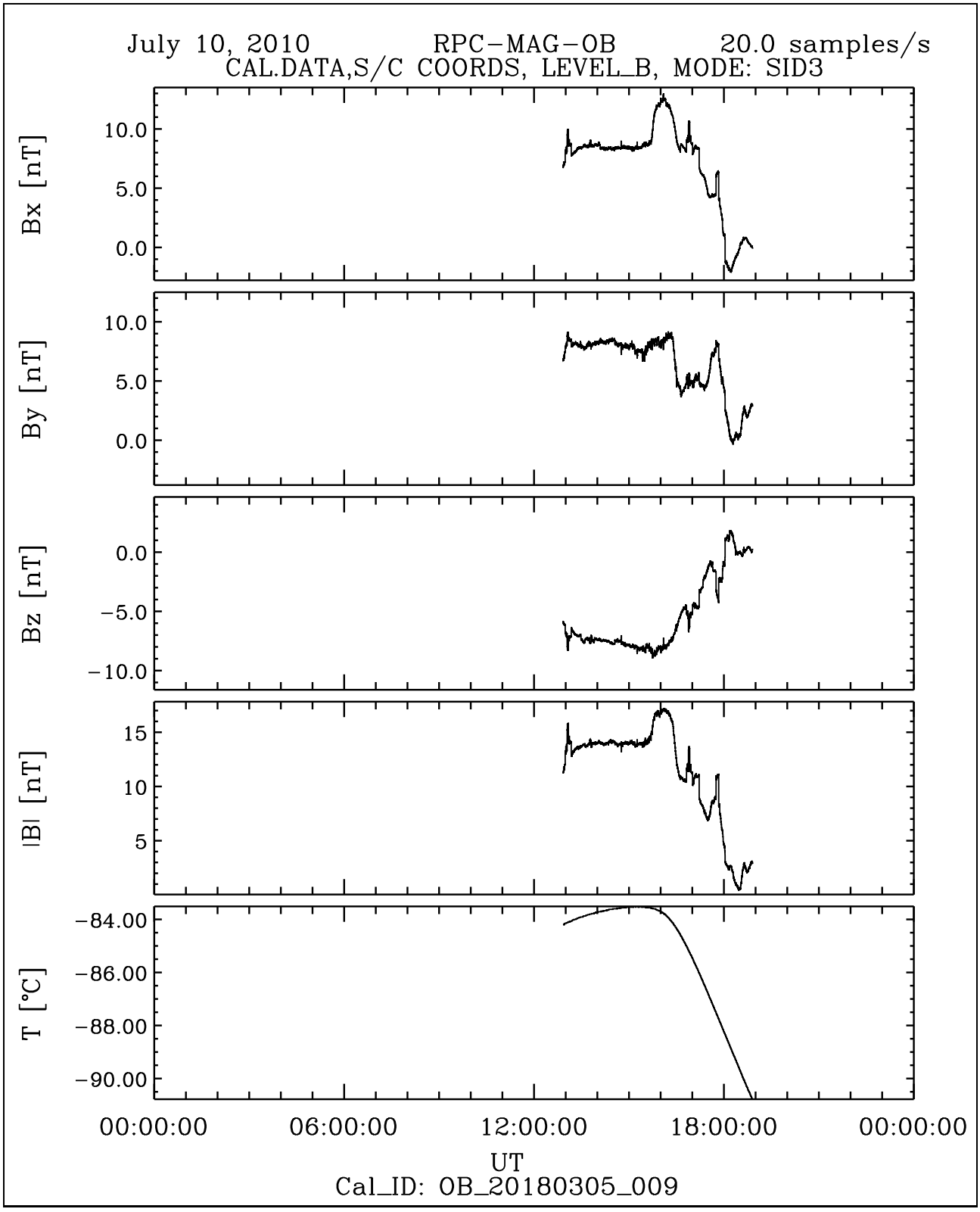

Figure 24: File: RPCMAG100710T1255_CLB_OB_M3_T0000_2400_009

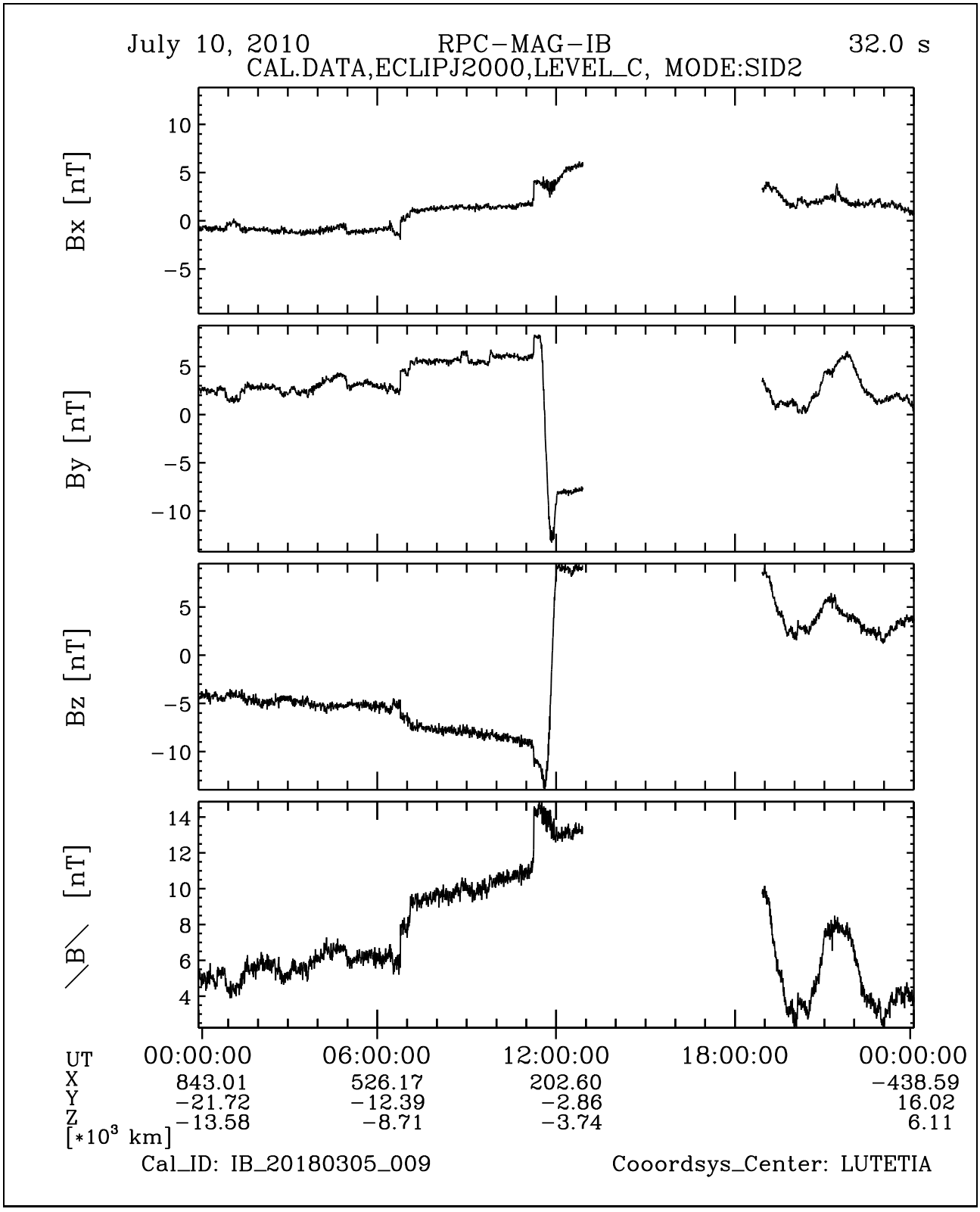

Figure 25: File: RPCMAG100710T0000_CLC_IB_M2_T0000_2400_009

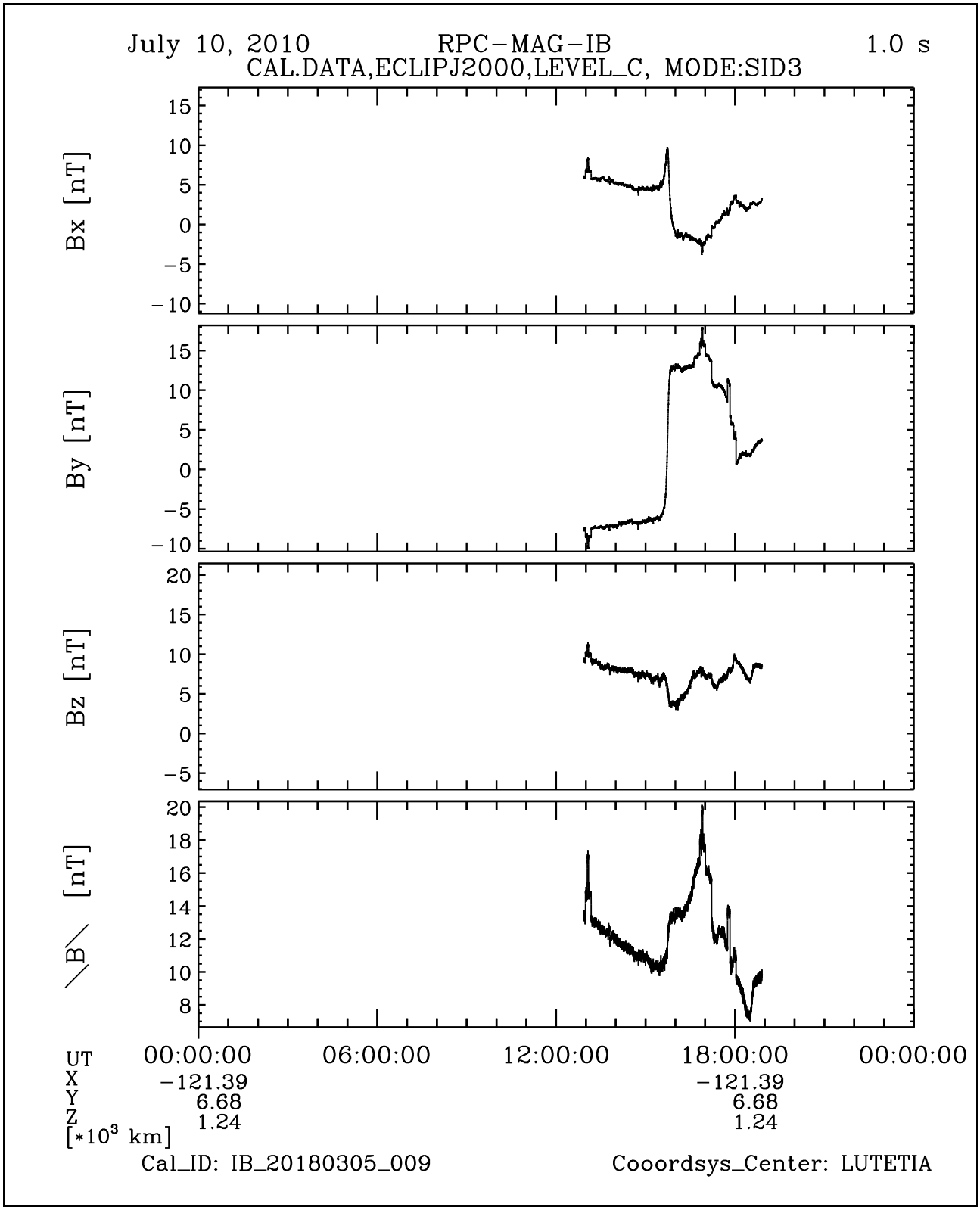

Figure 26: File: RPCMAG100710T1255_CLC_IB_M3_T0000_2400_009

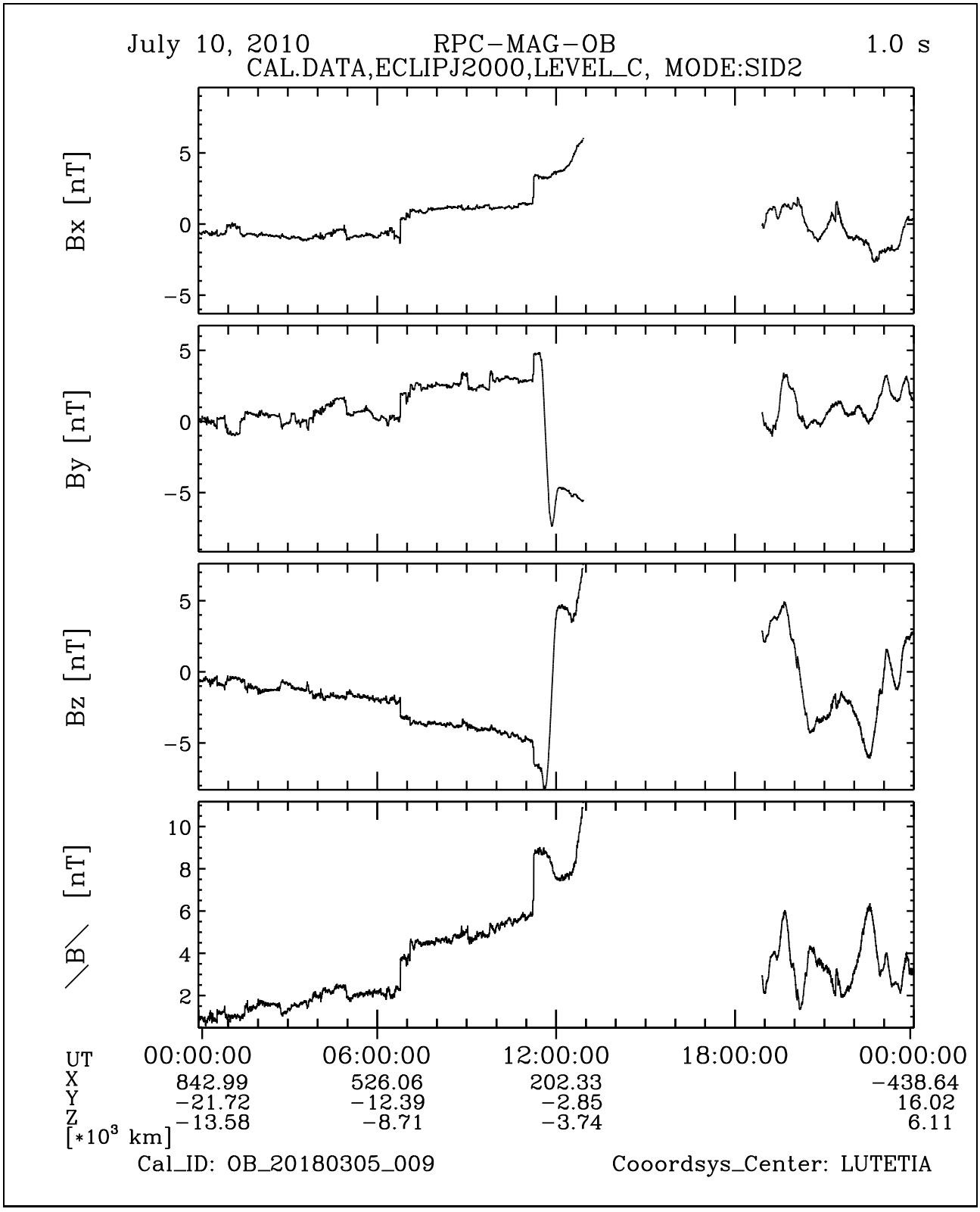

Figure 27: File: RPCMAG100710T0000_CLC_OB_M2_T0000_2400_009

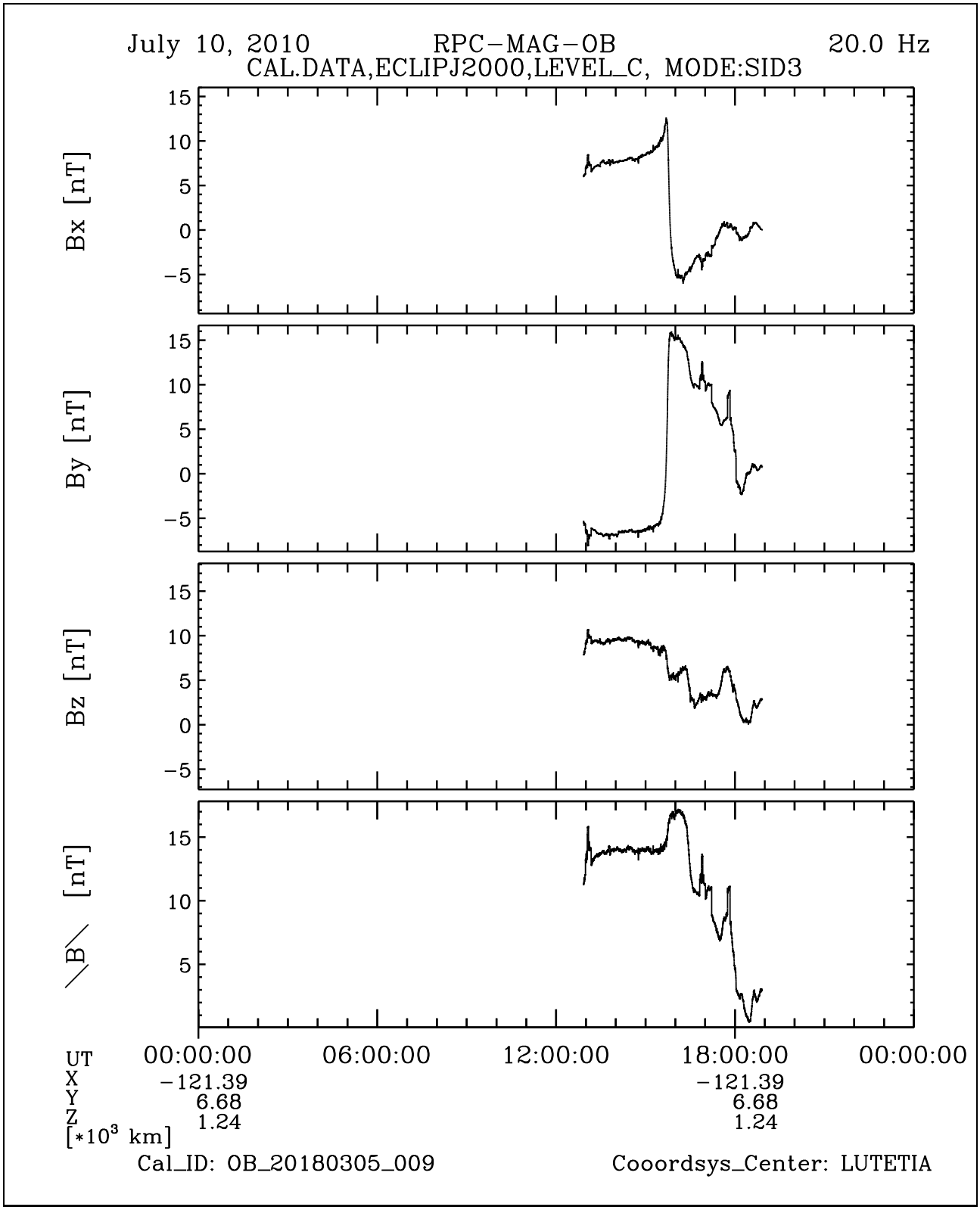

Figure 28: File: RPCMAG100710T1255_CLC_OB_M3_T0000_2400_009

3.5 July 11, 2010:

3.5.1 Actions

MAG stayed in SID 2. No problems occurred.

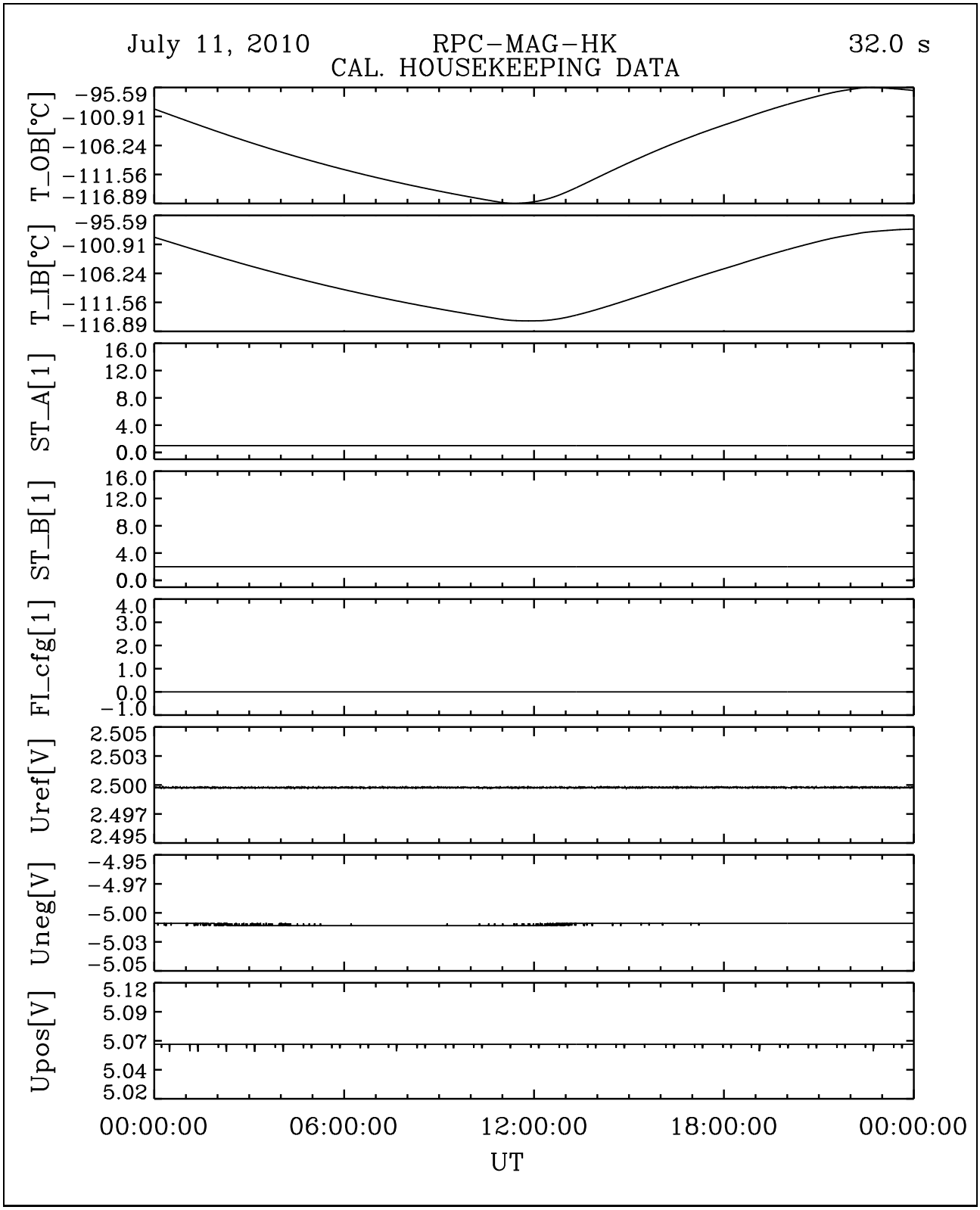

Figure 29: File: RPCMAG100711T0000_CLA_HK_P0000_2400

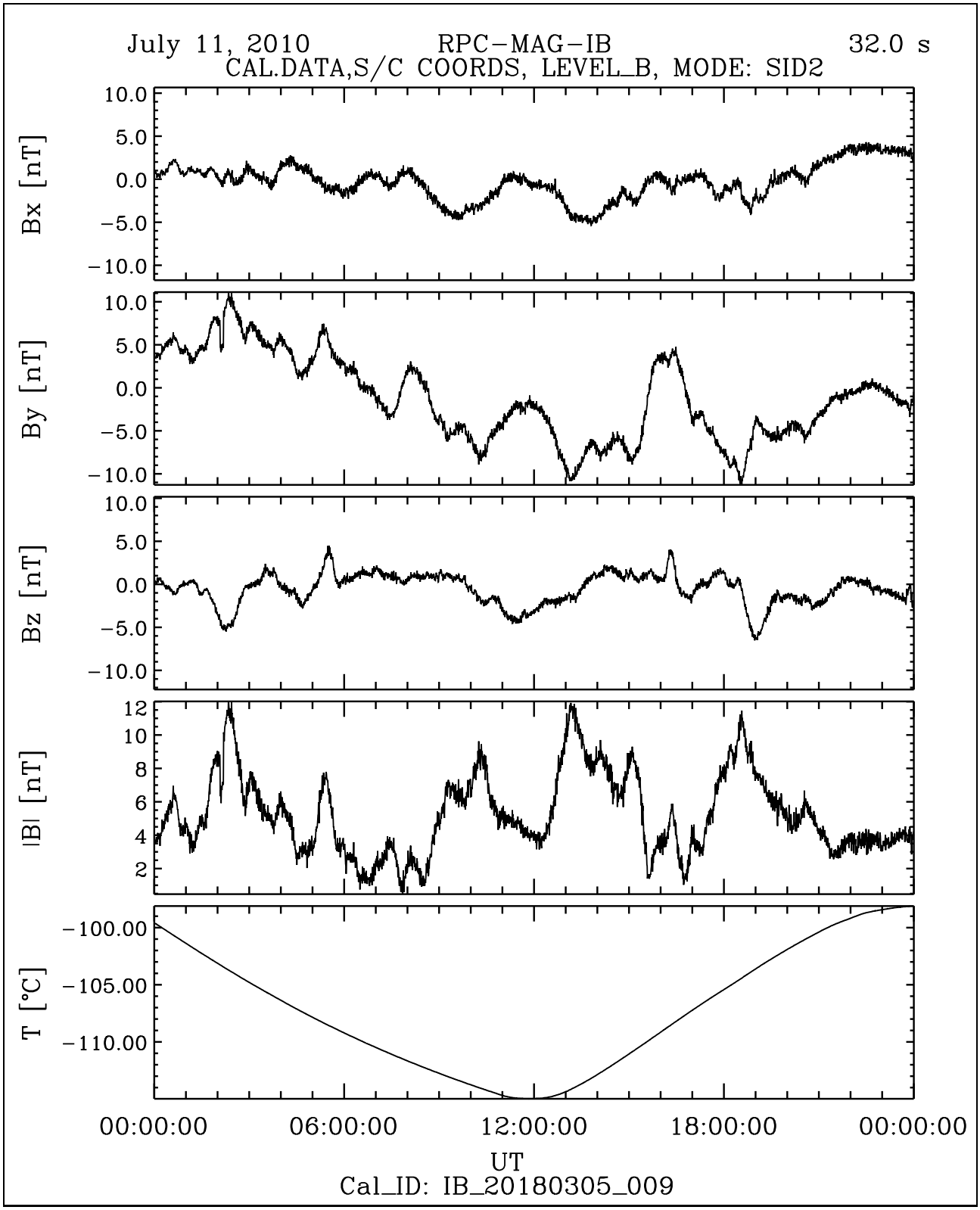

Figure 30: File: RPCMAG100711T0000_CLB_IB_M2_T0000_2400_009

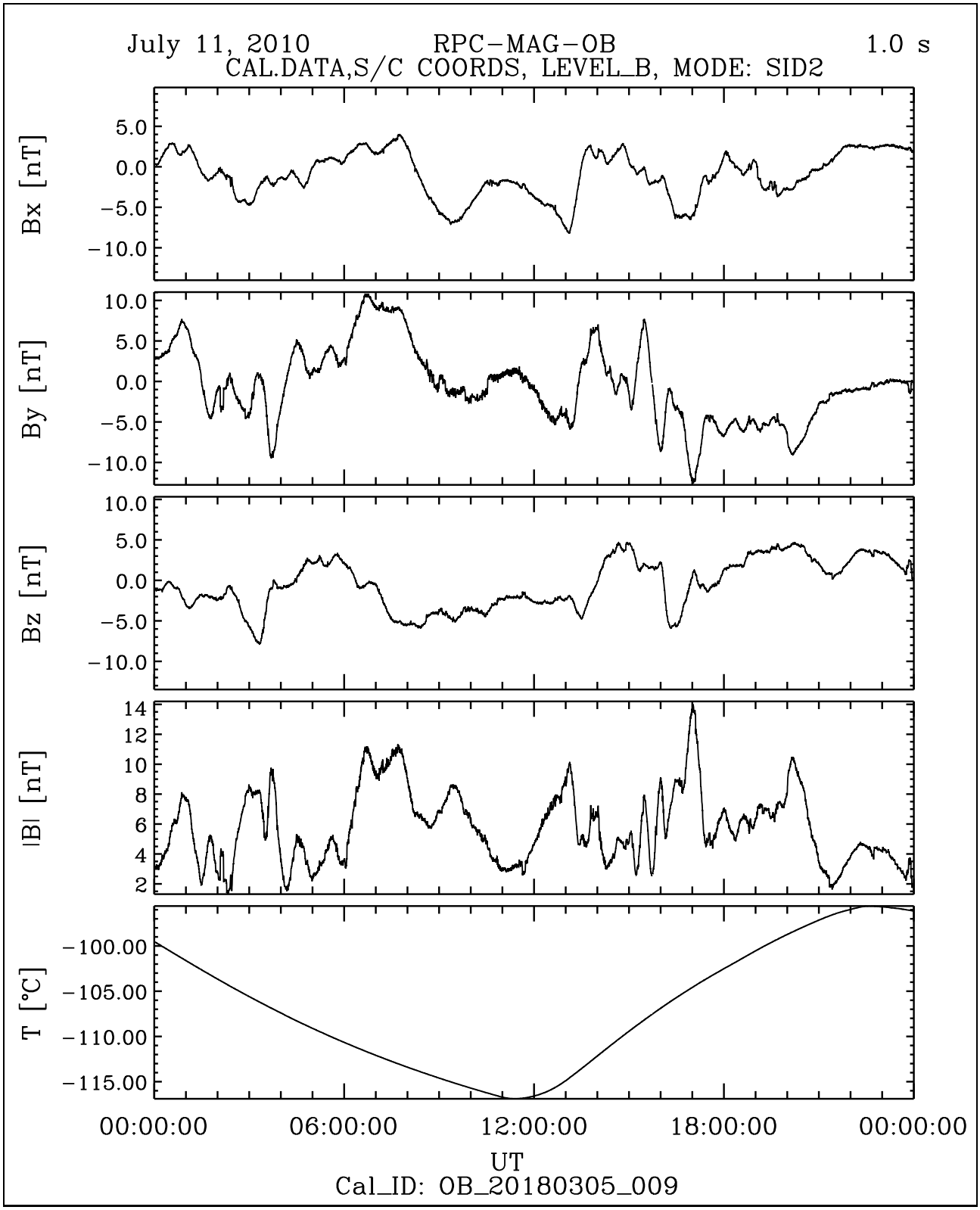

Figure 31: File: RPCMAG100711T0000_CLB_OB_M2_T0000_2400_009

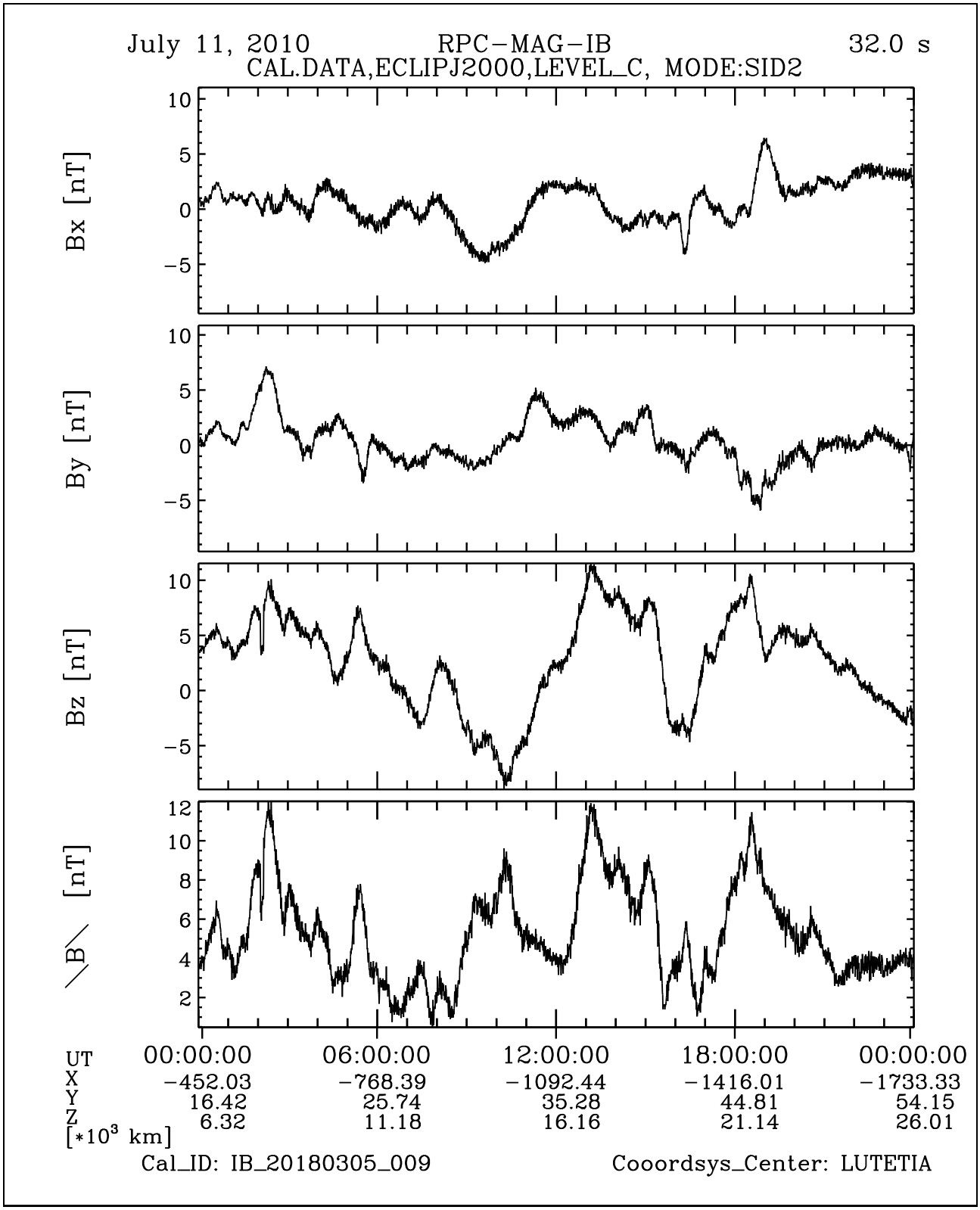

Figure 32: File: RPCMAG100711T0000_CLC_IB_M2_T0000_2400_009

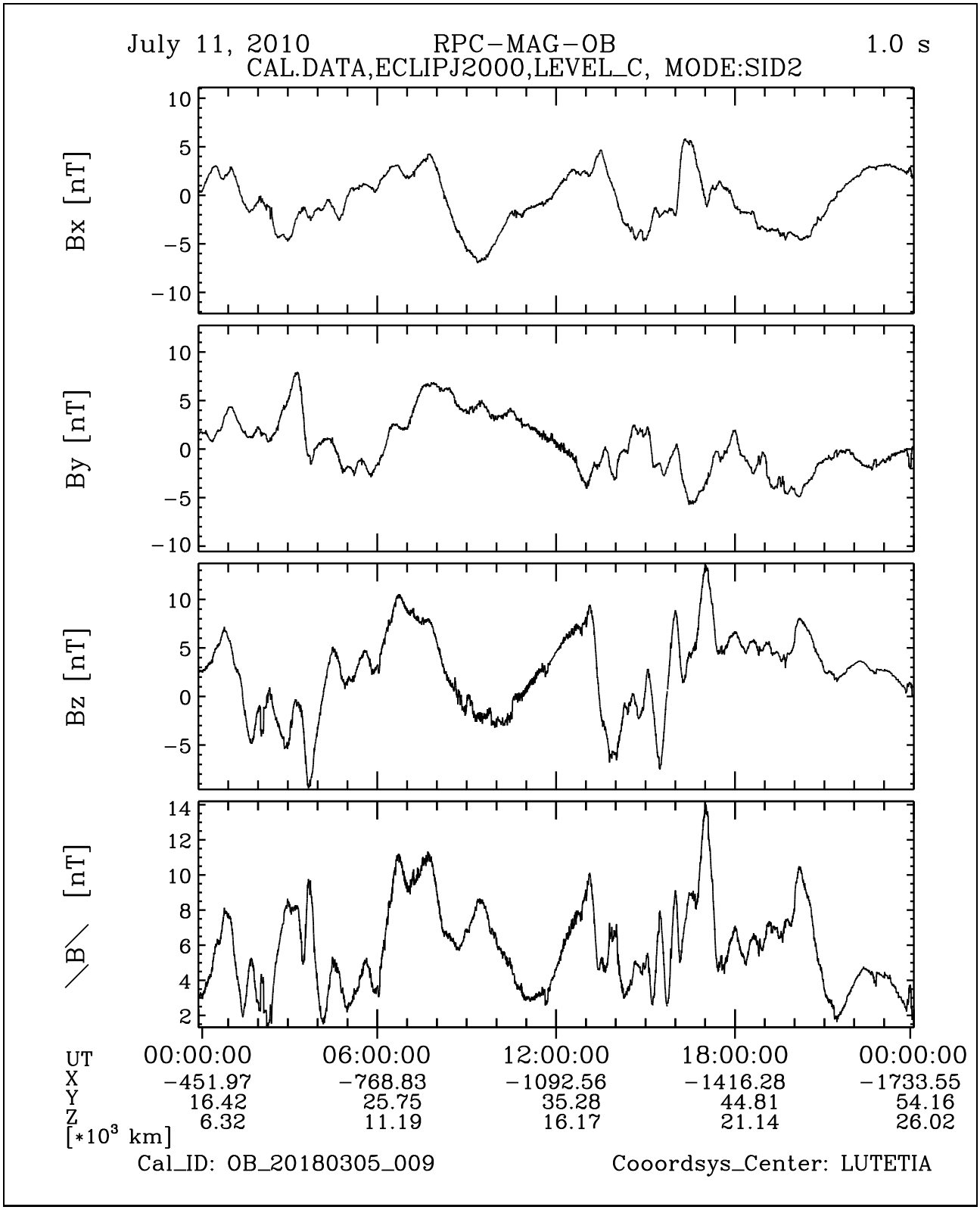

Figure 33: File: RPCMAG100711T0000_CLC_OB_M2_T0000_2400_009

3.6 July 12, 2010:

3.6.1 Actions

MAG stayed in SID 2. No problems occurred.

3.6.2 Plots of Calibrated Data

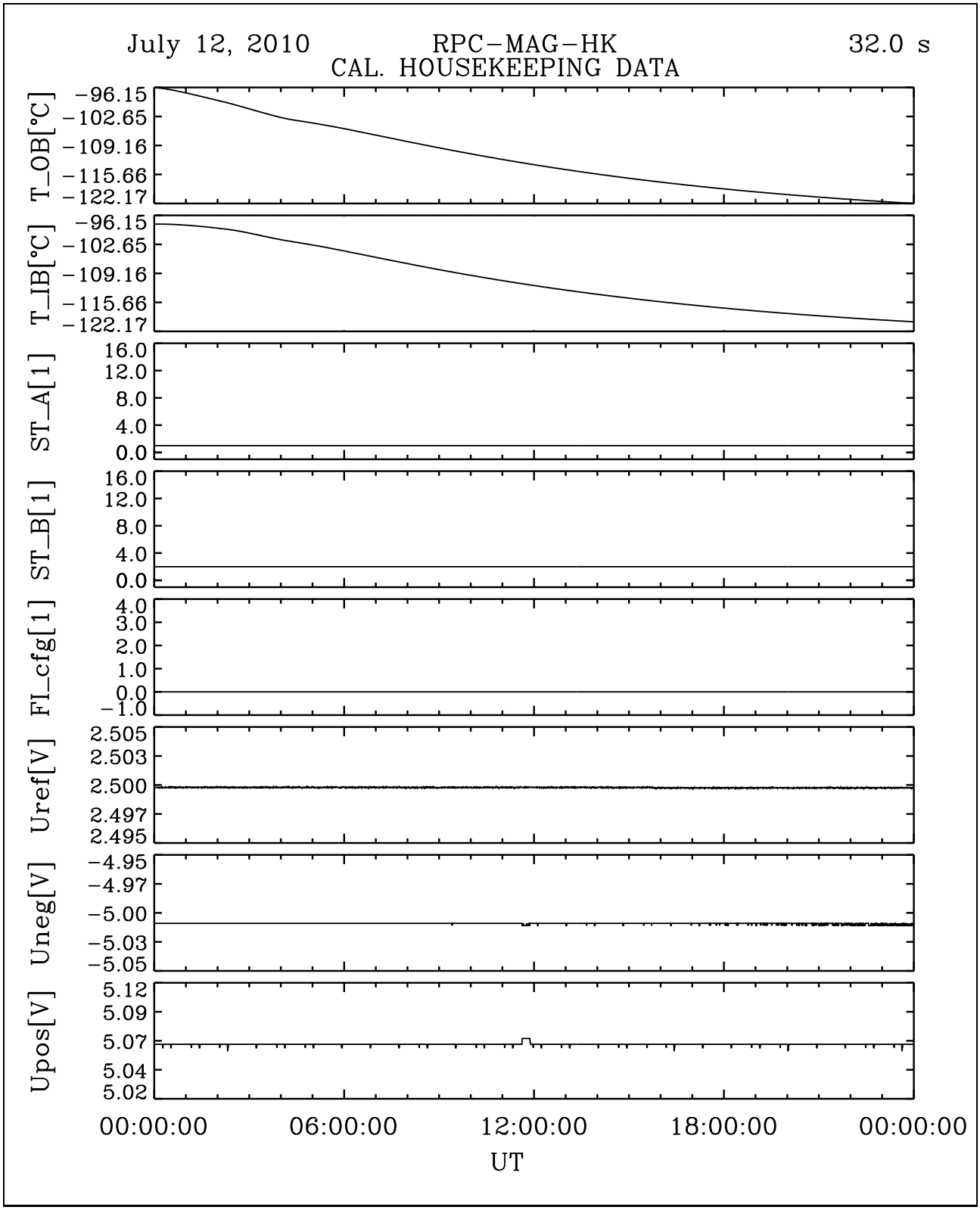

Figure 34: File: RPCMAG100712T0000_CLA_HK_P0000_2400

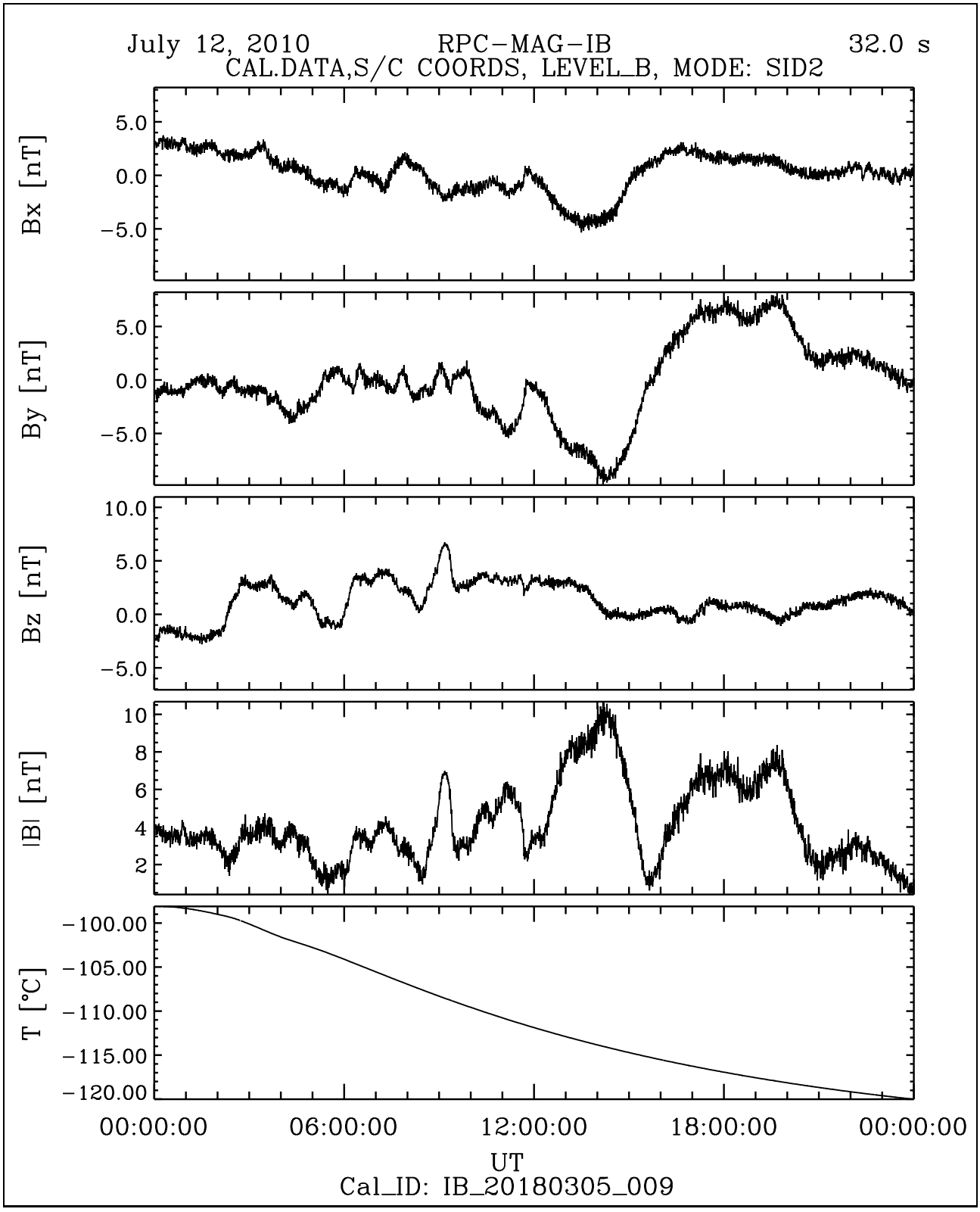

Figure 35: File: RPCMAG100712T0000_CLB_IB_M2_T0000_2400_009

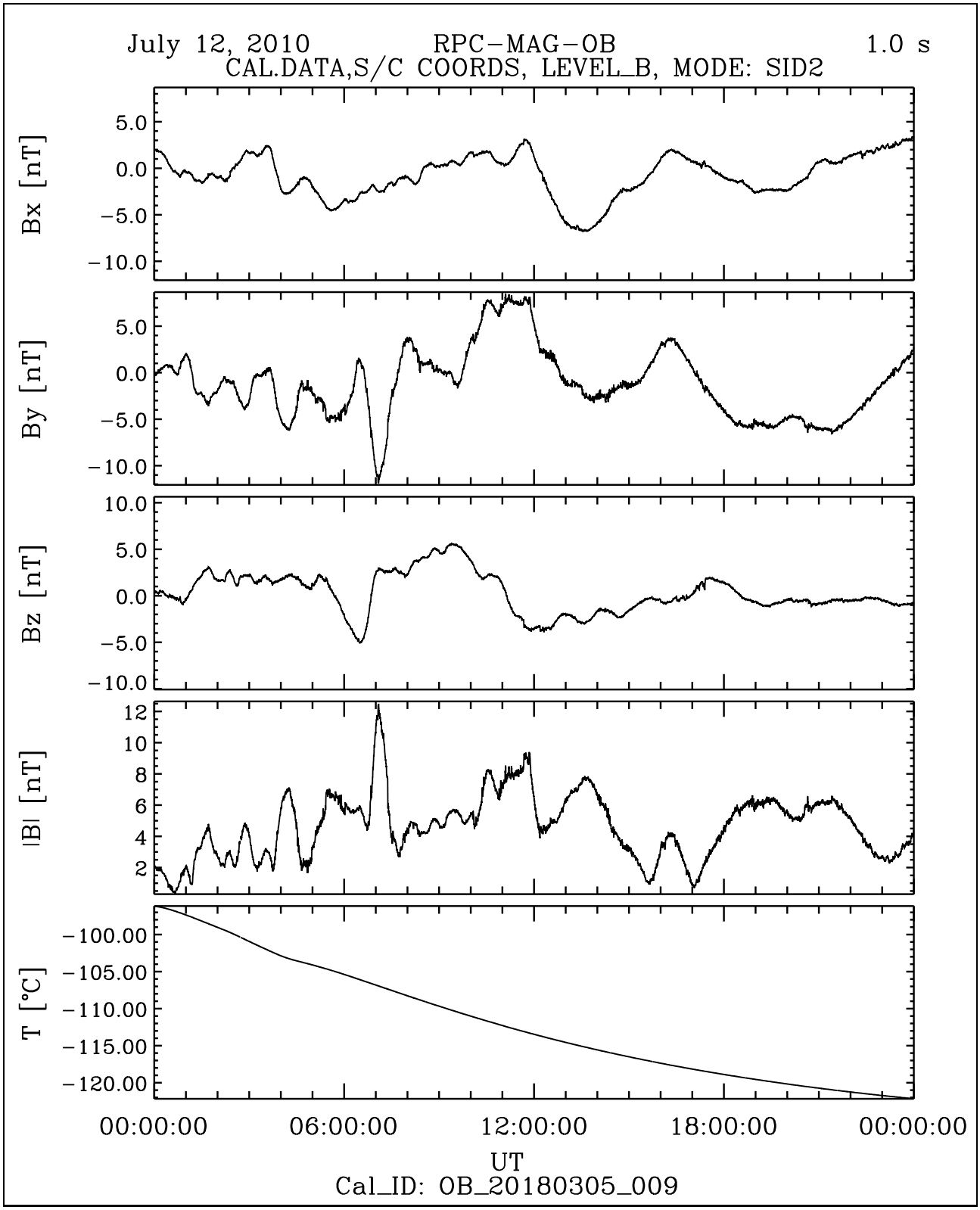

Figure 36: File: RPCMAG100712T0000_CLB_OB_M2_T0000_2400_009

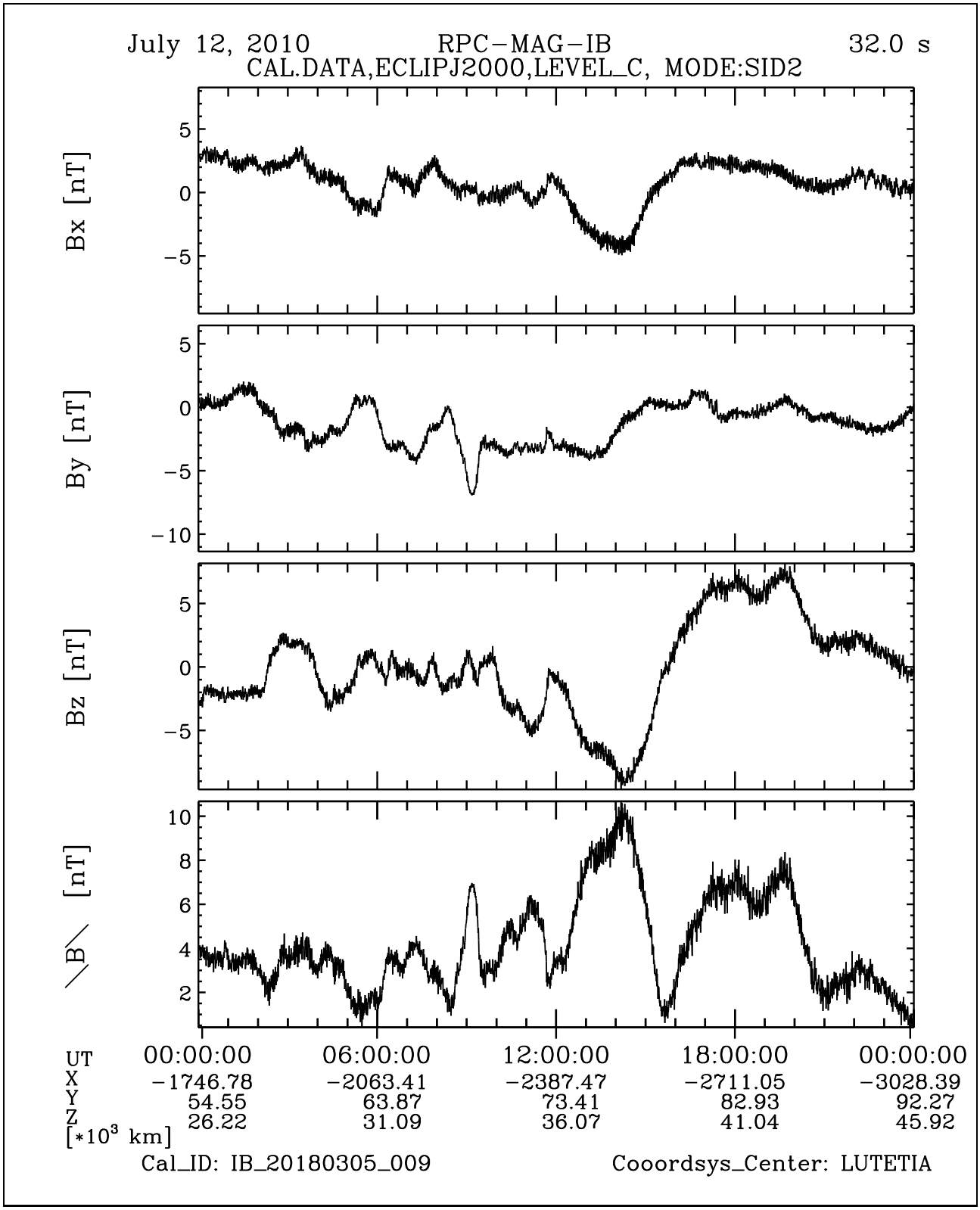

Figure 37: File: RPCMAG100712T0000_CLC_IB_M2_T0000_2400_009

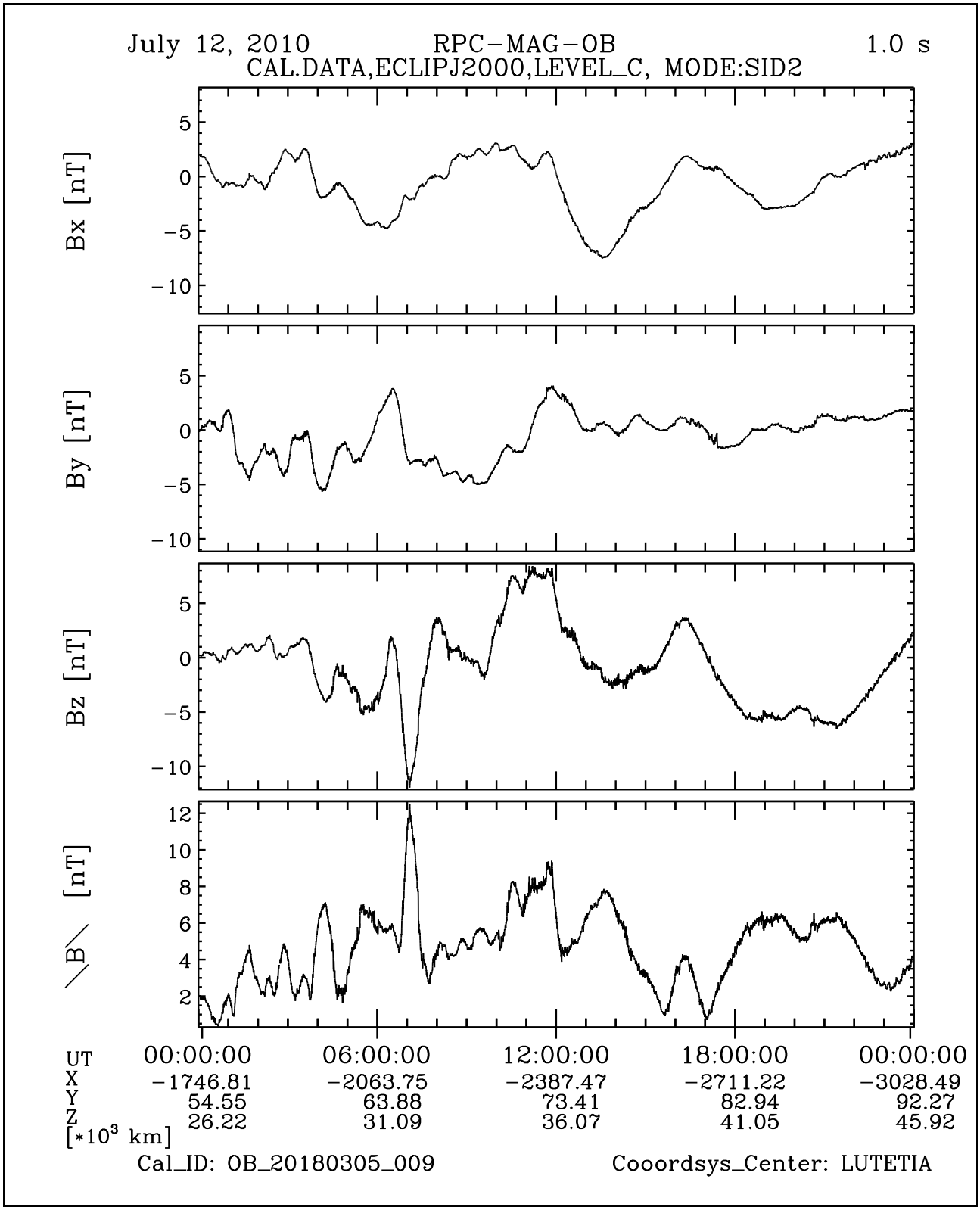

Figure 38: File: RPCMAG100712T0000_CLC_OB_M2_T0000_2400_009

3.7 July 13, 2010:

3.7.1 Actions

MAG stayed in SID 2 until 16:00. Then the instrument was switched off as the flyby campaign ended. No problems occurred.

Between 10:00 and 15:00 an interesting Solar wind signature is seen. It might be a CME. RPC-IES recognizes huge density fluctuations and an increasing speed in the same time interval.

3.7.2 Plots of Calibrated Data

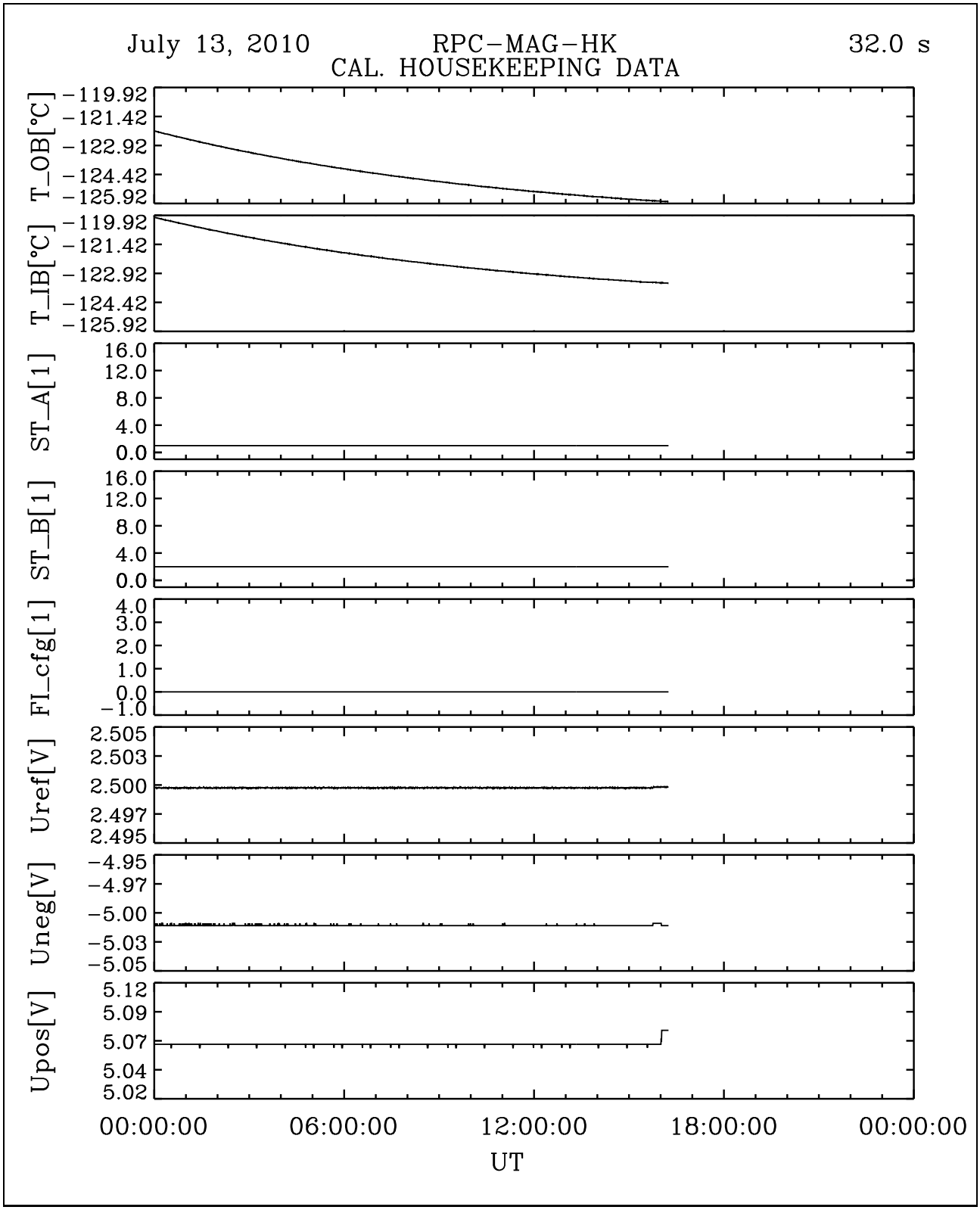

Figure 39: File: RPCMAG100713T0000_CLA_HK_P0000_2400

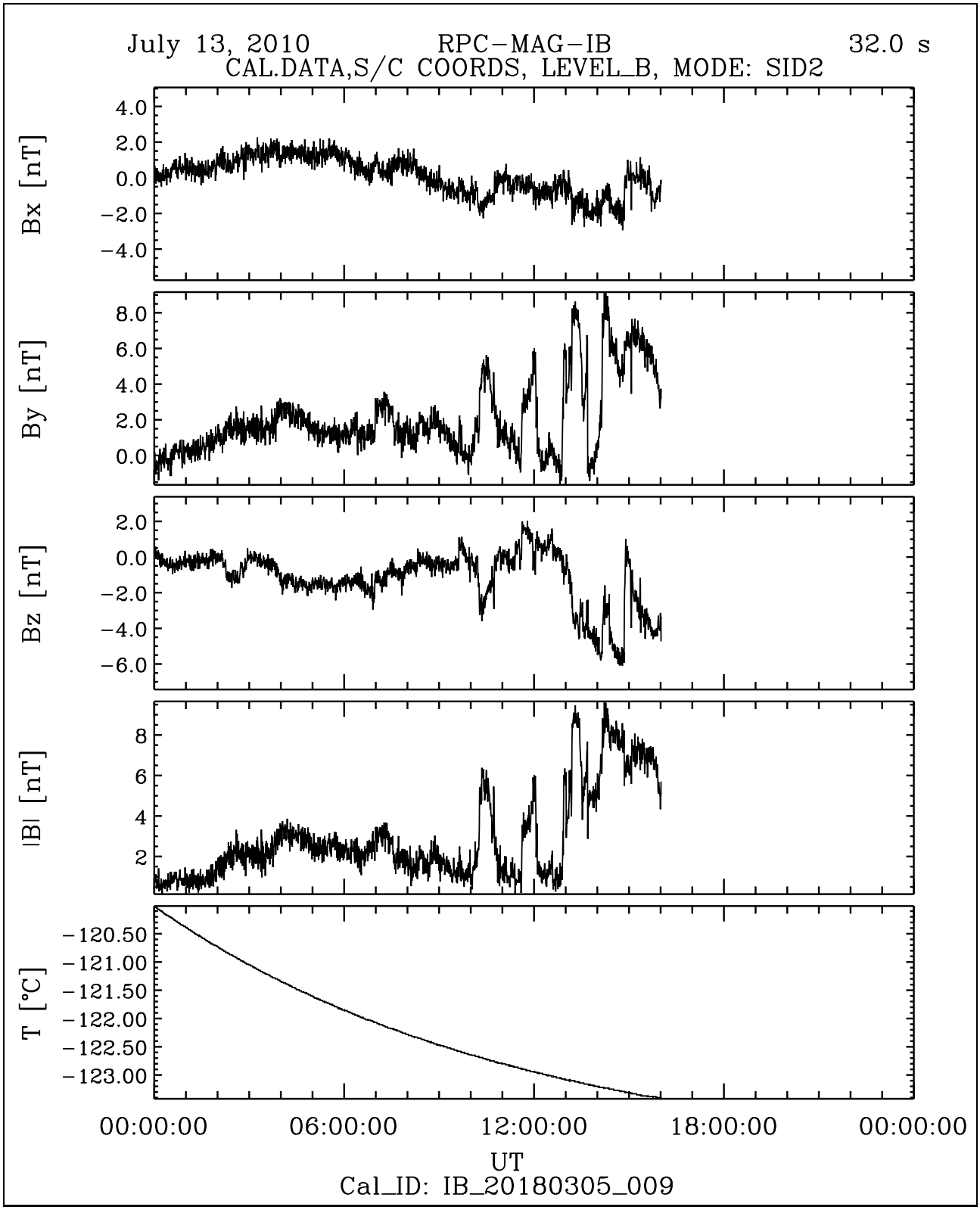

Figure 40: File: RPCMAG100713T0000_CLB_IB_M2_T0000_2400_009

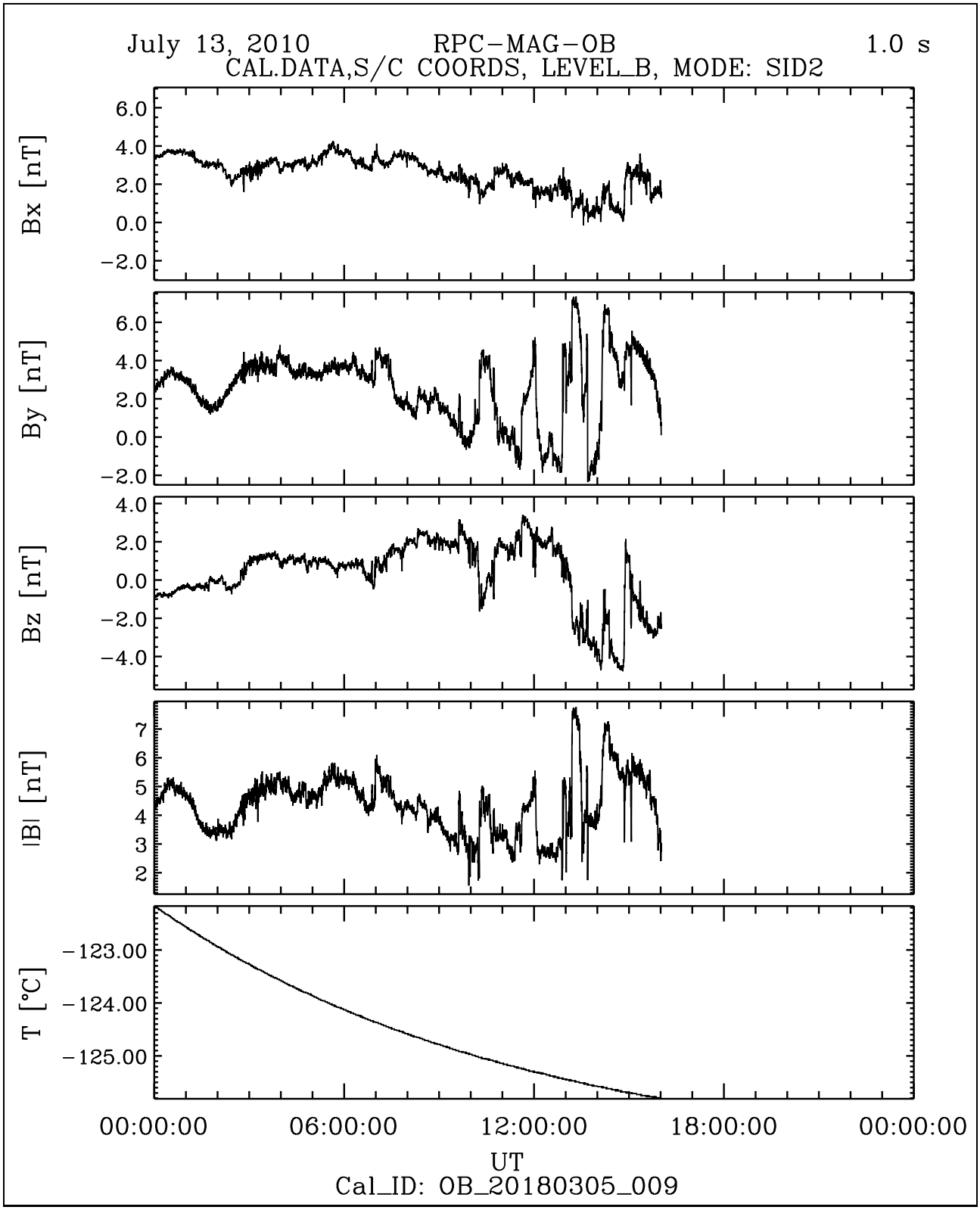

Figure 41: File: RPCMAG100713T0000_CLB_OB_M2_T0000_2400_009

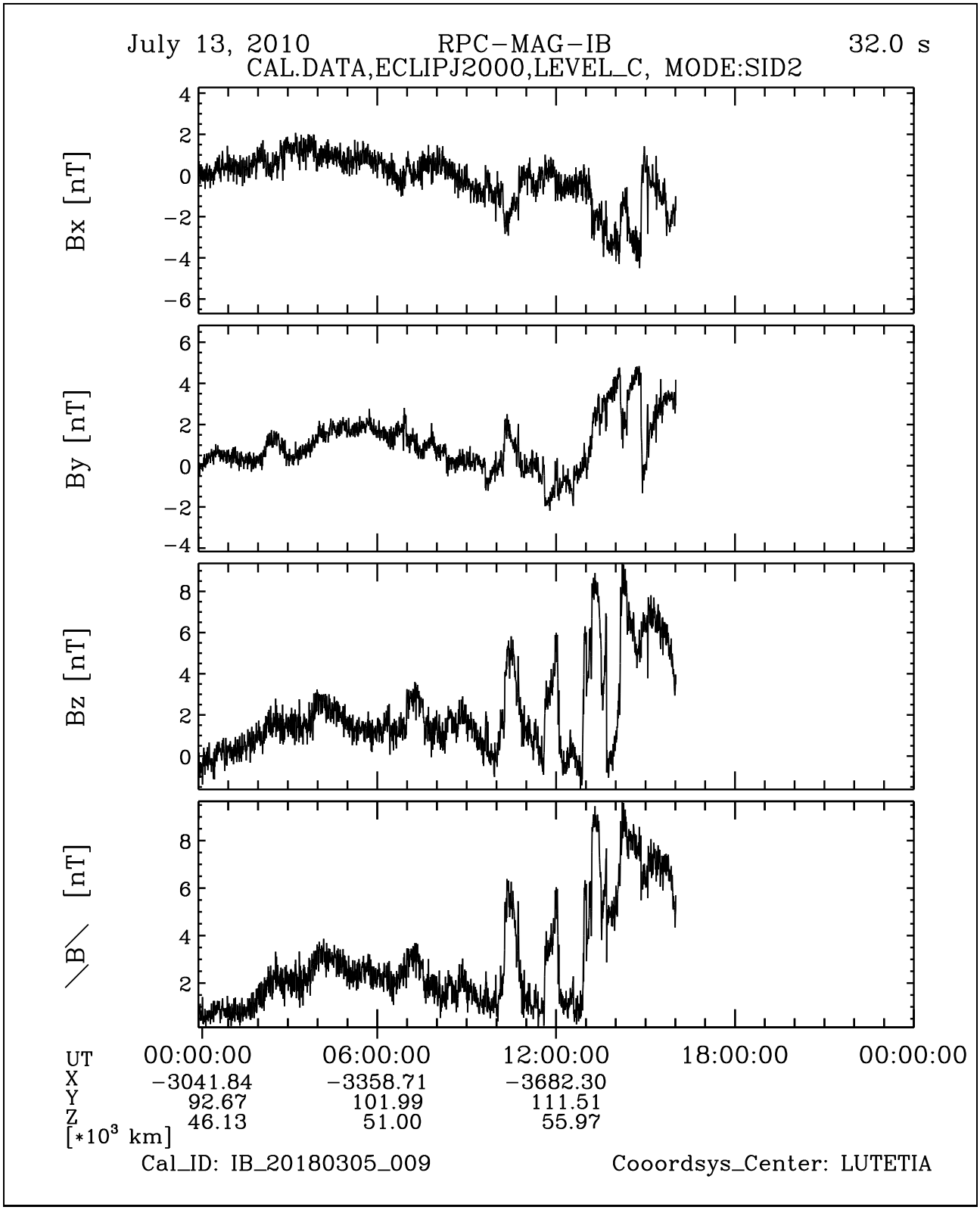

Figure 42: File: RPCMAG100713T0000_CLC_IB_M2_T0000_2400_009

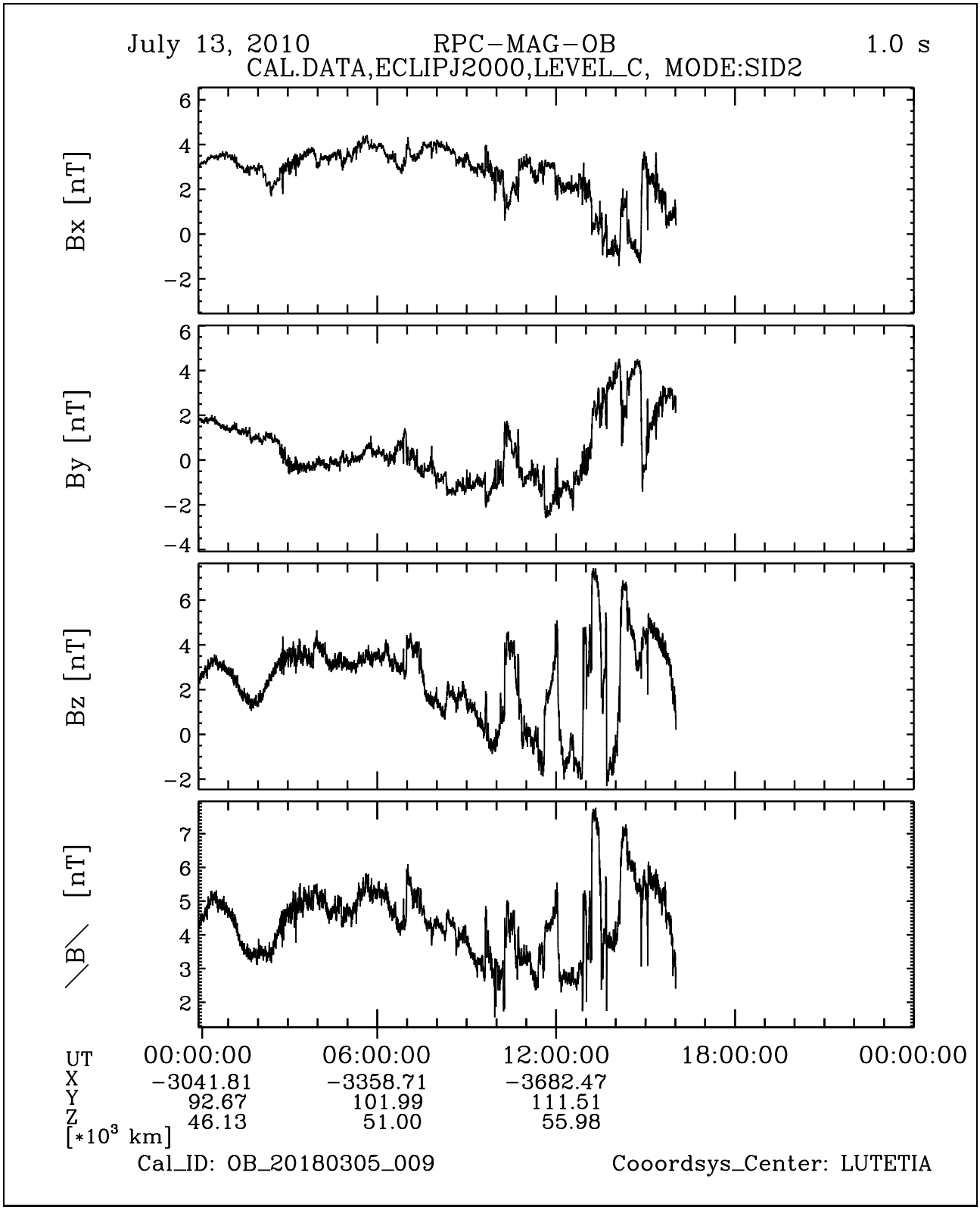

Figure 43: File: RPCMAG100713T0000_CLC_OB_M2_T0000_2400_009

4 Comparison between OB,IB and ROMAP: The Influence of the Sensor Temperature and of other Disturbers

In this section we compare the measured data of the OB Sensor with the IB ones. The investigation is done with 1 s averaged LEVEL_F data (s/c coordinates) for various days.

From earlier mission phases we know, that the OB and IB data match very well at times where the both sensors feel the same temperature *variation*. When the temperature changes are different, then the magnetic field data diverge as well. We do see this effect still in a reduced way although a the new calibration model 009 has been applied using data from the complete ROSETTA mission. On short time scales different heat capacities and micro physical hysteresis effects of the sensors core material may cause this behavior.

At the actual mission phase we see - as already recognized in many phases before - that the OB and IB data are sometimes different also if the temperature behavior is the same. This is clear indication there are active disturbers on the s/c.

For July, 10 some disturbers could be identified. There was activity from the COSAC and the PTOLEMY instruments. The impact of these instruments is indicated in Figure 44 for the OB sensor and additionally for the LANDER magnetometer ROMAP in Figure 45. The difference of the impacts is in the order of a few hundred nT.

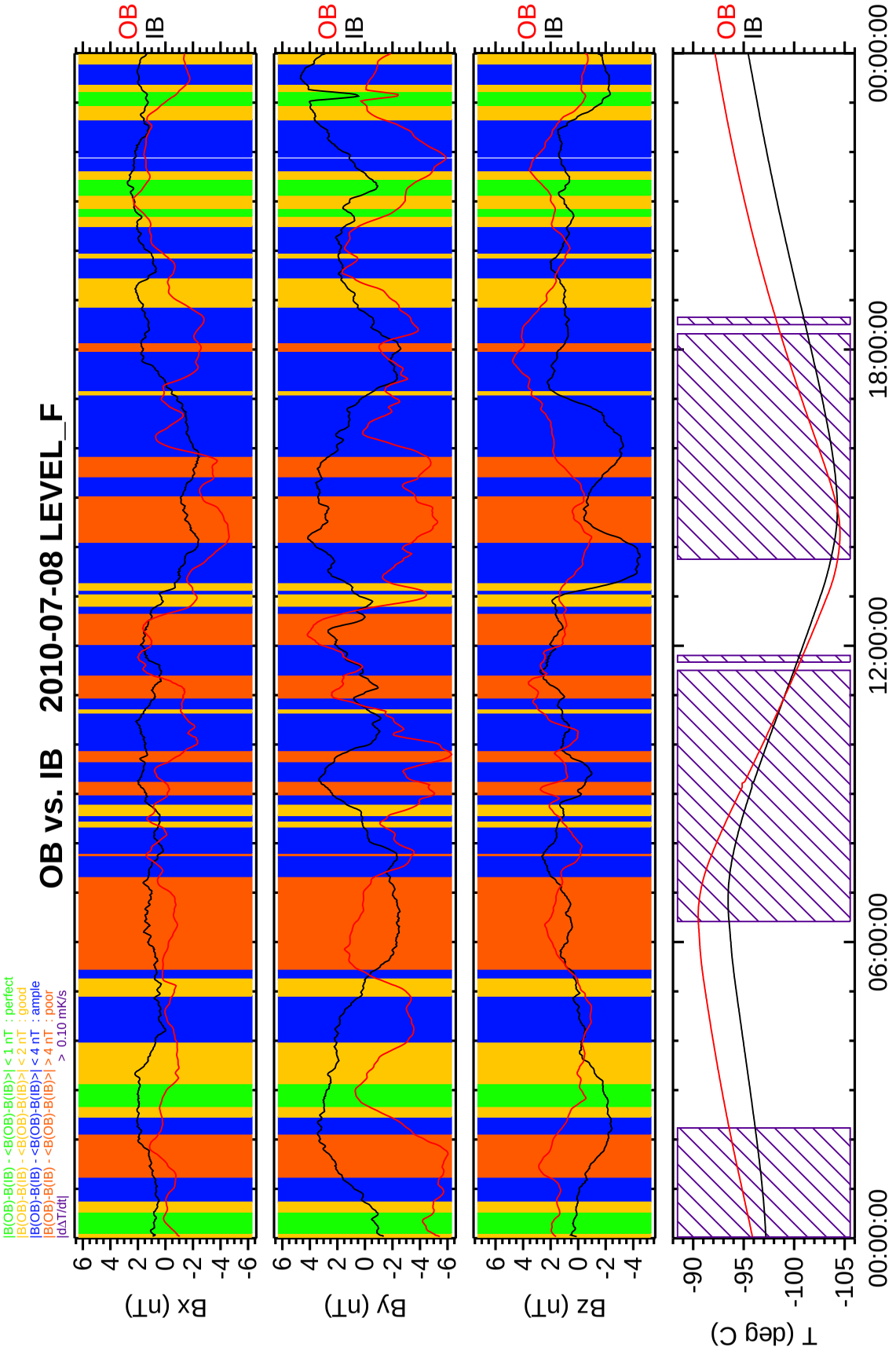
OB vs. IB 2010-07-08 LEVEL_F
|B(OB)-B(IB) - <B(OB)-B(IB)>| < 1 nT : perfect
|B(OB)-B(IB) - <B(OB)-B(IB)>| < 2 nT : good
|B(OB)-B(IB) - <B(OB)-B(IB)>| < 4 nT : ample
|B(OB)-B(IB) - <B(OB)-B(IB)>| > 4 nT : poor
|dΔT/dt| > 0.10 mK/s
OB
IB
Bx (nT)
By (nT)
Bz (nT)
T (deg C)
00:00:00
06:00:00
12:00:00
18:00:00
00:00:00

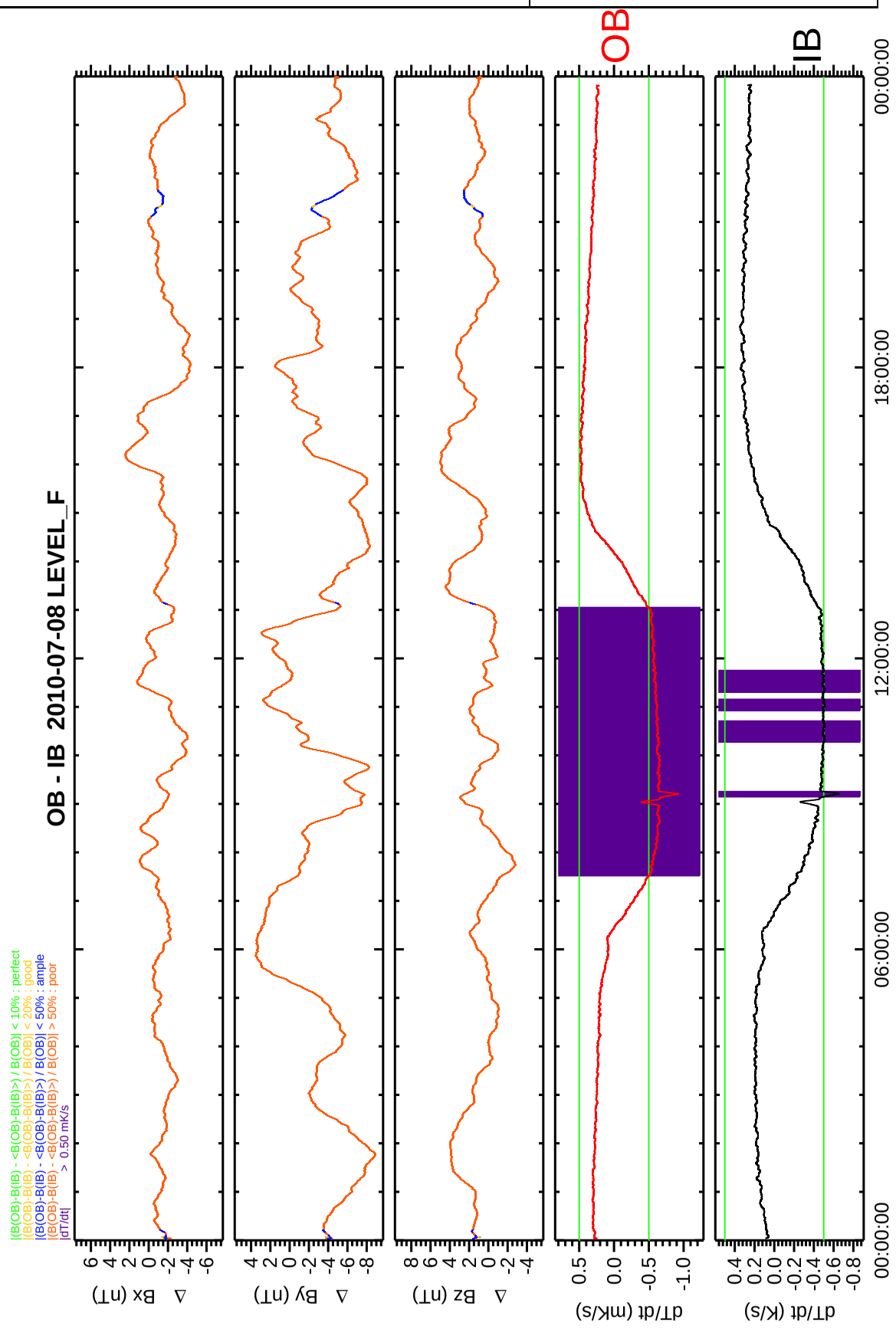
OB - IB 2010-07-08 LEVEL_F
OB
IB
Δ Bx (nT)
Δ By (nT)
Δ Bz (nT)
dT/dt (mK/s)
dT/dt (K/s)
00:00:00
06:00:00
12:00:00
18:00:00
00:00:00
|(B(OB)-B(IB) - <B(OB)-B(IB)>) / B(OB)| < 10% : perfect
|(B(OB)-B(IB) - <B(OB)-B(IB)>) / B(OB)| < 20% : good
|(B(OB)-B(IB) - <B(OB)-B(IB)>) / B(OB)| < 50% : ample
|(B(OB)-B(IB) - <B(OB)-B(IB)>) / B(OB)| > 50% : poor
|dT/dt| > 0.50 mK/s

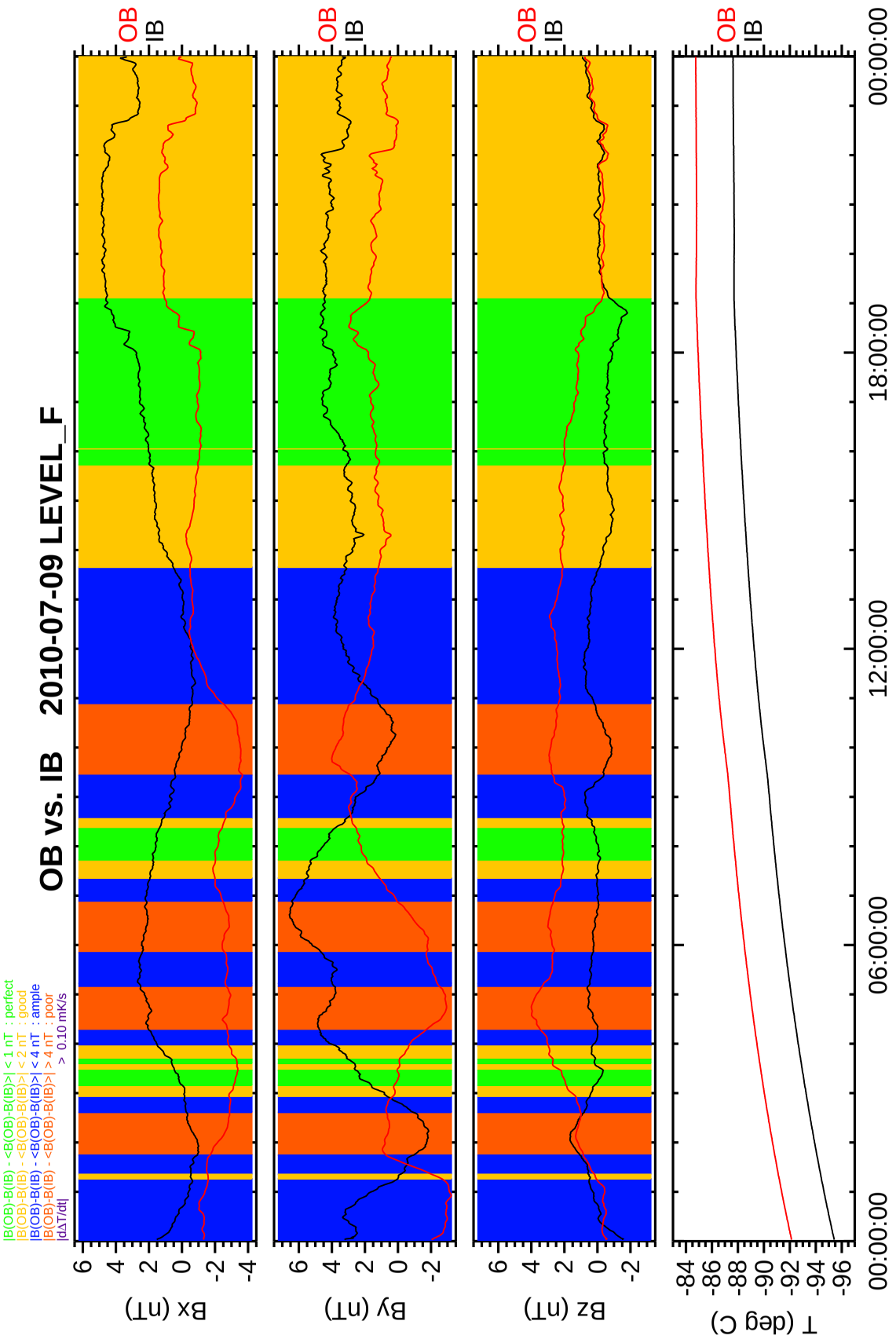
OB vs. IB 2010-07-09 LEVEL_F
|B(OB)-B(IB) - <B(OB)-B(IB)>| < 1 nT : perfect
|B(OB)-B(IB) - <B(OB)-B(IB)>| < 2 nT : good
|B(OB)-B(IB) - <B(OB)-B(IB)>| < 4 nT : ample
|B(OB)-B(IB) - <B(OB)-B(IB)>| > 4 nT : poor
|dΔT/dt| > 0.10 mK/s
OB
IB
Bx (nT)
By (nT)
Bz (nT)
T (deg C)
00:00:00
06:00:00
12:00:00
18:00:00
00:00:00

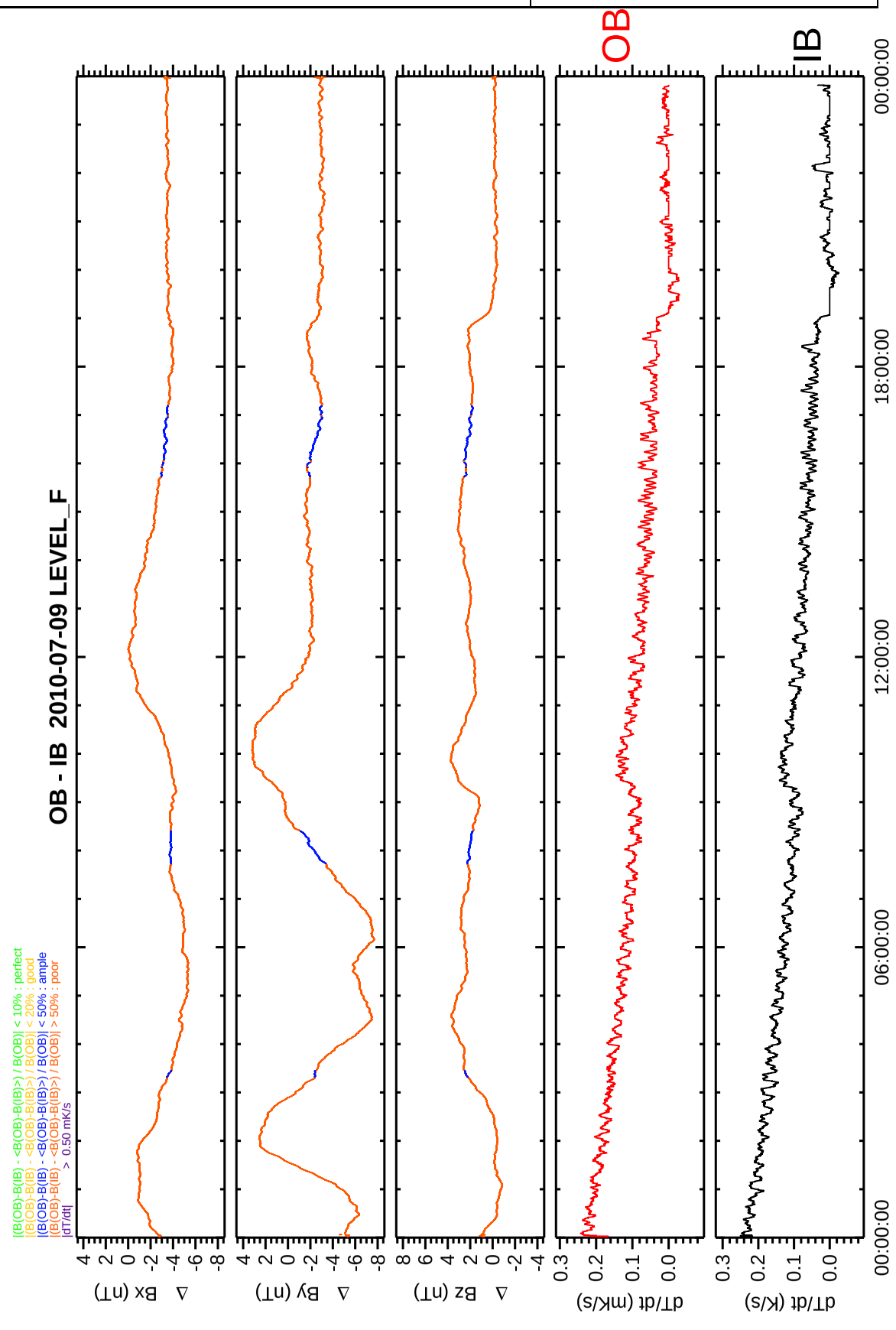
OB - IB 2010-07-09 LEVEL_F
|B(OB)-B(IB) - <B(OB)-B(IB)>| / B(OB)| < 10% : perfect
|B(OB)-B(IB) - <B(OB)-B(IB)>| / B(OB)| < 20% : good
|B(OB)-B(IB) - <B(OB)-B(IB)>| / B(OB)| < 50% : ample
|B(OB)-B(IB) - <B(OB)-B(IB)>| / B(OB)| > 50% : poor
|dT/dt| > 0.50 mK/s
Δ Bx (nT)
Δ By (nT)
Δ Bz (nT)
dT/dt (mK/s)
dT/dt (K/s)
OB
IB
00:00:00
06:00:00
12:00:00
18:00:00
00:00:00

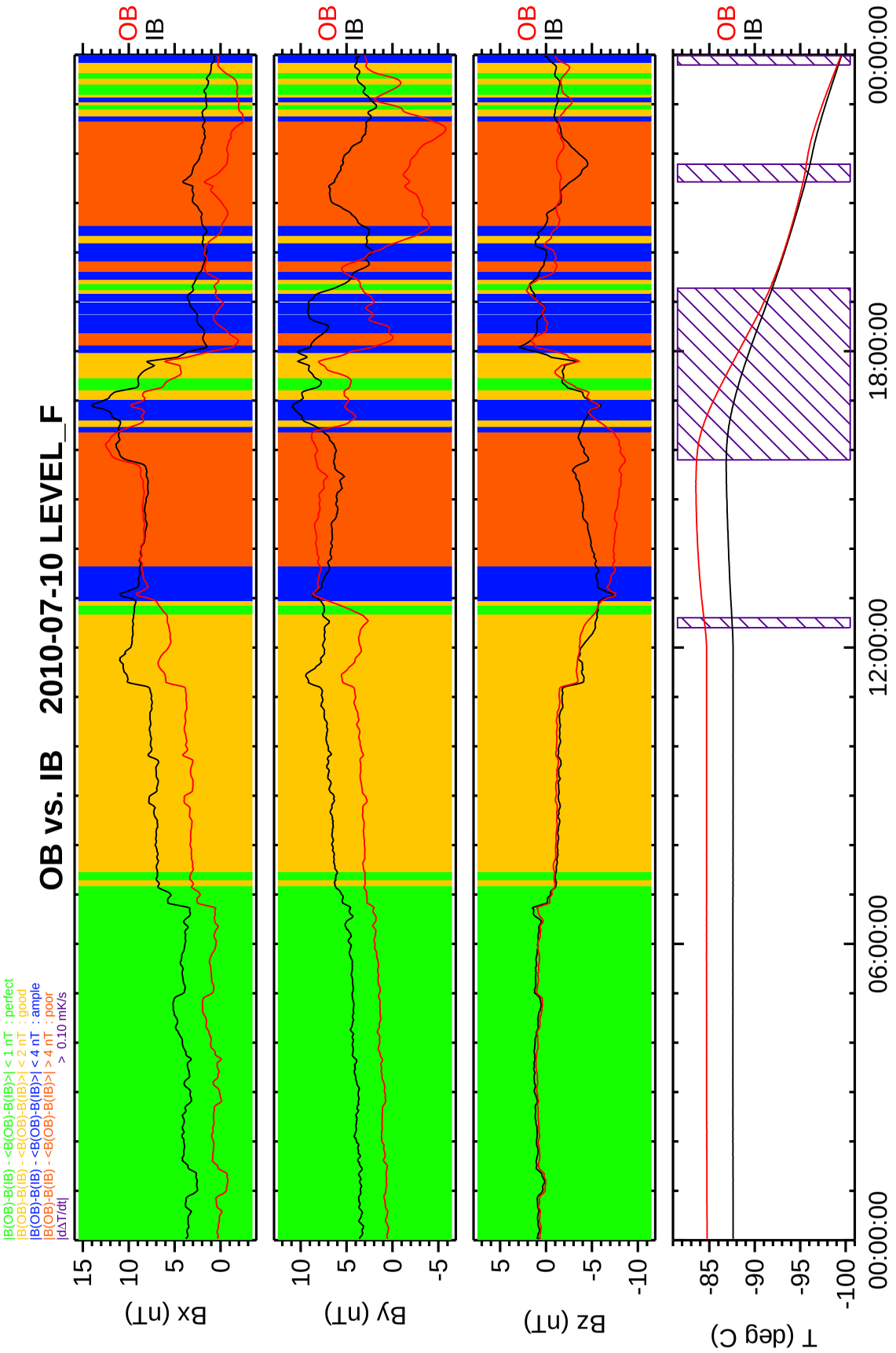
OB vs. IB 2010-07-10 LEVEL_F
|B(OB)-B(IB) - <B(OB)-B(IB)>| < 1 nT : perfect
|B(OB)-B(IB) - <B(OB)-B(IB)>| < 2 nT : good
|B(OB)-B(IB) - <B(OB)-B(IB)>| < 4 nT : ample
|B(OB)-B(IB) - <B(OB)-B(IB)>| > 4 nT : poor
|dΔT/dt| > 0.10 mK/s
OB
IB
Bx (nT)
By (nT)
Bz (nT)
T (deg C)
00:00:00
06:00:00
12:00:00
18:00:00
00:00:00

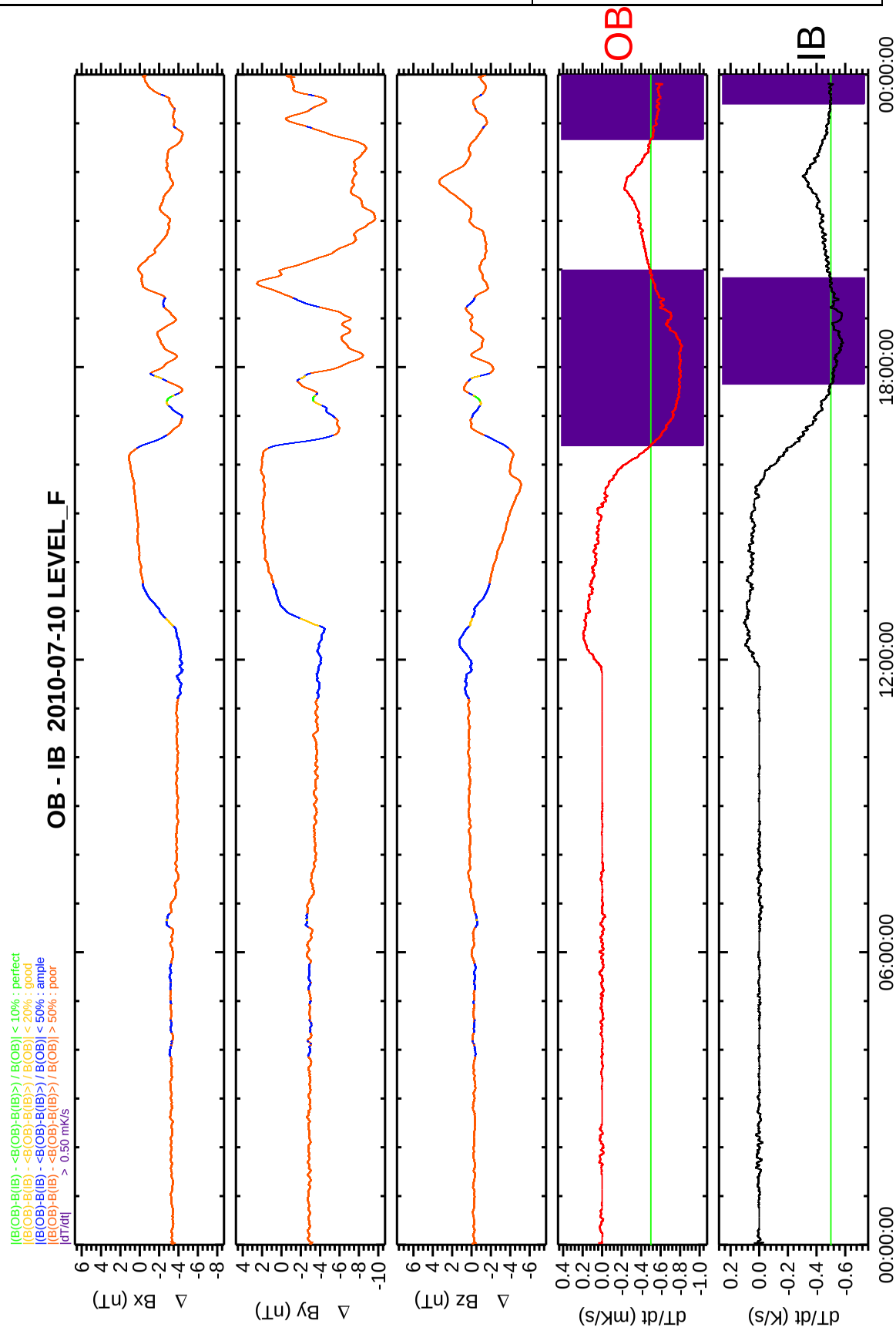
OB - IB 2010-07-10 LEVEL_F
|(B(OB)-B(IB) - <B(OB)-B(IB)>) / B(OB)| < 10% : perfect
|(B(OB)-B(IB) - <B(OB)-B(IB)>) / B(OB)| < 20% : good
|(B(OB)-B(IB) - <B(OB)-B(IB)>) / B(OB)| < 50% : ample
|(B(OB)-B(IB) - <B(OB)-B(IB)>) / B(OB)| > 50% : poor
|dT/dt| > 0.50 mK/s
Δ Bx (nT)
Δ By (nT)
Δ Bz (nT)
dT/dt (mK/s)
dT/dt (K/s)
OB
IB
00:00:00
06:00:00
12:00:00
18:00:00
00:00:00

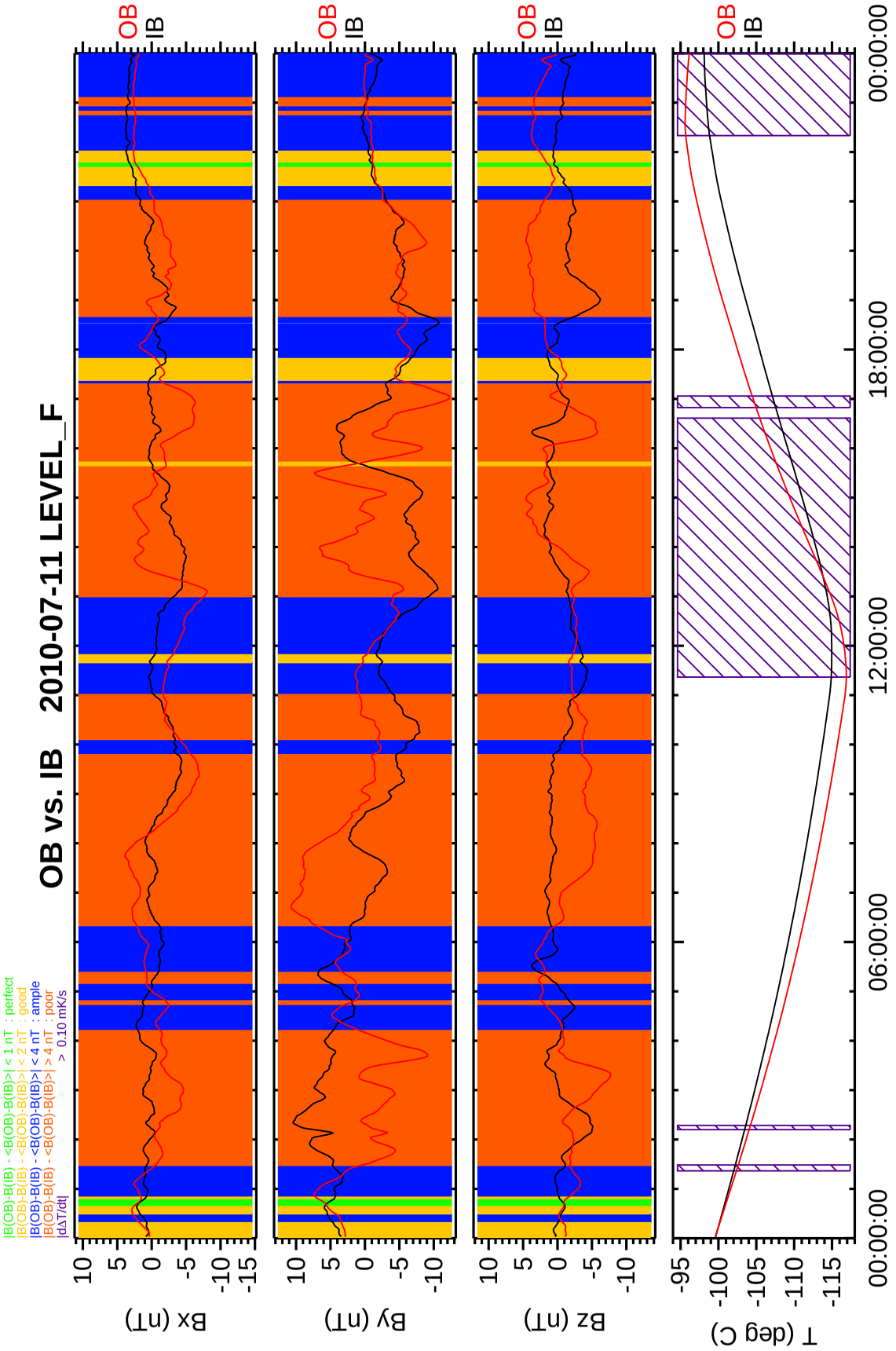
OB vs. IB 2010-07-11 LEVEL_F
|B(OB)-B(IB) - <B(OB)-B(IB)>| < 1 nT : perfect
|B(OB)-B(IB) - <B(OB)-B(IB)>| < 2 nT : good
|B(OB)-B(IB) - <B(OB)-B(IB)>| < 4 nT : ample
|B(OB)-B(IB) - <B(OB)-B(IB)>| > 4 nT : poor
|dΔT/dt| > 0.10 mK/s
OB
IB
Bx (nT)
By (nT)
Bz (nT)
T (deg C)
00:00:00
06:00:00
12:00:00
18:00:00
00:00:00

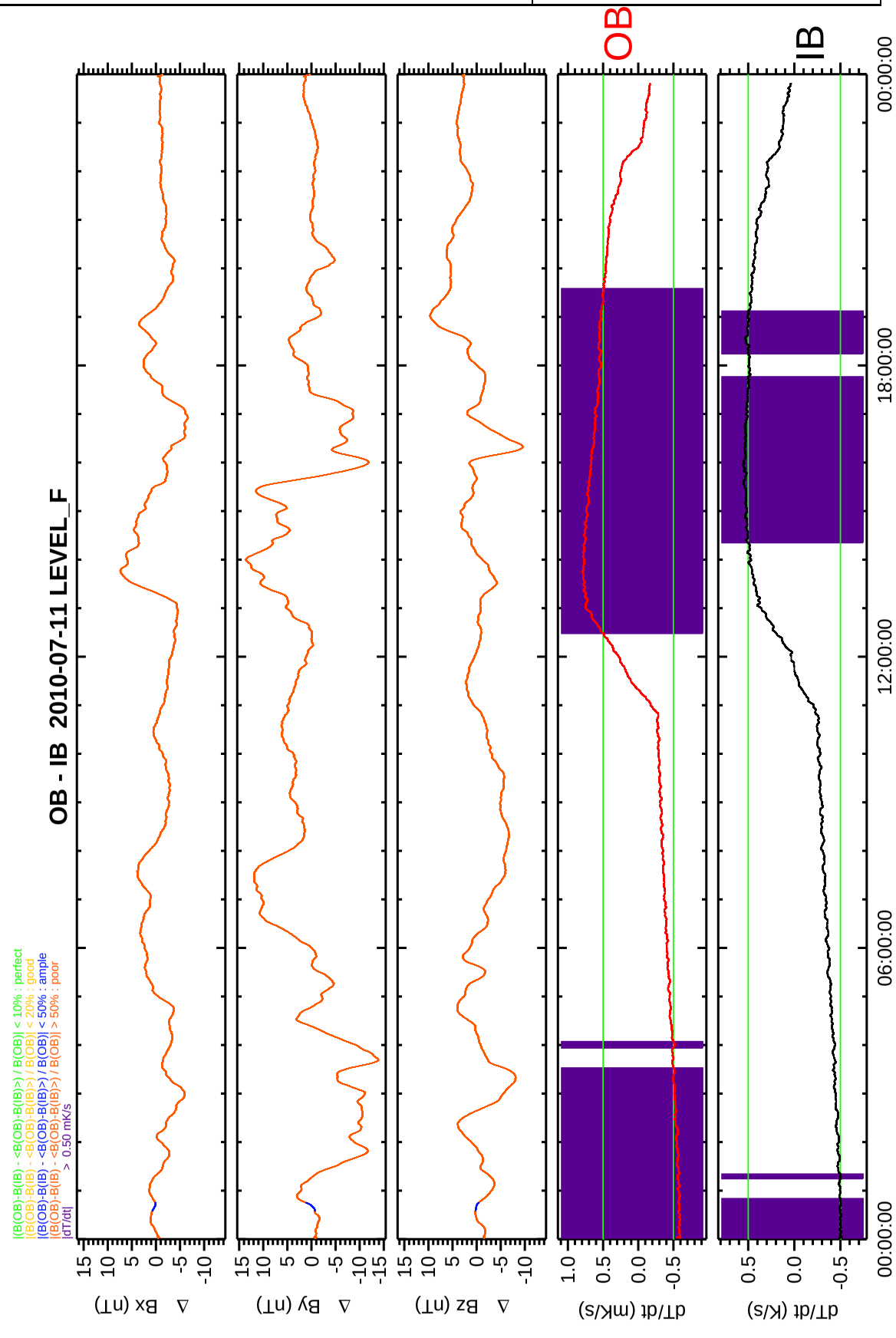
OB - IB 2010-07-11 LEVEL_F
OB
IB
Δ Bx (nT)
Δ By (nT)
Δ Bz (nT)
dT/dt (mK/s)
dT/dt (K/s)
00:00:00
06:00:00
12:00:00
18:00:00
00:00:00
|(B(OB)-B(IB) - <B(OB)-B(IB)>) / B(OB)| < 10% : perfect
|(B(OB)-B(IB) - <B(OB)-B(IB)>) / B(OB)| < 20% : good
|(B(OB)-B(IB) - <B(OB)-B(IB)>) / B(OB)| < 50% : ample
|(B(OB)-B(IB) - <B(OB)-B(IB)>) / B(OB)| > 50% : poor
|dT/dt| > 0.50 mK/s

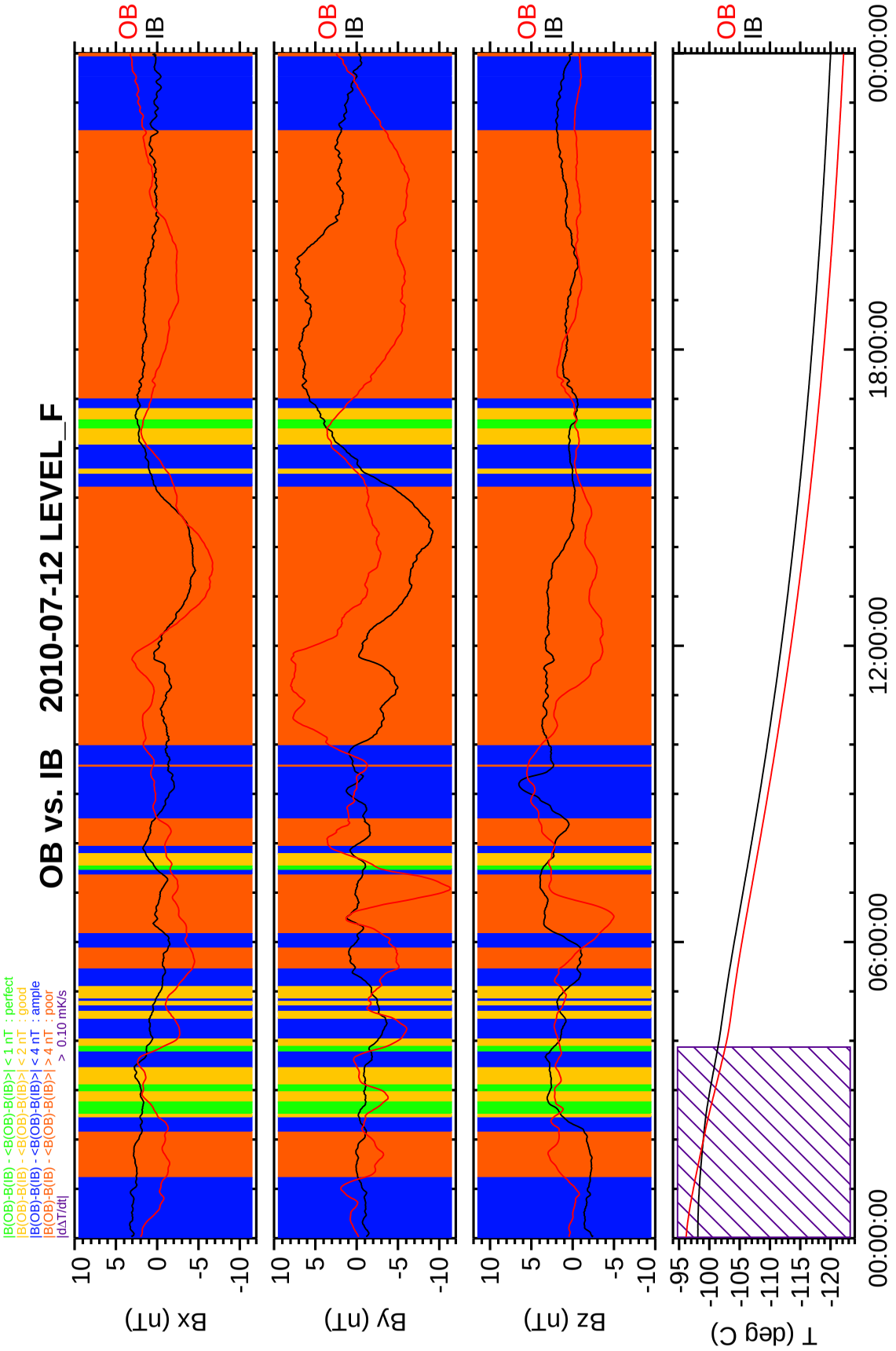
OB vs. IB 2010-07-12 LEVEL_F
|B(OB)-B(IB) - <B(OB)-B(IB)>| < 1 nT : perfect
|B(OB)-B(IB) - <B(OB)-B(IB)>| < 2 nT : good
|B(OB)-B(IB) - <B(OB)-B(IB)>| < 4 nT : ample
|B(OB)-B(IB) - <B(OB)-B(IB)>| > 4 nT : poor
|dΔT/dt| > 0.10 mK/s
OB
IB
Bx (nT)
By (nT)
Bz (nT)
T (deg C)
10
5
0
-5
-10
-95
-100
-105
-110
-115
-120
00:00:00
06:00:00
12:00:00
18:00:00
00:00:00

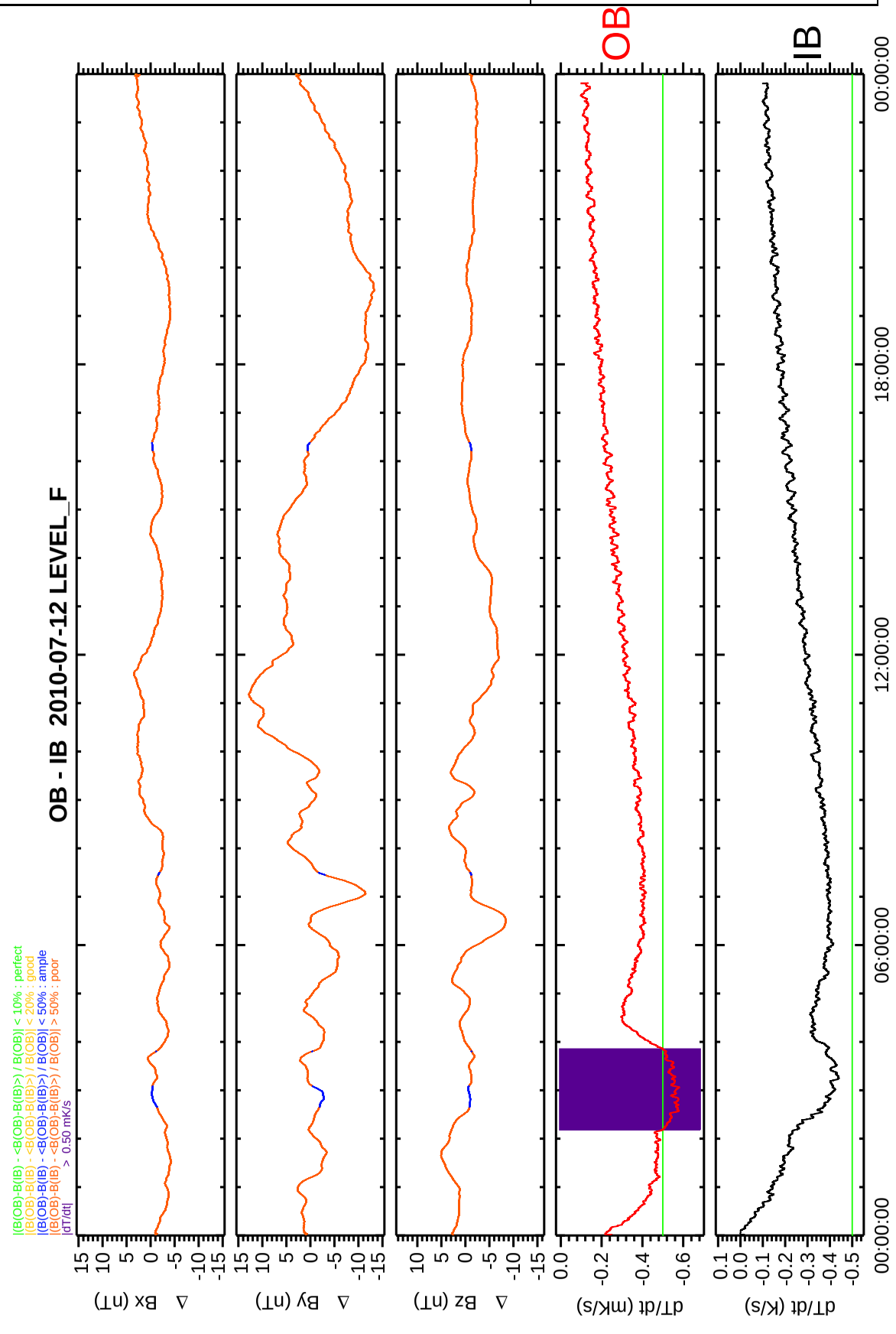
OB - IB 2010-07-12 LEVEL_F
|(B(OB)-B(IB) - <B(OB)-B(IB)>) / B(OB)| < 10% : perfect
|(B(OB)-B(IB) - <B(OB)-B(IB)>) / B(OB)| < 20% : good
|(B(OB)-B(IB) - <B(OB)-B(IB)>) / B(OB)| < 50% : ample
|(B(OB)-B(IB) - <B(OB)-B(IB)>) / B(OB)| > 50% : poor
|dT/dt| > 0.50 mK/s
Δ Bx (nT)
Δ By (nT)
Δ Bz (nT)
dT/dt (mK/s)
dT/dt (K/s)
OB
IB
00:00:00
06:00:00
12:00:00
18:00:00
00:00:00

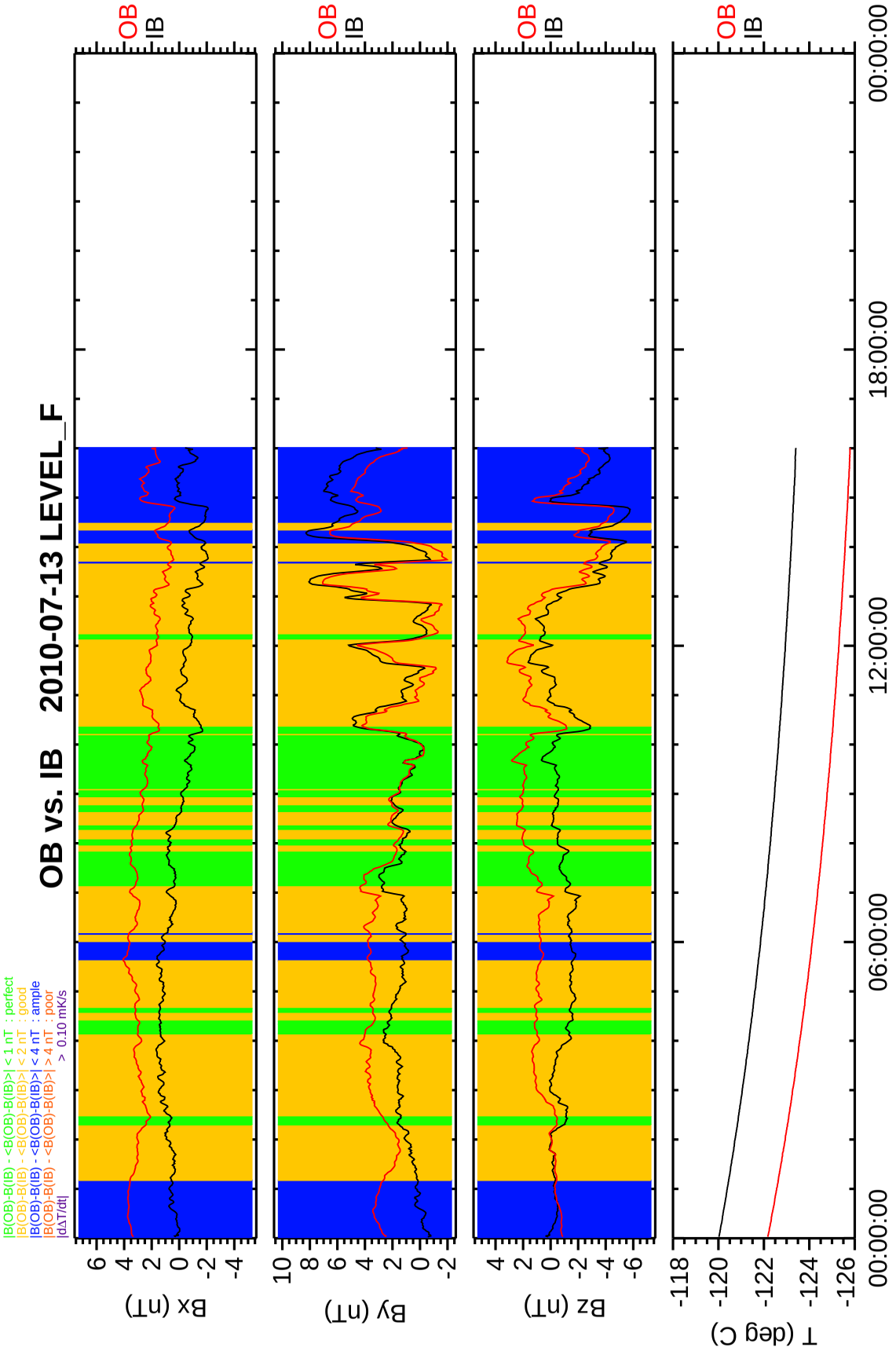
OB vs. IB 2010-07-13 LEVEL_F
|B(OB)-B(IB) - <B(OB)-B(IB)>| < 1 nT : perfect
|B(OB)-B(IB) - <B(OB)-B(IB)>| < 2 nT : good
|B(OB)-B(IB) - <B(OB)-B(IB)>| < 4 nT : ample
|B(OB)-B(IB) - <B(OB)-B(IB)>| > 4 nT : poor
|dΔT/dt| > 0.10 mK/s
OB
IB
Bx (nT)
By (nT)
Bz (nT)
T (deg C)
00:00:00
06:00:00
12:00:00
18:00:00
00:00:00

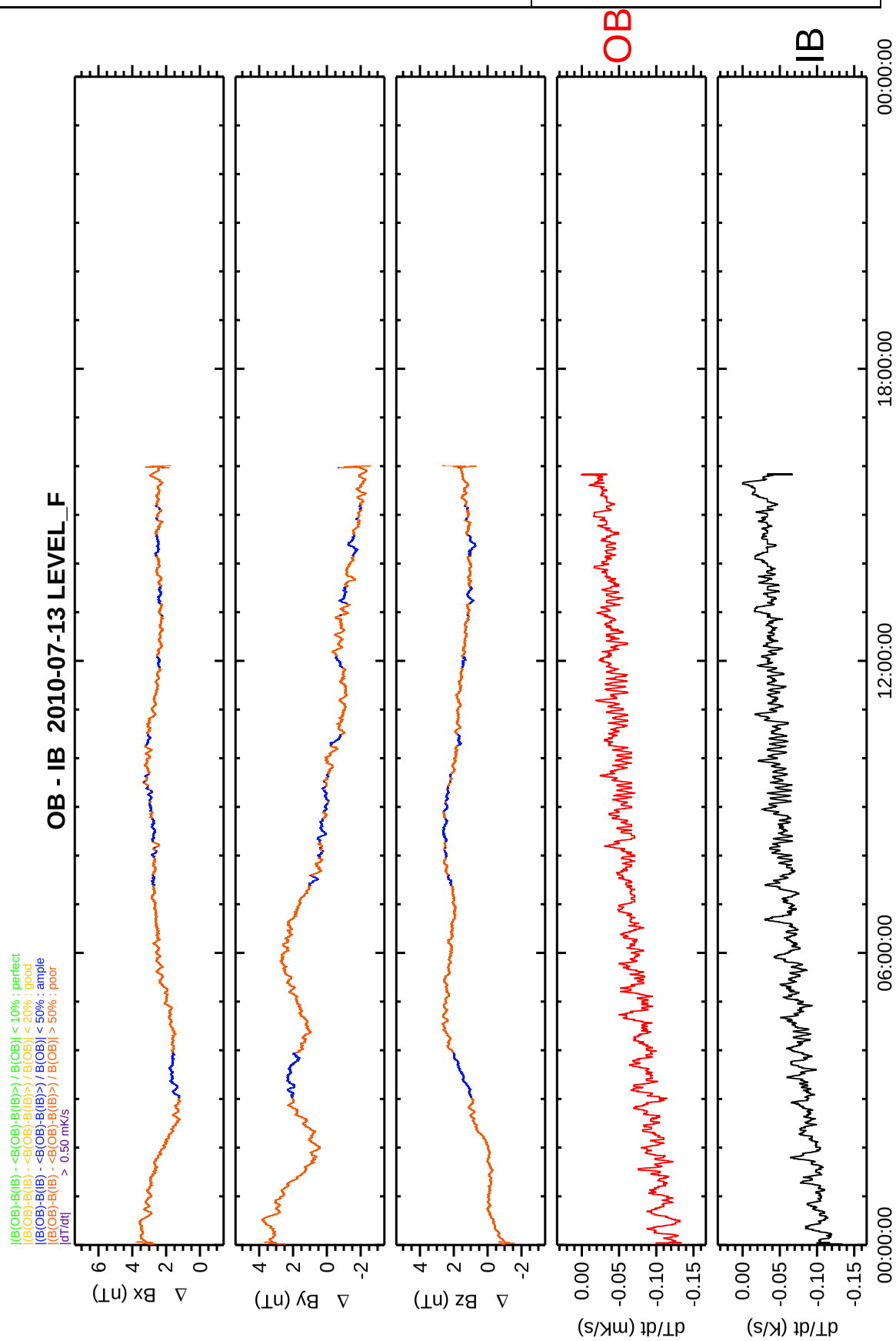
OB - IB 2010-07-13 LEVEL_F
OB
IB
Δ Bx (nT)
Δ By (nT)
Δ Bz (nT)
dT/dt (mK/s)
dT/dt (K/s)
00:00:00
06:00:00
12:00:00
18:00:00
00:00:00
|(B(OB)-B(IB) - <B(OB)-B(IB)>) / B(OB)| < 10% : perfect
|(B(OB)-B(IB) - <B(OB)-B(IB)>) / B(OB)| < 20% : good
|(B(OB)-B(IB) - <B(OB)-B(IB)>) / B(OB)| < 50% : ample
|(B(OB)-B(IB) - <B(OB)-B(IB)>) / B(OB)| > 50% : poor
|dT/dt| > 0.50 mK/s

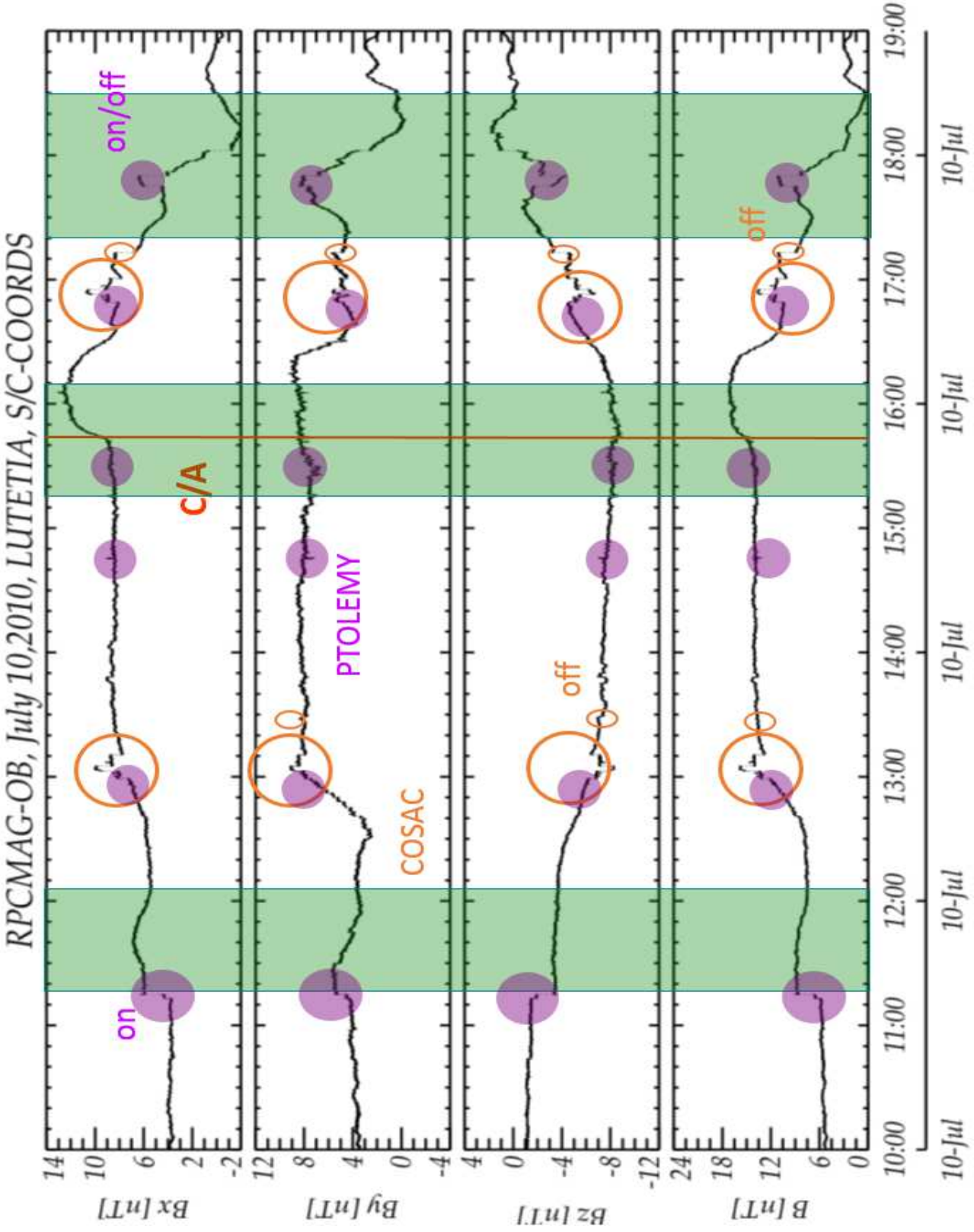

Figure 44: The COSAC and PTOLEMY disturbances as seen by RPC-MAG-OB

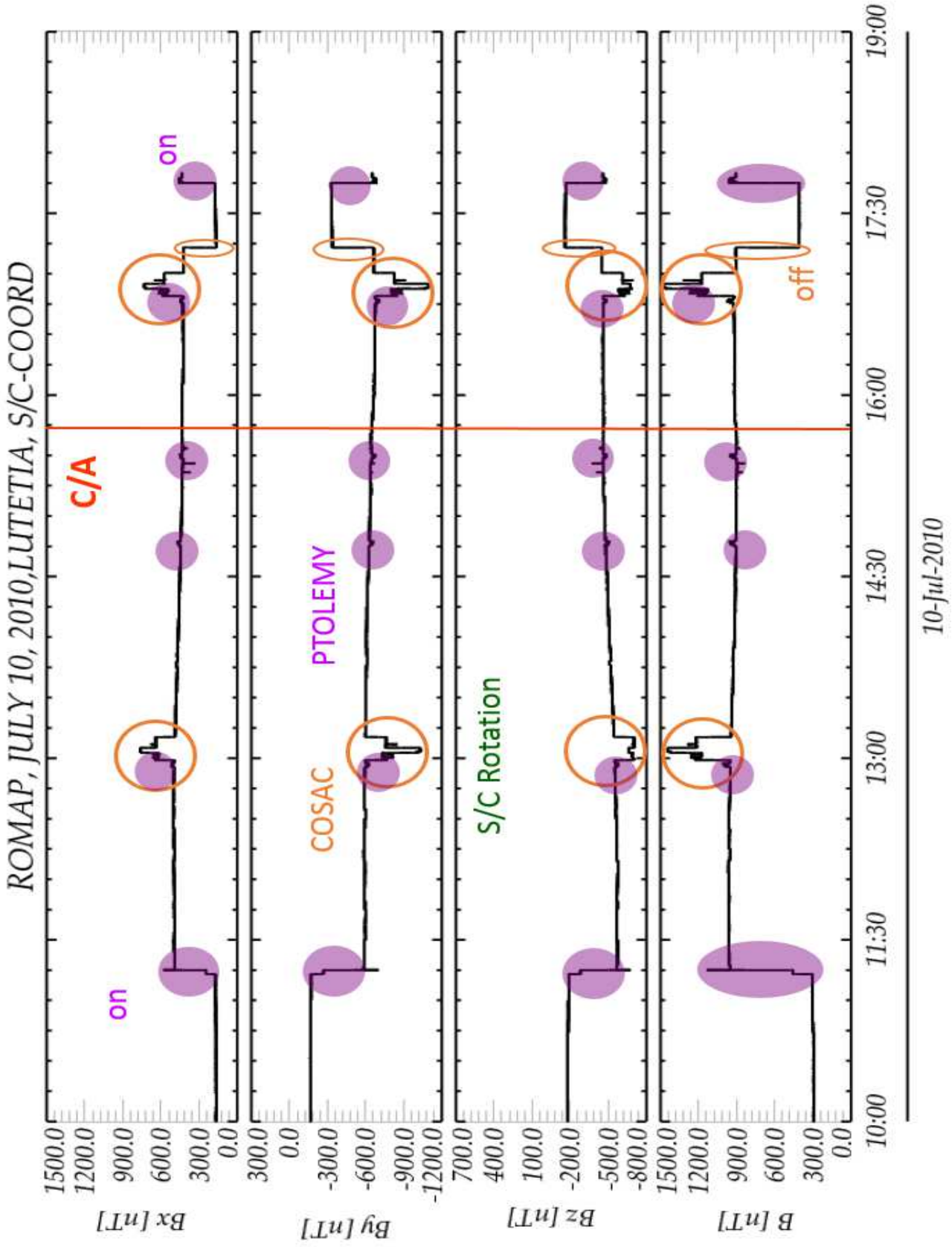

Figure 45: The COSAC and PTOLEMY disturbances as seen by ROMAP

5 Dynamic Spectra of the Fly-By

This section shows the dynamic spectra of the OB sensor in LEVEL_C = ECLIPJ2000 coordinates. As the sensor was operated as primary sensor in NORMAL mode, SID2, for most of the time the maximum resolvable frequency is 0.5 Hz. Around the closest approach time (2010-07-10T15:44) RPCMAG was set to Burstmode (20 Hz sampling rate) starting at 2010-07-10T12:55 8 and ending at 2010-07-10T18:54

All the tilted lines in the spectra are caused by the Reaction wheels as usual. The 3.2 Hz lines are caused by the LAP instrument.

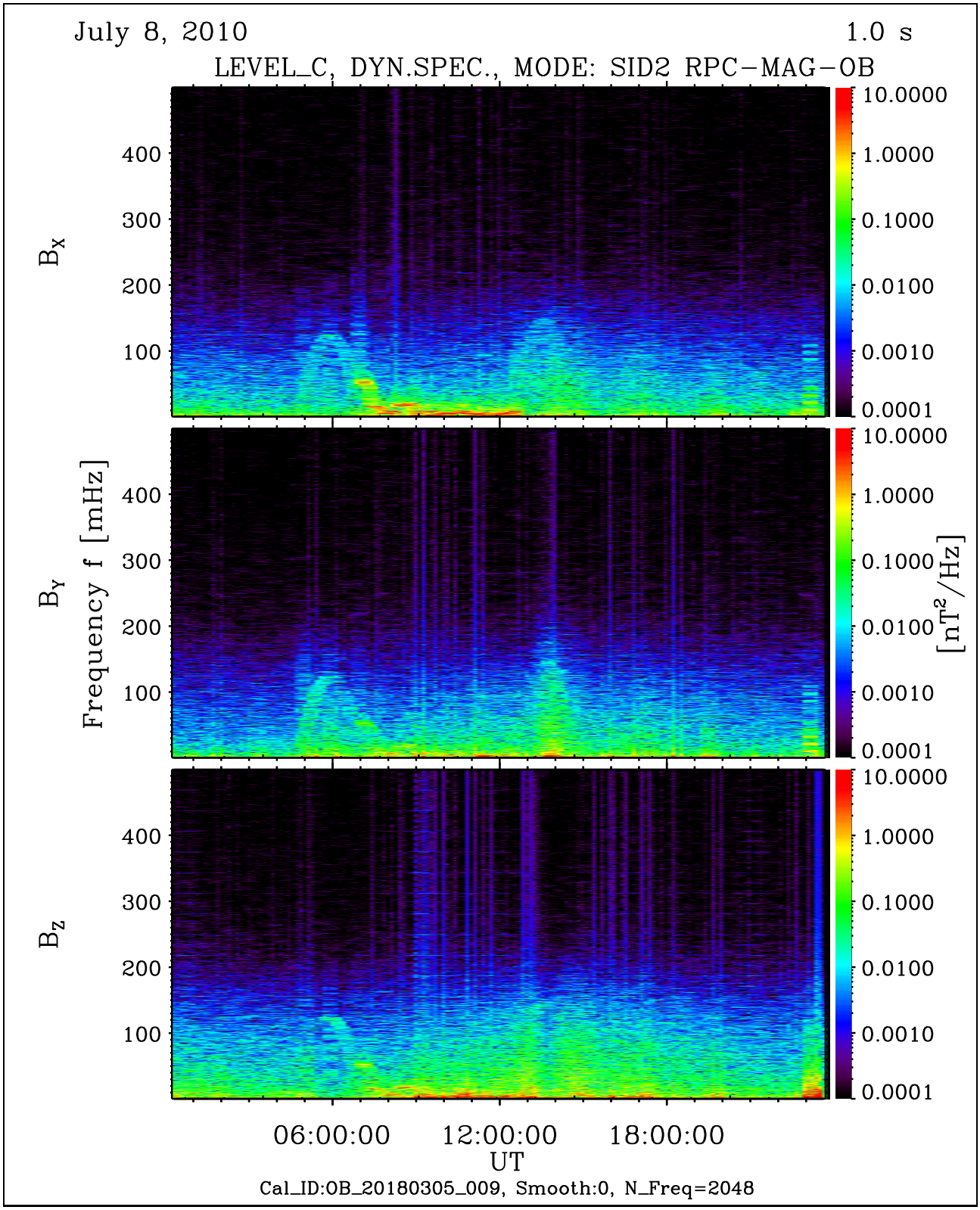

Figure 46: File: RPCMAG100708T0000_CLC_OB_M2_DS0_500_009

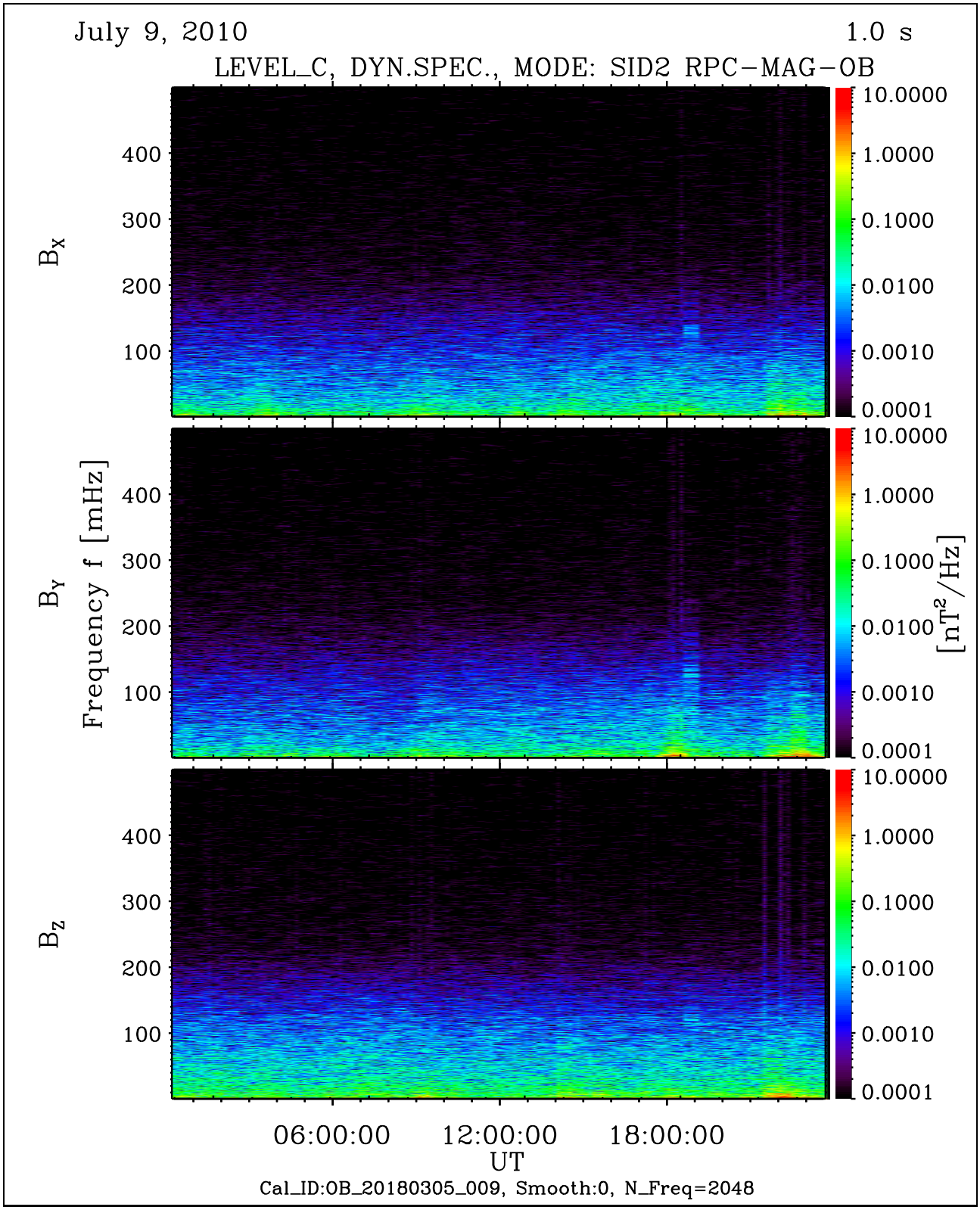

Figure 47: File: RPCMAG100709T0000_CLC_OB_M2_DS0_500_009

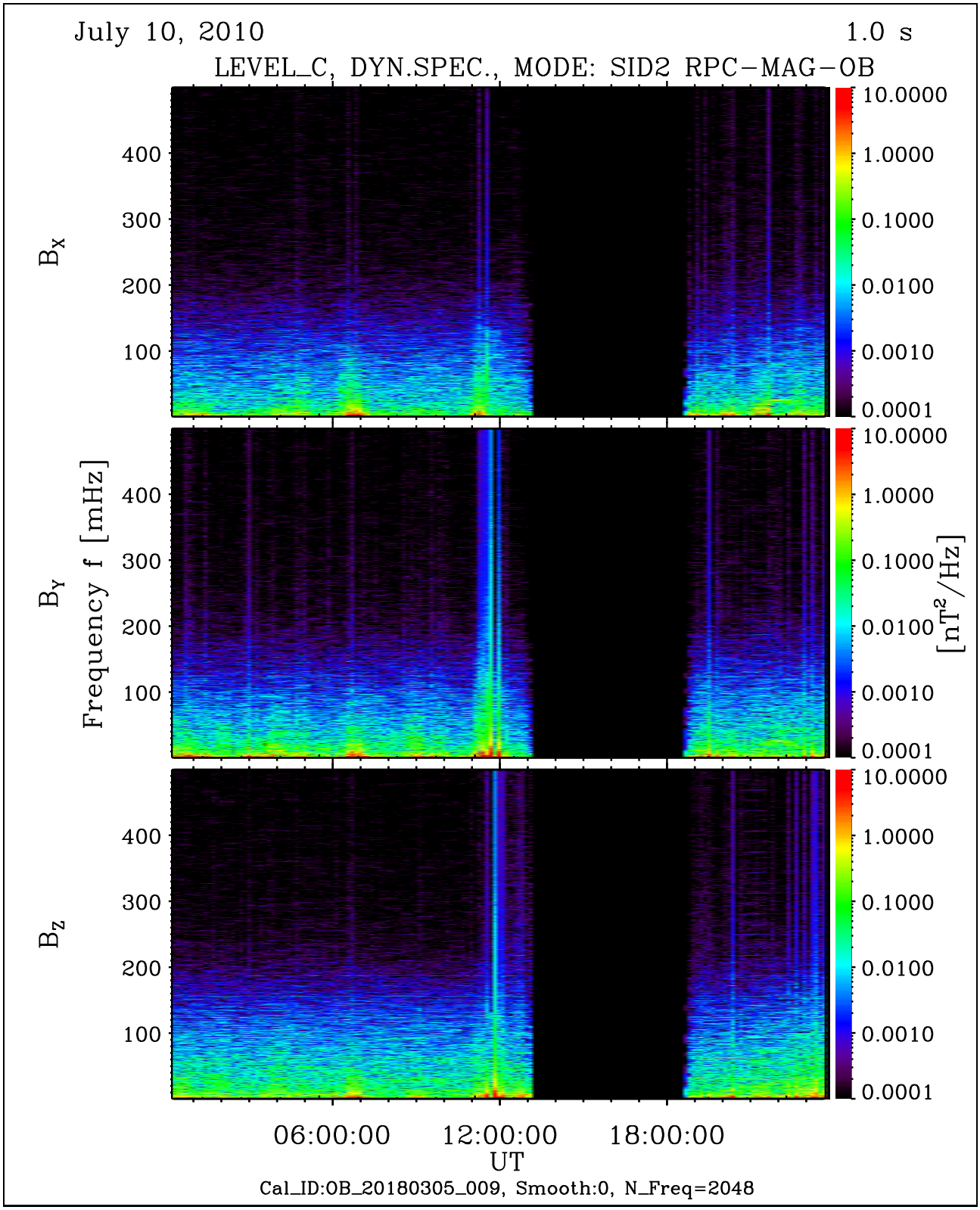

Figure 48: File: RPCMAG100710T0000_CLC_OB_M2_DS0_500_009

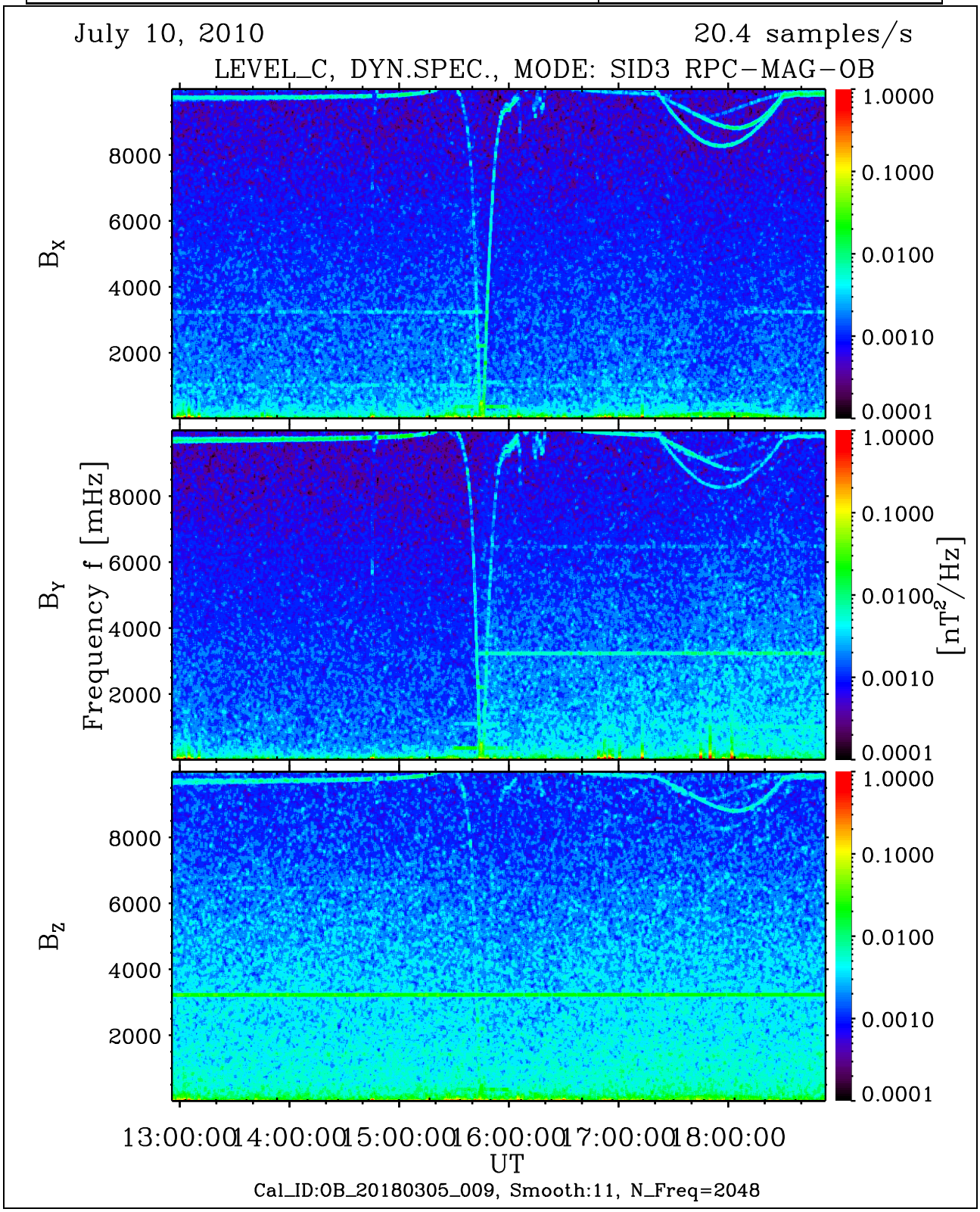

Figure 49: File: RPCMAG100710T1255_CLC_OB_M3_DS0_10000_009

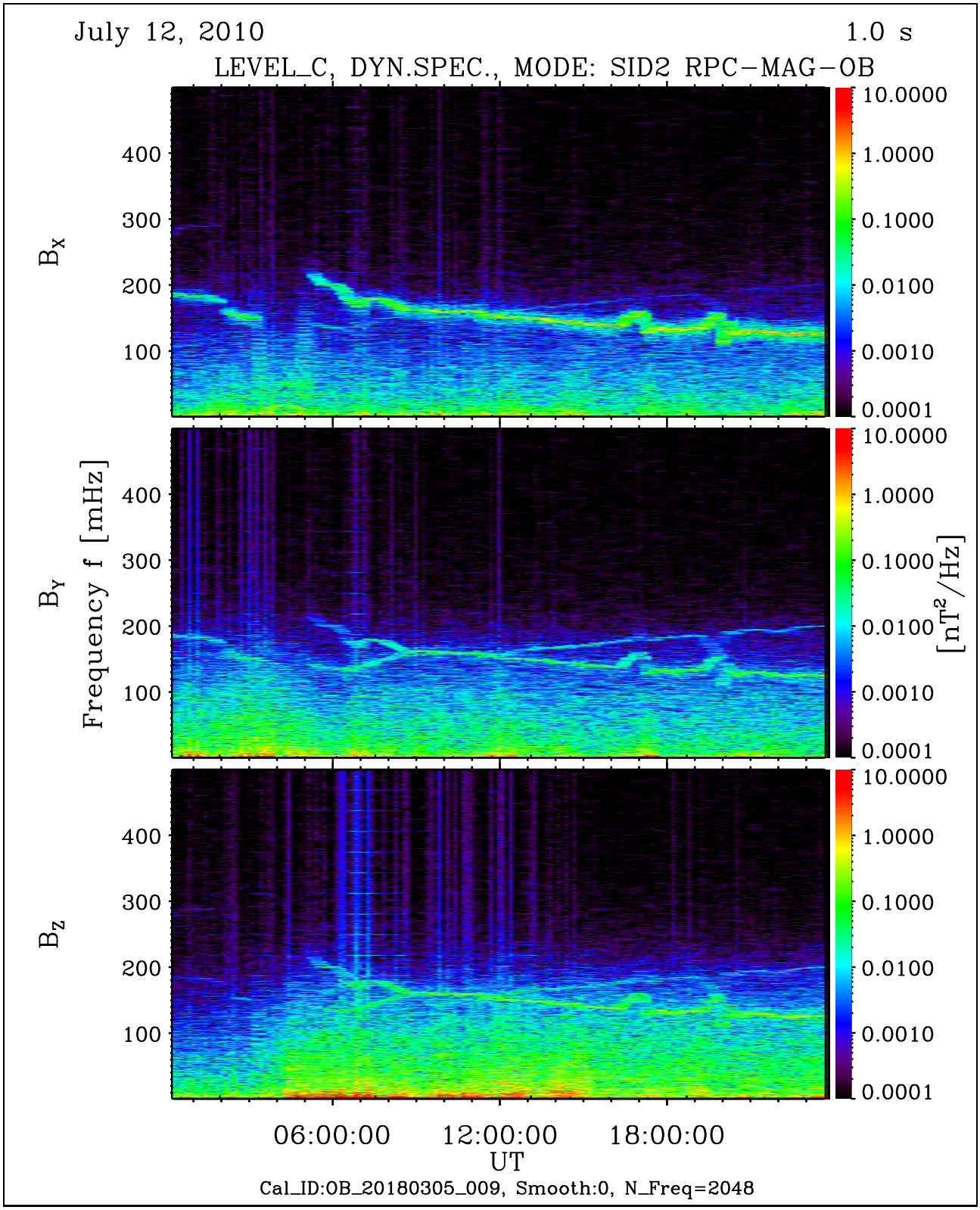

Figure 50: File: RPCMAG100712T0000_CLC_OB_M2_DS0_500_009

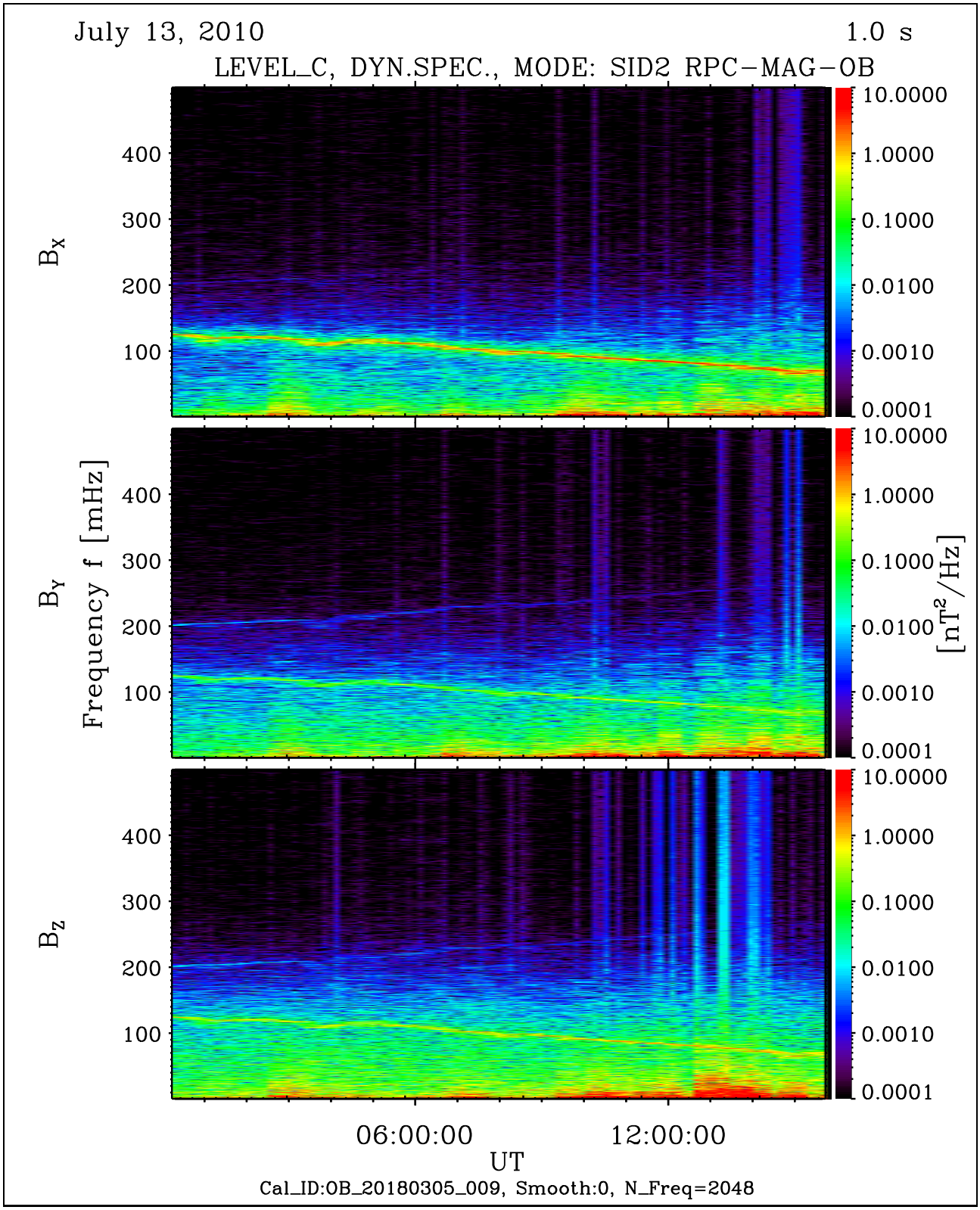

Figure 51: File: RPCMAG100713T0000_CLC_OB_M2_DS0_500_009

6 Dynamic Spectra of ROSETTAs REACTION WHEELS

This section shows the spectra of ROSETTAs Reaction Wheels (RW). There are 4 different wheels rotating with different frequencies. The plots do not show the original rotation frequencies but the signatures that would be expected using an data acquisition system operating at 1 Hz sampling frequency (or 20 Hz in Burst mode) without any aliasing filter. These signatures are expected to be seen on the OB sensor operated in NORMAL mode (sometimes) and always in BURST mode.

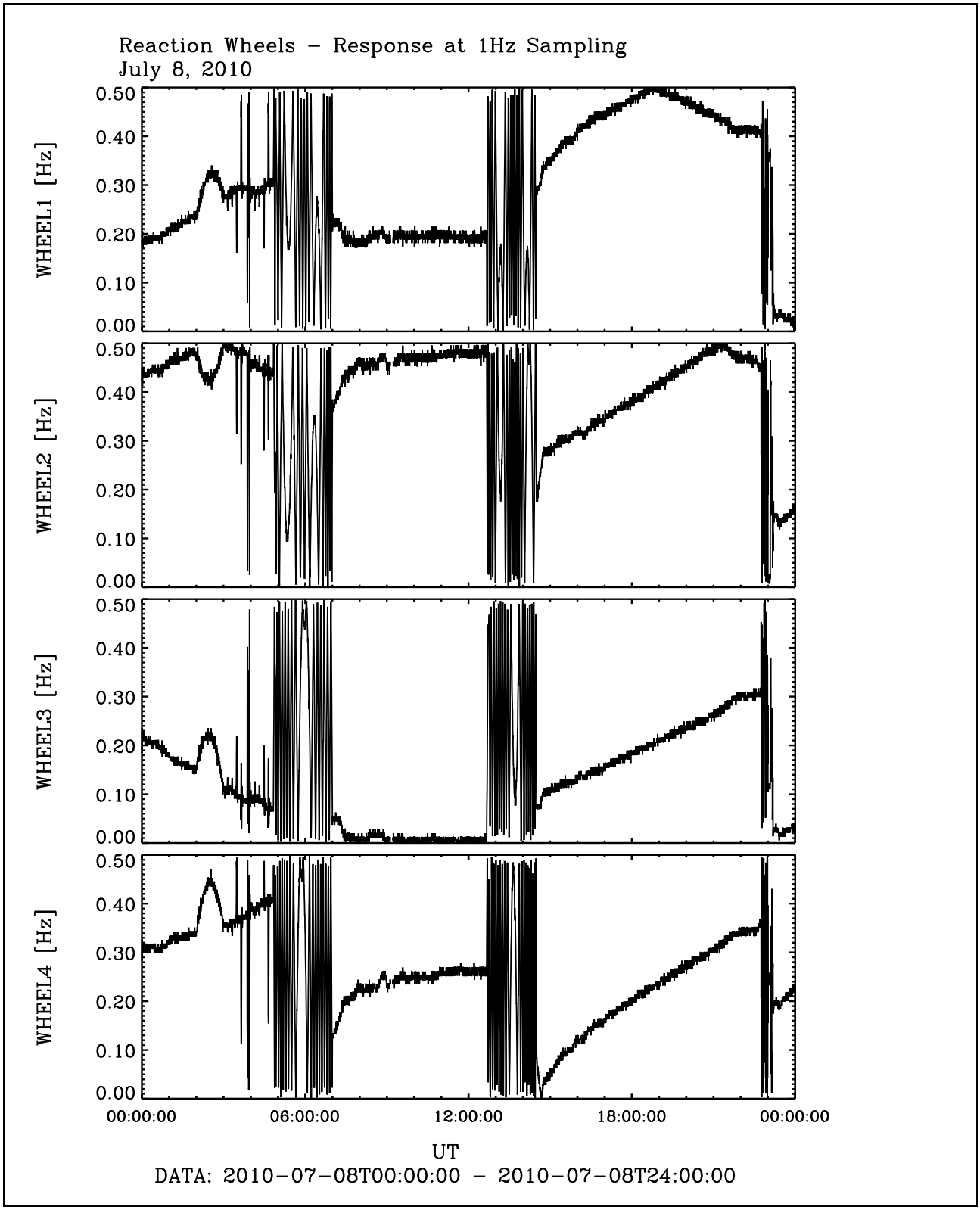

Figure 52: File: wheels_1Hz_Sampling2010-07-08T00-00

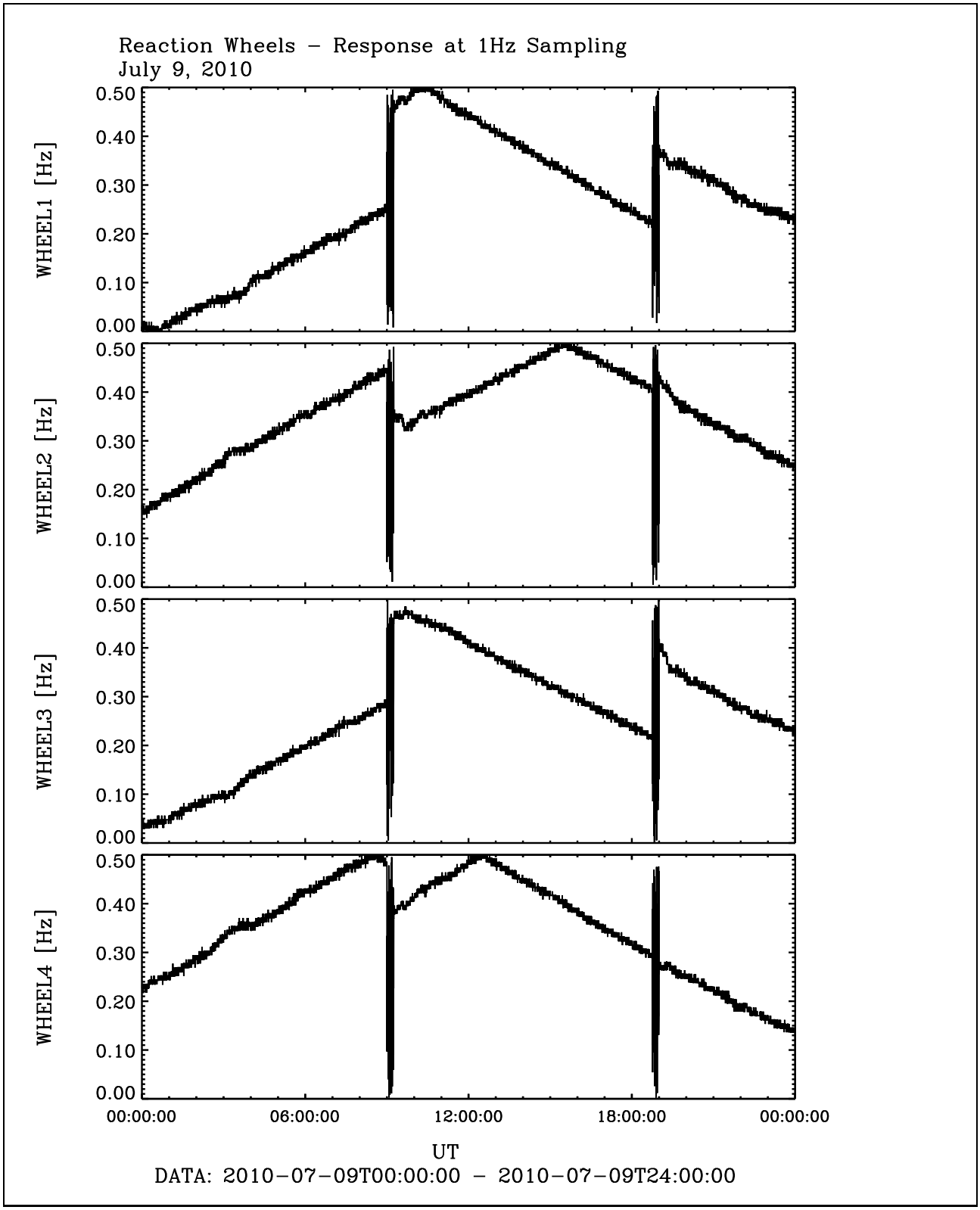

Figure 53: File: wheels_1Hz_Sampling2010-07-09T00-00

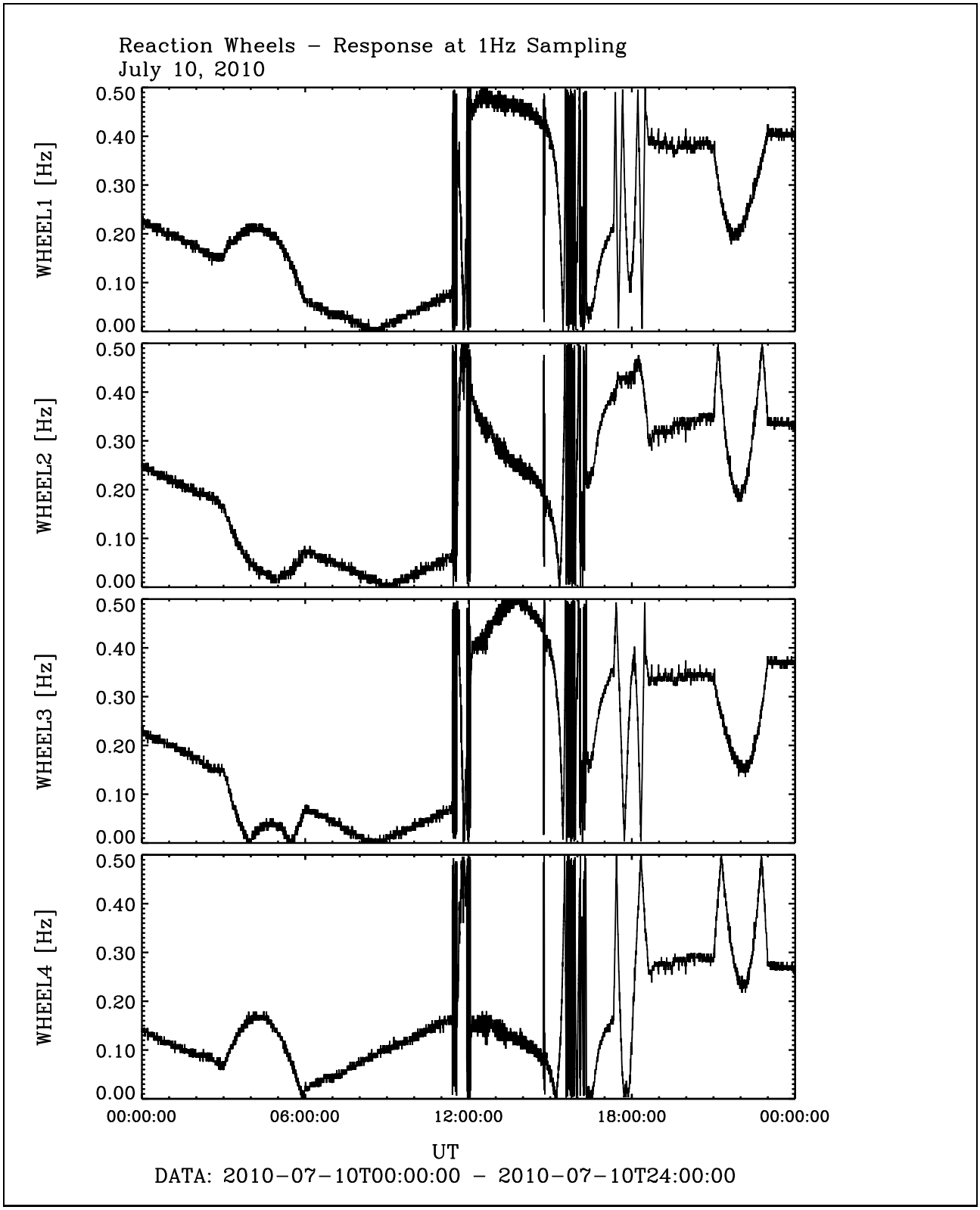

Figure 54: File: wheels_1Hz_Sampling2010-07-10T00-00

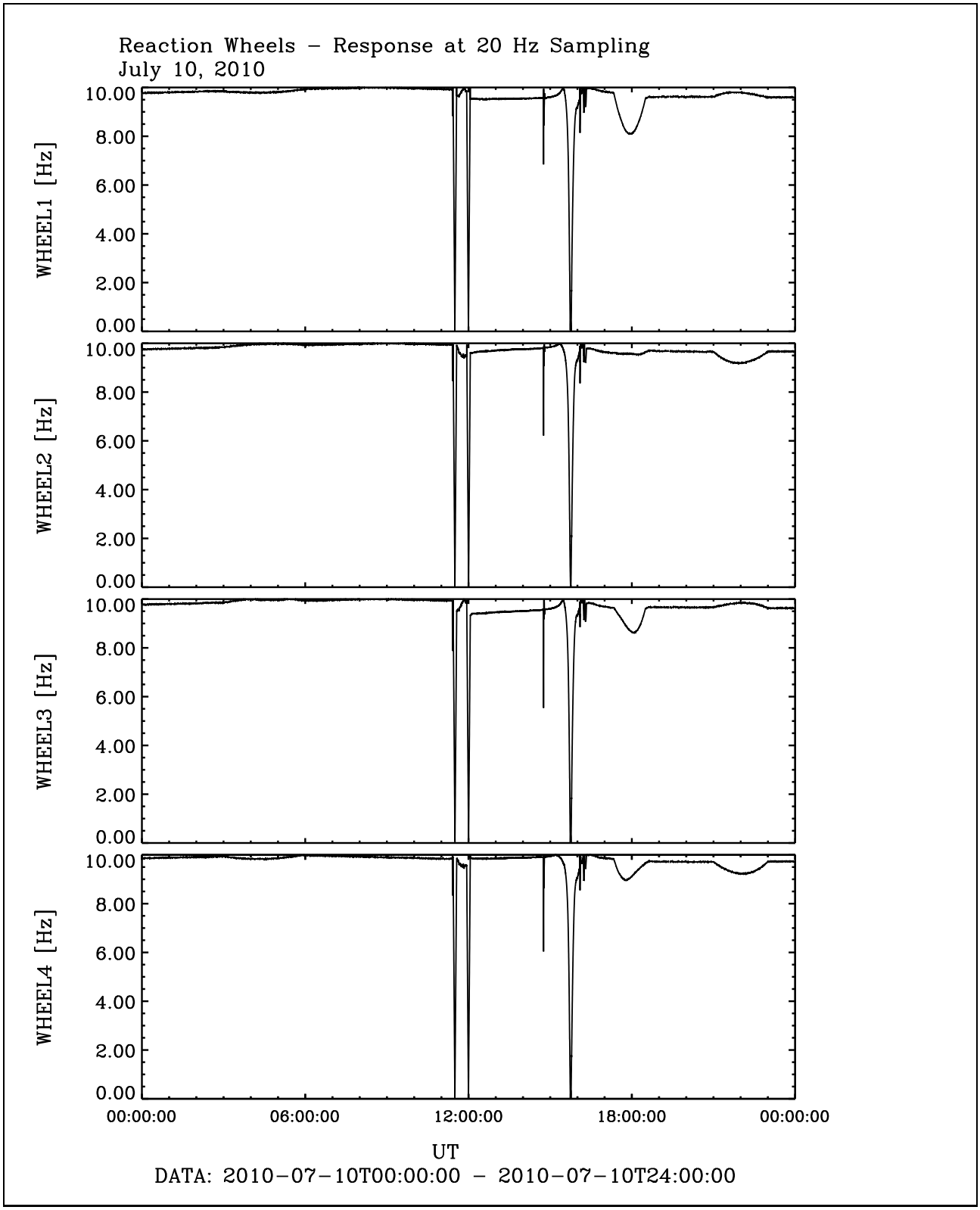

Figure 55: File: wheels_20Hz_Sampling2010-07-10T00-00

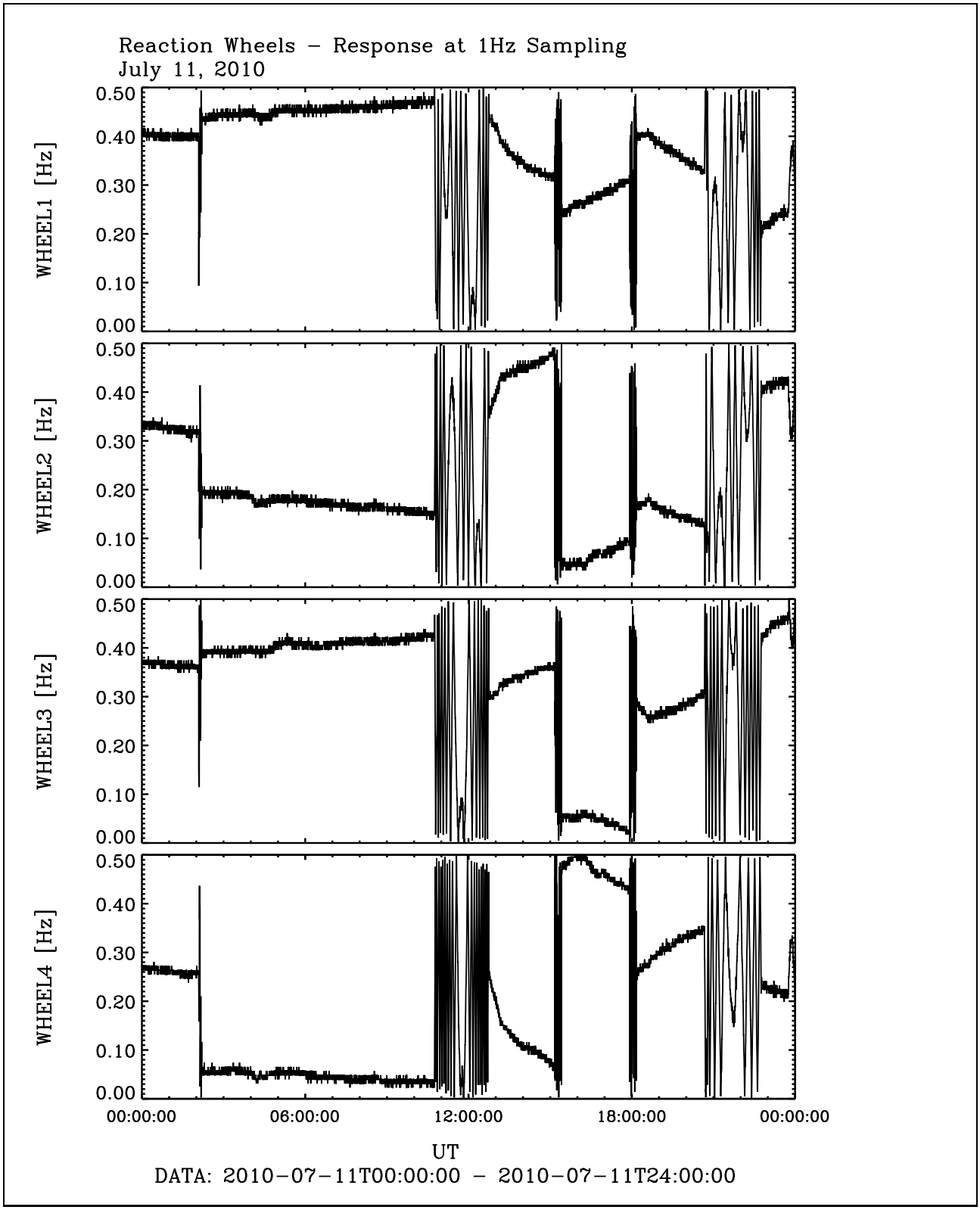

Figure 56: File: wheels_1Hz_Sampling2010-07-11T00-00

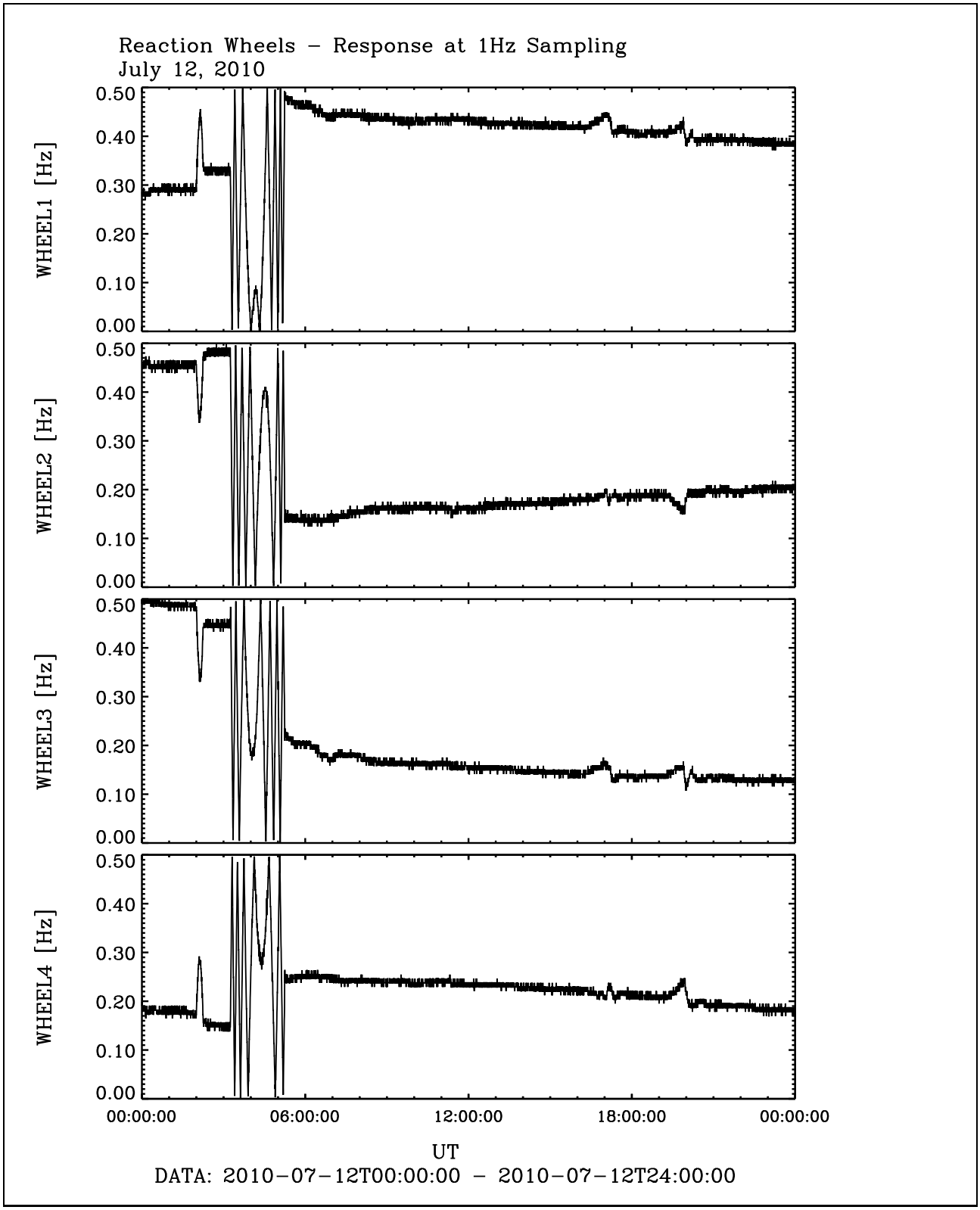

Figure 57: File: wheels_1Hz_Sampling2010-07-12T00-00

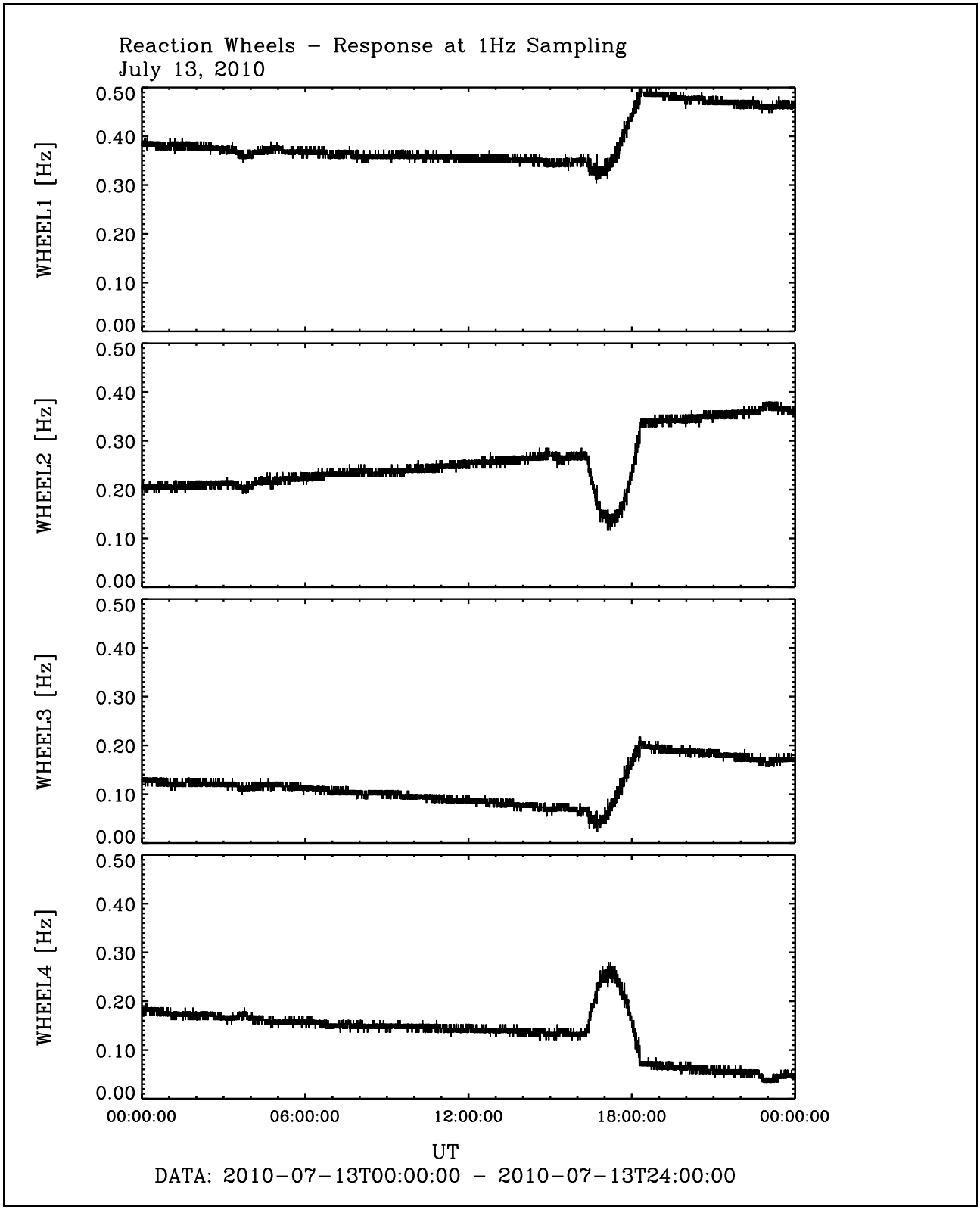

Figure 58: File: wheels_1Hz_Sampling2010-07-13T00-00

6.1 Reaction Wheel and LAP Disturbance corrected Data

The following plot shows the dynamic spectrum of the LEVEL_H data for July 10 - the only day where the instrument was put into burstmode and where therefore a reaction wheel impact elimination algorithm could be applied. These data have been purged from ROSETTAs reaction wheel disturbance and also from the disturbance of the LAP instrument. The Plot is only shown for the primary sensor.

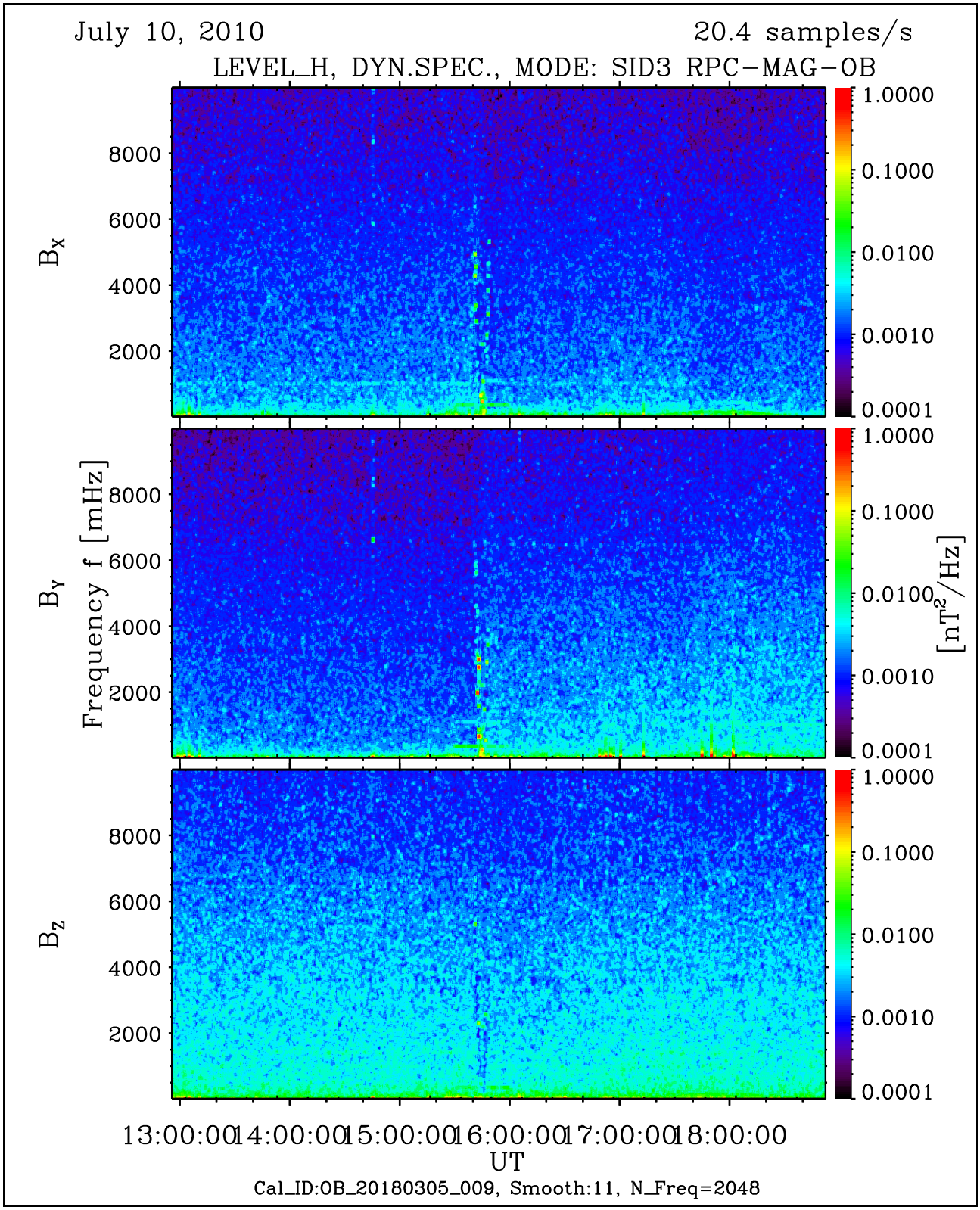

Figure 59: File: RPCMAG100710T1255_CLH_OB_M3_DS0_10000_009

7 Solar Array Rotation Angles and High Gain Antenna Orientation

To get an idea, whether the rotation of the Solar arrays or the movement of the High Gain Antenna (HGA) has an influence of the magnetic field data, the following plots have been generated. Each figure shows

- in the upper panel
  the rotation angle of the solar arrays (angle between the solar array normal and the spacecraft $x_{\mathrm{S/C}}$ axis
- in the two lower panels
  the projected rotation angle in the spacecraft $xy_{\mathrm{S/C}}$-Plane and the projected rotation angle in the spacecraft $xz_{\mathrm{S/C}}$-Plane. Both angles are displayed wrt. the x-axis.

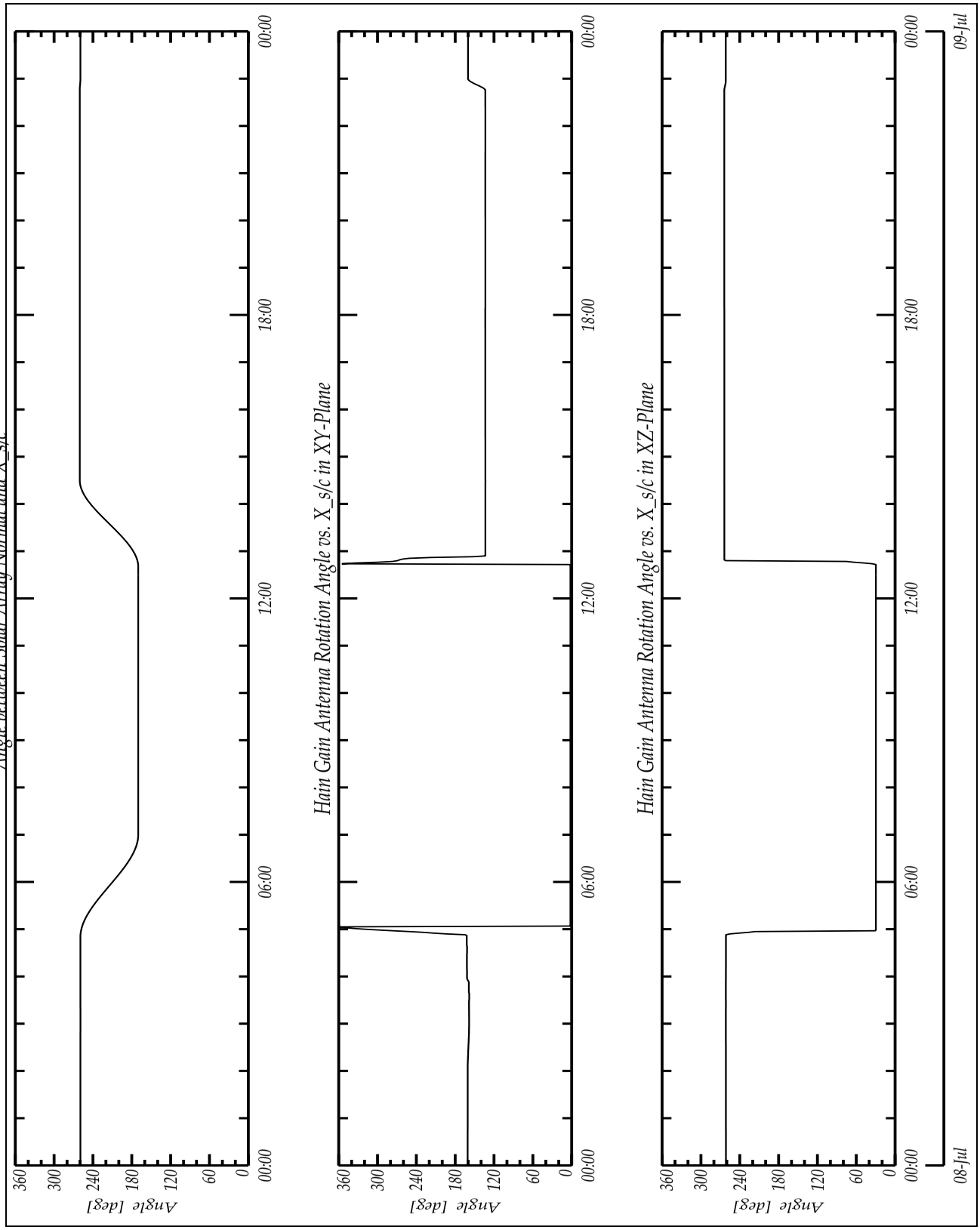

Figure 60: File: Solar Array and HGA Rotation Angles of 2010-07-08

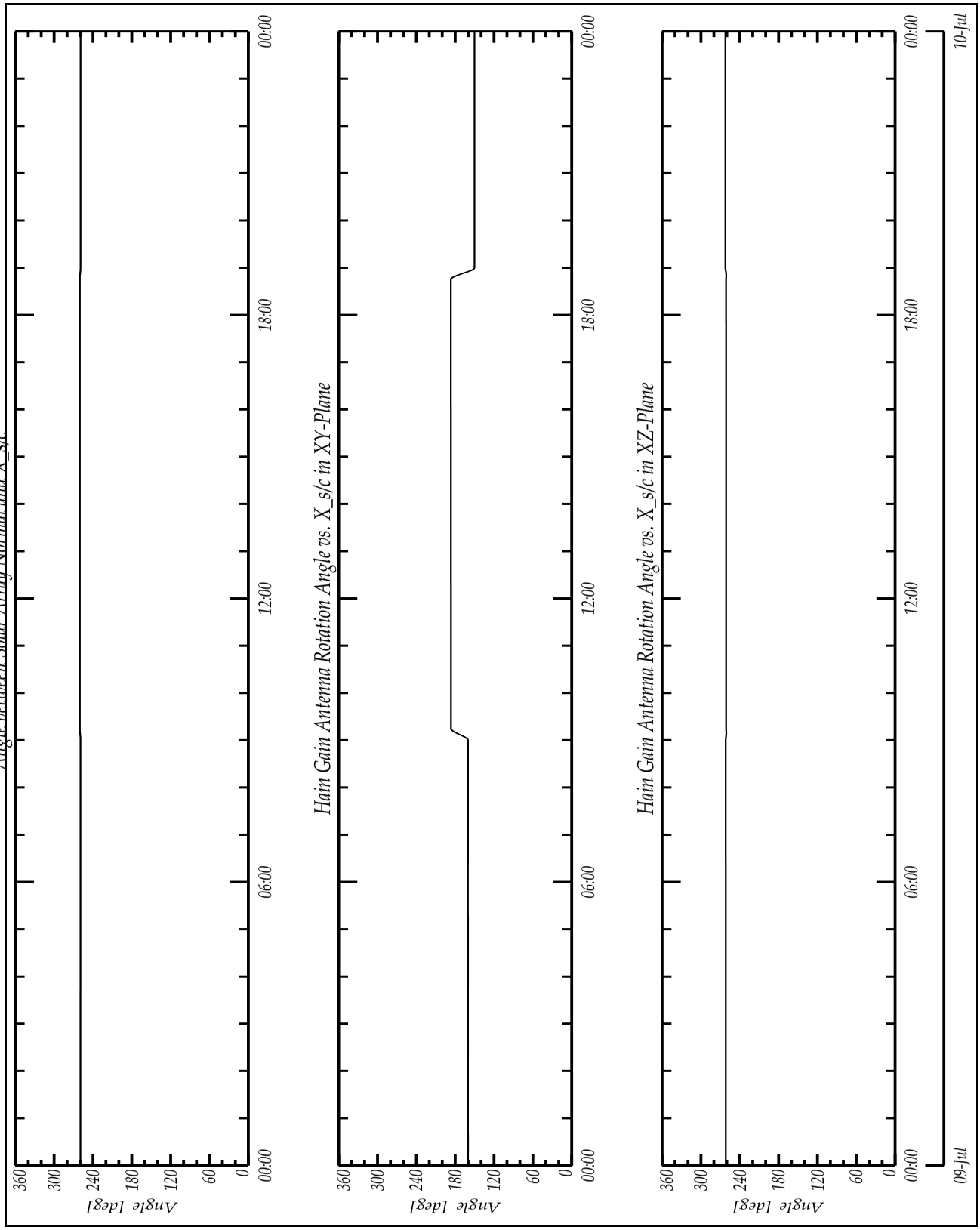

Figure 61: File: Solar Array and HGA Rotation Angles of 2010-07-09

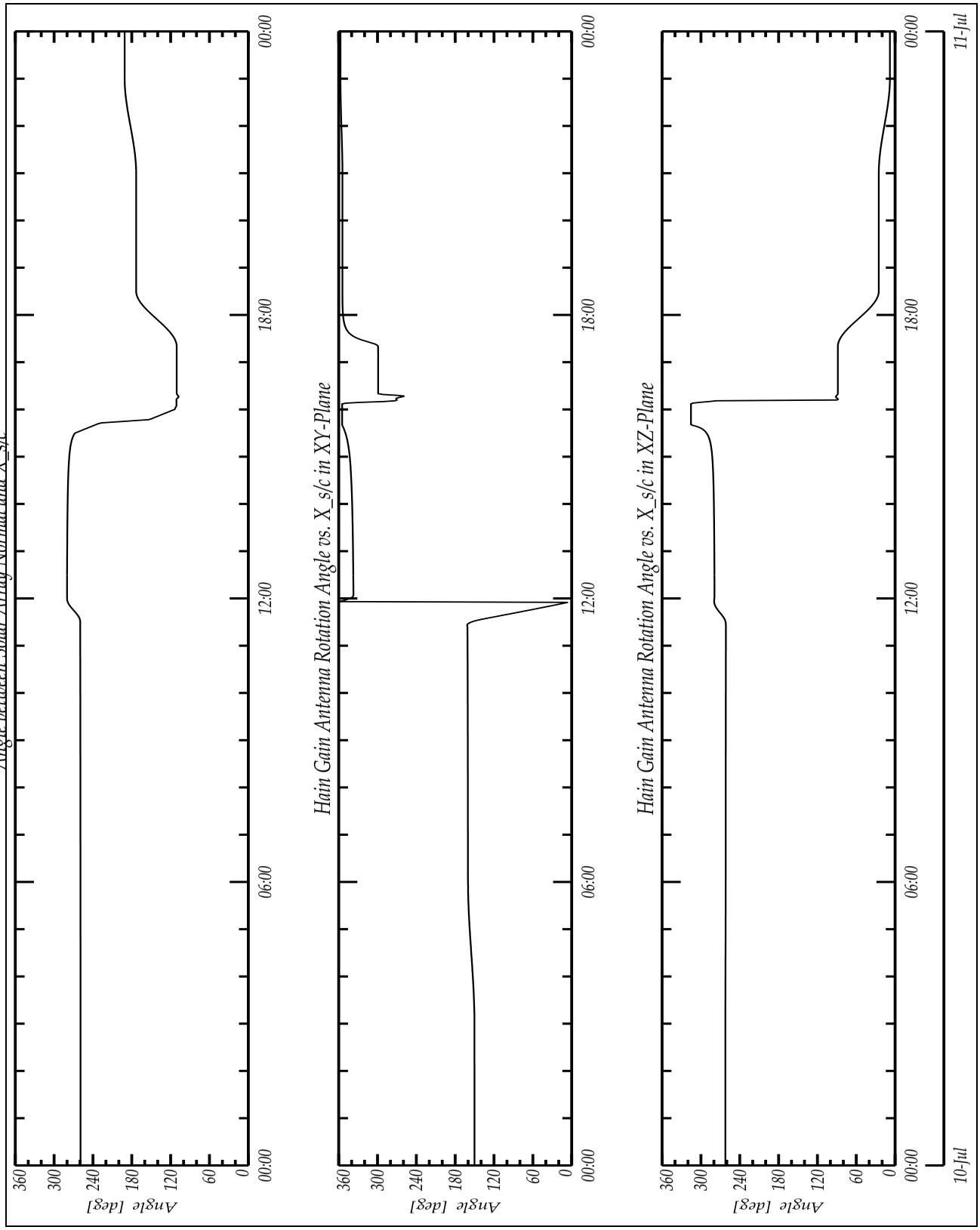

Figure 62: File: Solar Array and HGA Rotation Angles of 2010-07-10

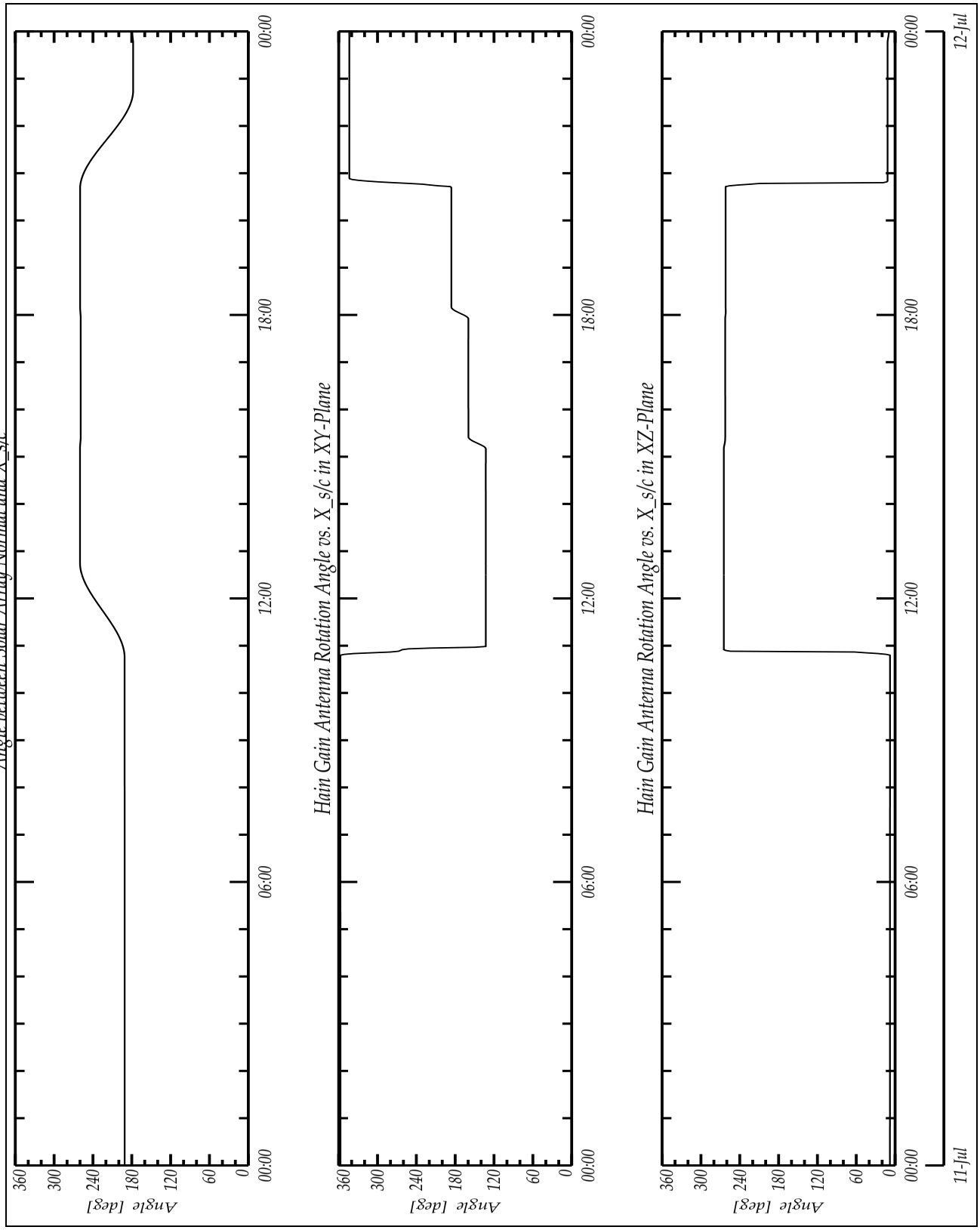

Figure 63: File: Solar Array and HGA Rotation Angles of 2010-07-11

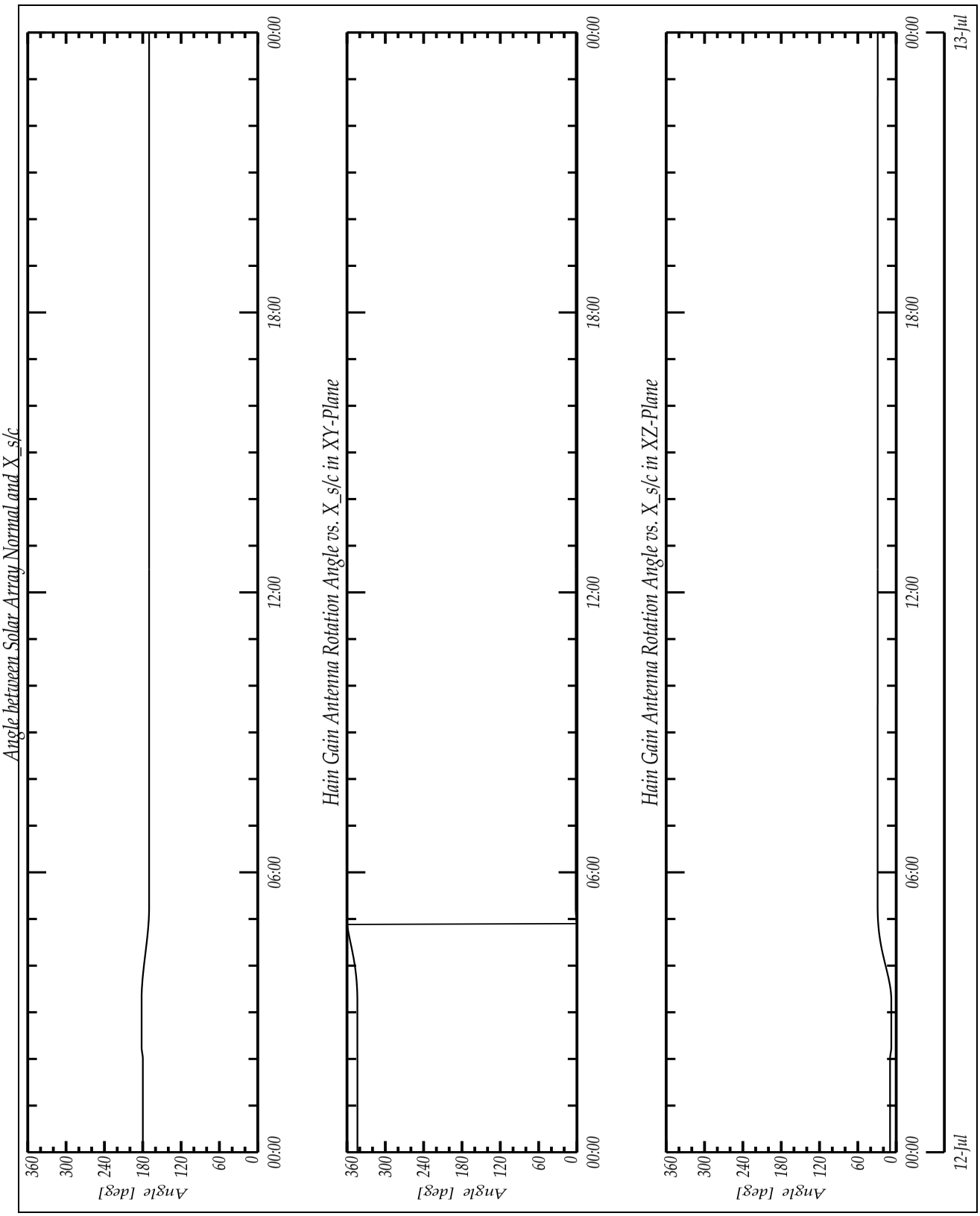

Figure 64: File: Solar Array and HGA Rotation Angles of 2010-07-12

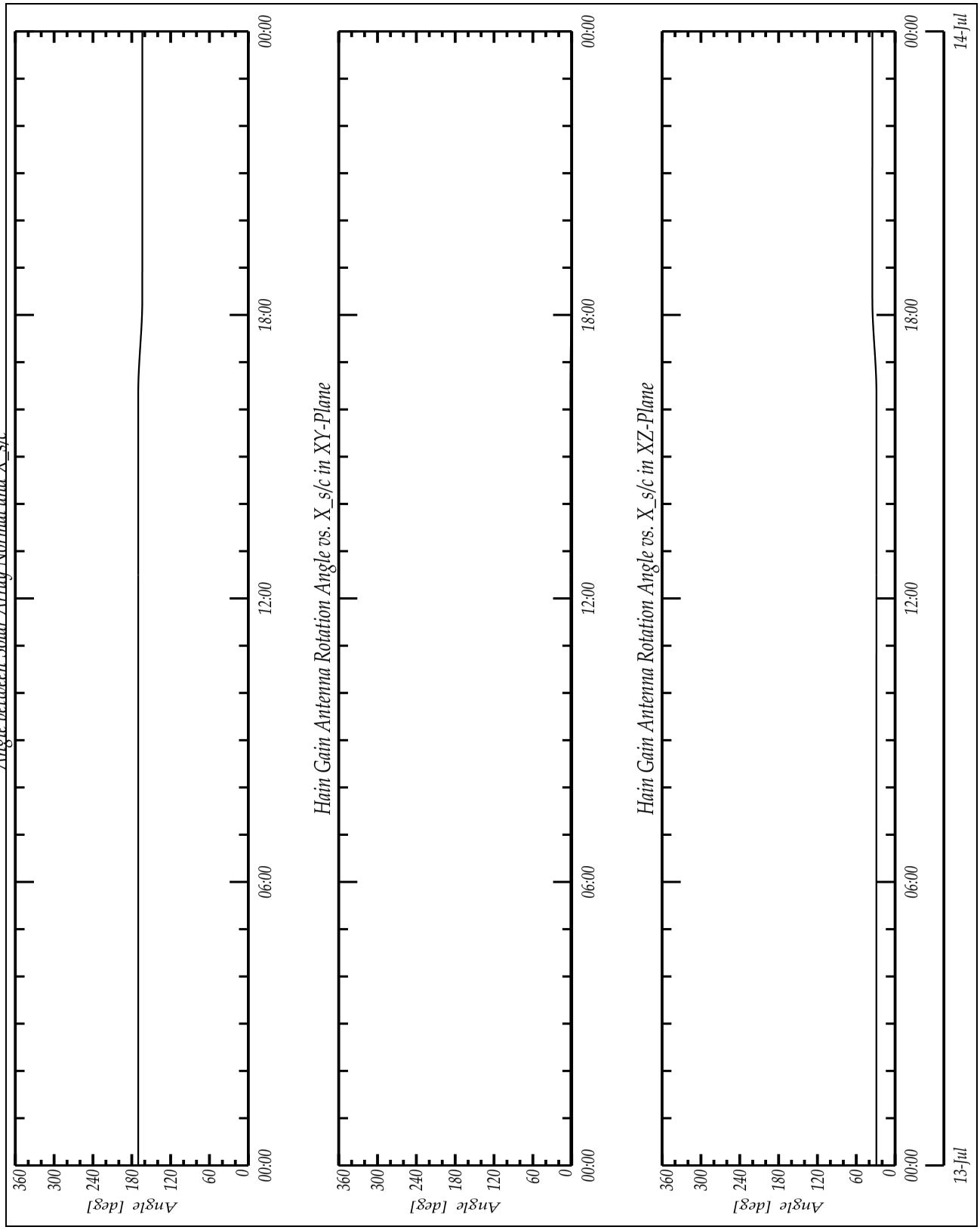

Figure 65: File: Solar Array and HGA Rotation Angles of 2010-07-13

8 Temperature profile during the FlyBy

The following figure shows the measured temperatures of the OB and IB sensor during the flyby. The lower panels of the graph show the angles between x–, y–, and z–axis of the s/c frame and the sun direction.

The analysis of these plots shows that - as expected - most of the temperature changes are related to attitude changes.

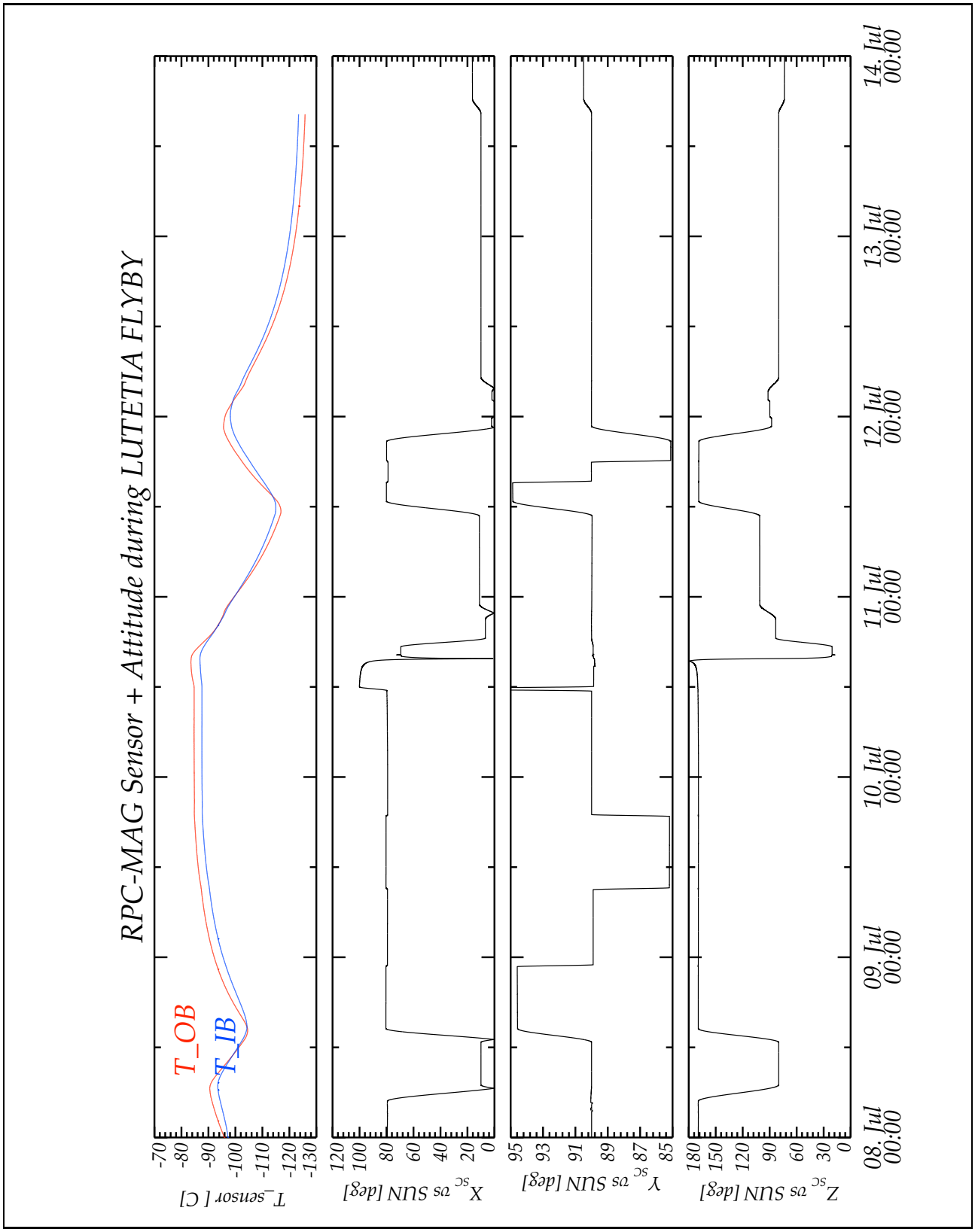

Figure 66: Measured Sensor Temperatures and attitudes during the complete FlyBy cam-

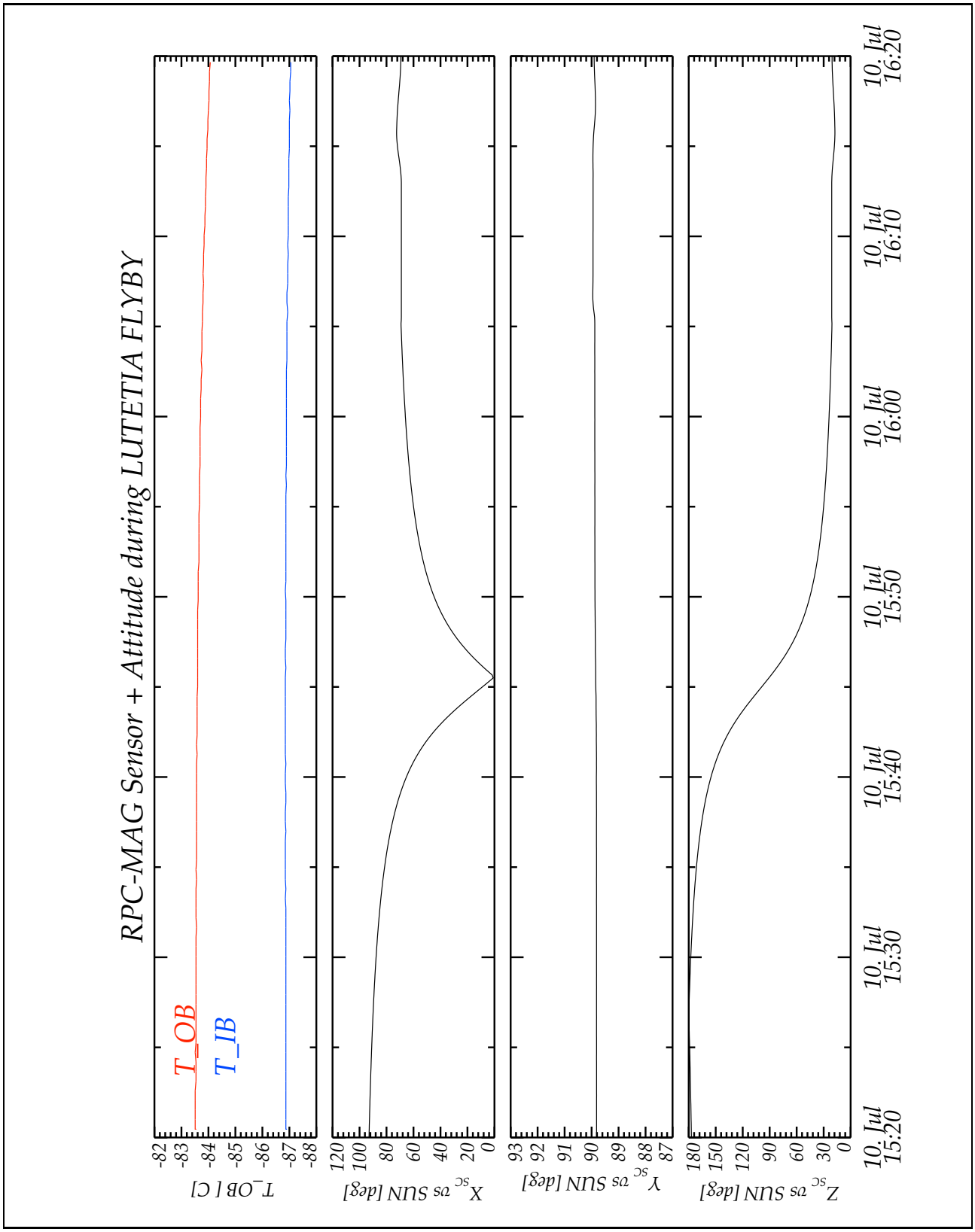

Figure 67: Measured Sensor Temperatures and attitudes during the very LUTETIA FlyBy

9 Comparison with WIND Data

As usual the question arises whether the observed data can be put into context with "reference" data. As such reference source the NASA satellite WIND can be used, which provides magnetic field data observed at the Lagrange point L1 of Earth and Sun. During the AST2 time interval, the distance between ROSETTA/LUTETIA and WIND was about 2.7 AU. That means that the solar wind, propagating from the position of WIND to ROSETTA needs at least 10.45 days, assuming an average solar wind speed of 450 km/s. It is questionable whether the Parker spiral geometry fits to the celestial situation of the Sun, WIND and ROSETTA and whether such a long propagation distance maintains the plasma structure observed at WIND. A short investigation is, however, at least a tempting task.

The result of that study can be seen in Figure 68. Here the upper panel displays the low pass filtered magnetic field magnitude of the RPCMAG OB sensor. The second panel depicts the IB data, and the bottom panels shows the magnetic field magnitude observed at WIND. It has to be mentioned, that the WIND data have been shifted by the anticipated propagating time of 10.45 days.

Although the s/c was very noisy during the whole AST2 interval - which can be seen in the slightly different field magnitudes measured by the OB and IB sensor - there is a striking coincidence between OB/IB and the WIND observation. A roughly 12 h wide structure in the center of the observations can clearly be identified on all sensors and seem to be of the same origin. Although the three observations are not identical they give strong evidence of having measured the same plasma structure.

This part of the analysis also bears whitness to the reasonable quality of the new calibration model 009.

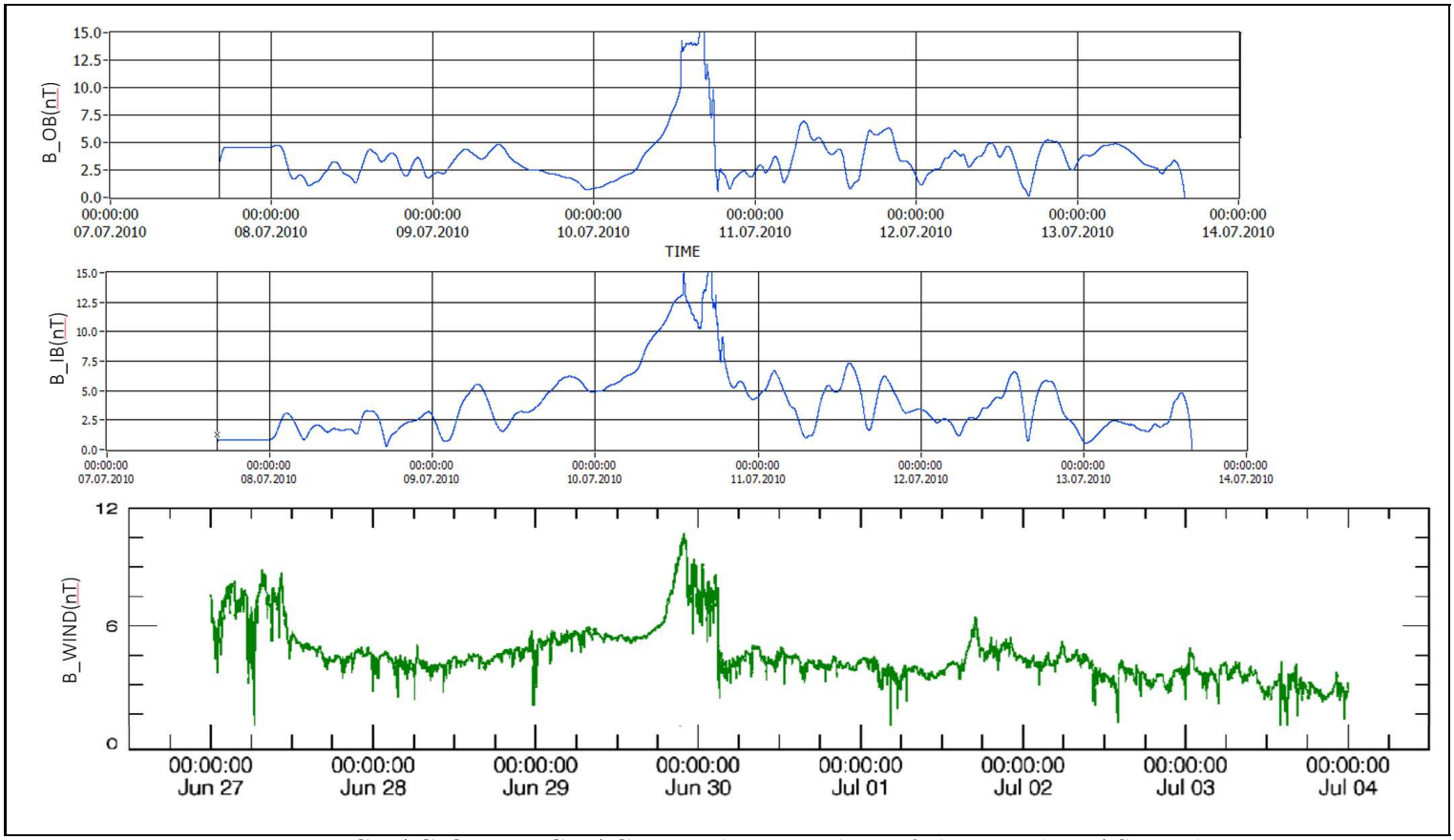

Figure 68: RPCMAG-OB, RPCMAG IB and WIND data of the complete AST2 Phase. WIND data have been shifted according to the anticipated solarwind propagation time of 10.45 days.

10 The very flyby

.

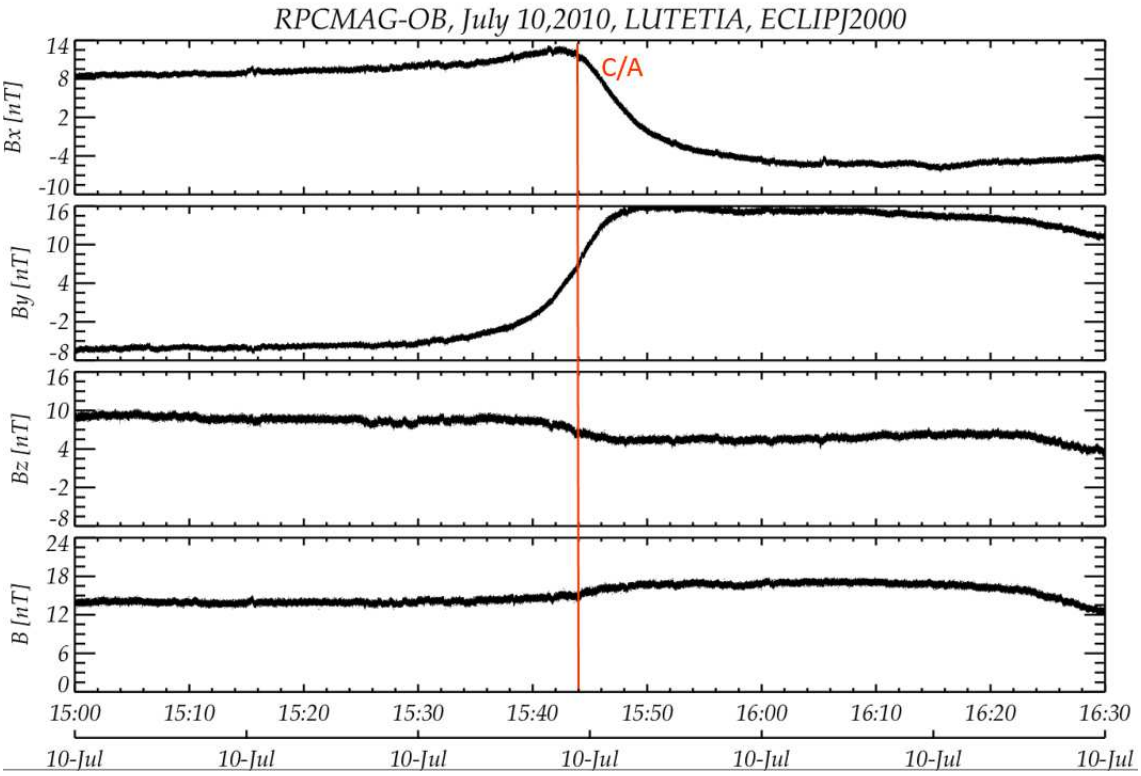

Figure 69: RPCMAG-OB data around C/A in ECLIPJ2000 coordinates.

Figure 69 shows the data of the RPCMAG-OB sensor in an interval of ± 45 minutes around closest approach. At the time of the very C/A the data do not show any interesting structure. The data are dominated by the rotation of the S/C according to Asteriod Flyby Mode (AFM). During the rotation the actual S/C disturbance field becomes visible, as the calibration is done using a global model not being able to take the magnetic configuration of the AFM into account.

In order to assess the Flyby a little bit more also the IB data have been inspected and overlayed (green data) on the OB data (black data) in Figure 70. It shows up that the overall timelines are nearly identical which is an indicator for the quality of the measurement.

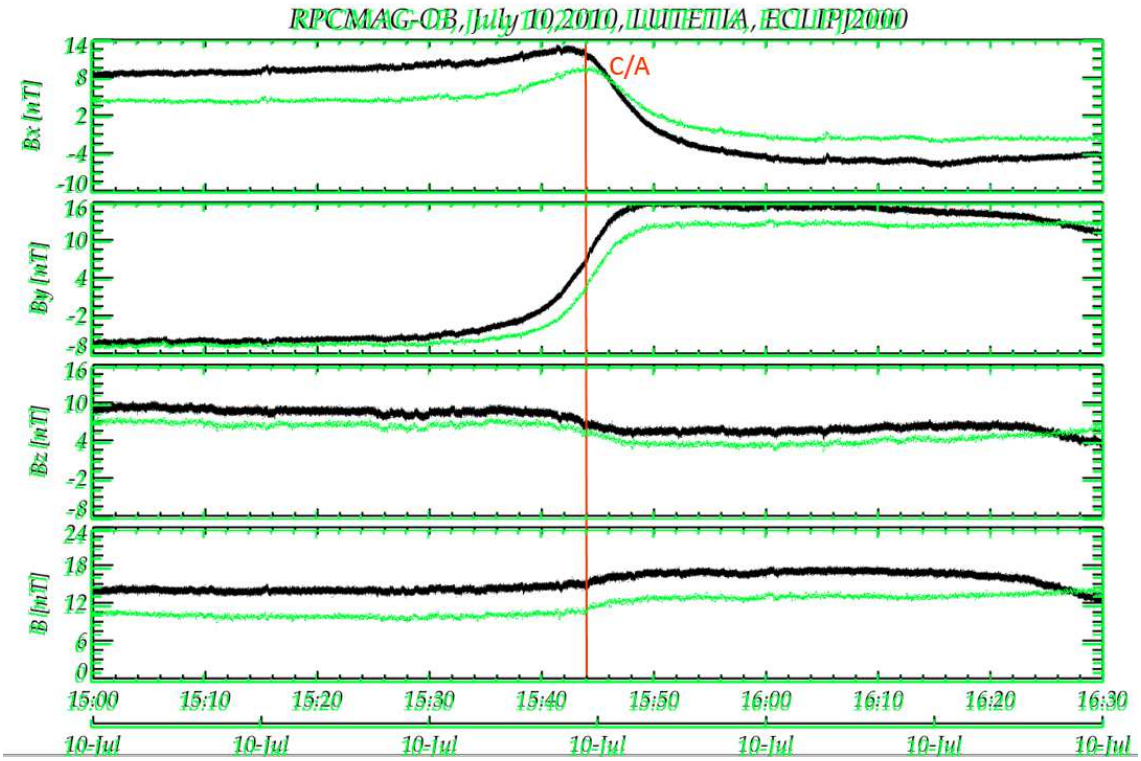

Figure 70: RPCMAG-OB and RPCMAG-IB data as overlay around C/A in ECLIPJ2000 coordinates.

Finally also the ROMAP data shall be shown. Figure 71 depicts all observed data by RPCMAG-OB, RPCMAG-IB and ROMAP, as a red overlay. Although the offset of the ROMAP data was unknown and the data are severely disturbed by the LANDER resp. Lander P/L a reasonable agreement of all datasets could be achieved at times.

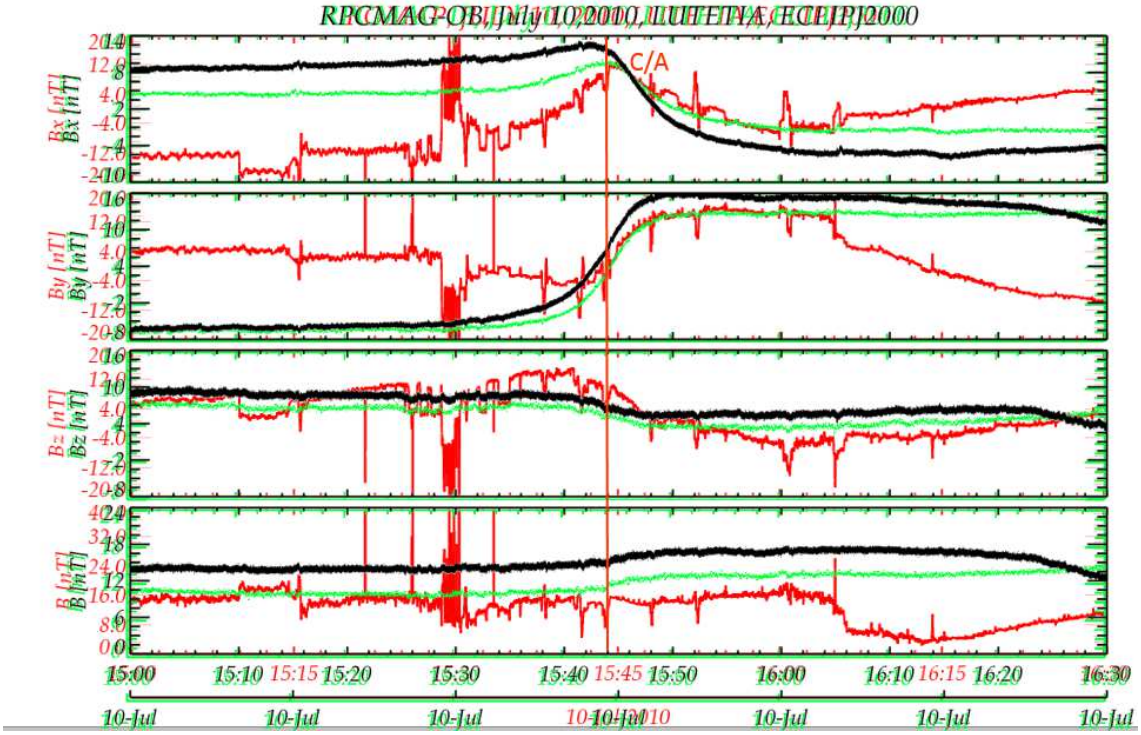

Figure 71: RPCMAG-OB and RPCMAG-IB data as overlay around C/A in ECLIPJ2000 coordinates.

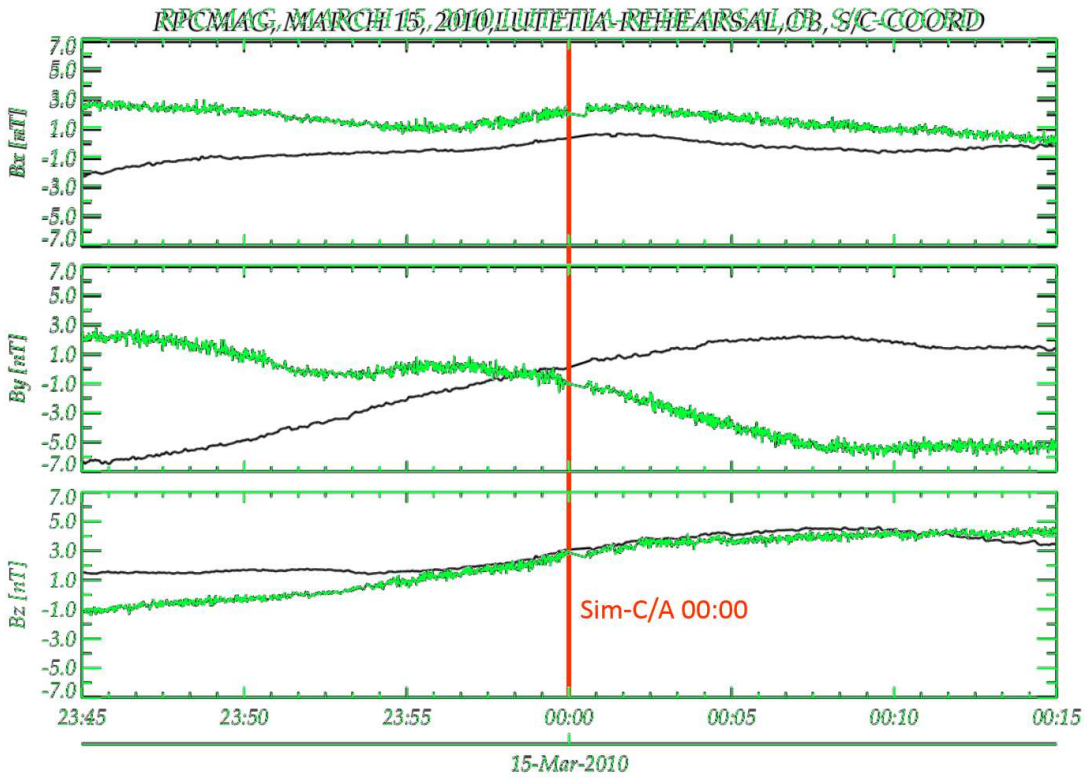

Figure 72: RPCMAG-OB and RPCMAG-IB data measured at the LUTETIA-FLYBY-REHEARSAL in March 2010. Simulated C/A is at 00:00

To get more information about real asteroidal signals and disturbances the data of the LUTETIA flyby rehearsal from March, 14 &15 2010 are taken into account. Figure 72 shows an overlay of RPCMAG-OB and RPCMAG-IB data. It can clearly be seen, that both timelines show different long term behavior, which is probably caused by huge activity of various instruments generating magnetic disturbance. Due to this, and due to the fact that the activities during the rehearsal were quite different to the ones of the real flyby, the rehearsal data do not gain any new information.

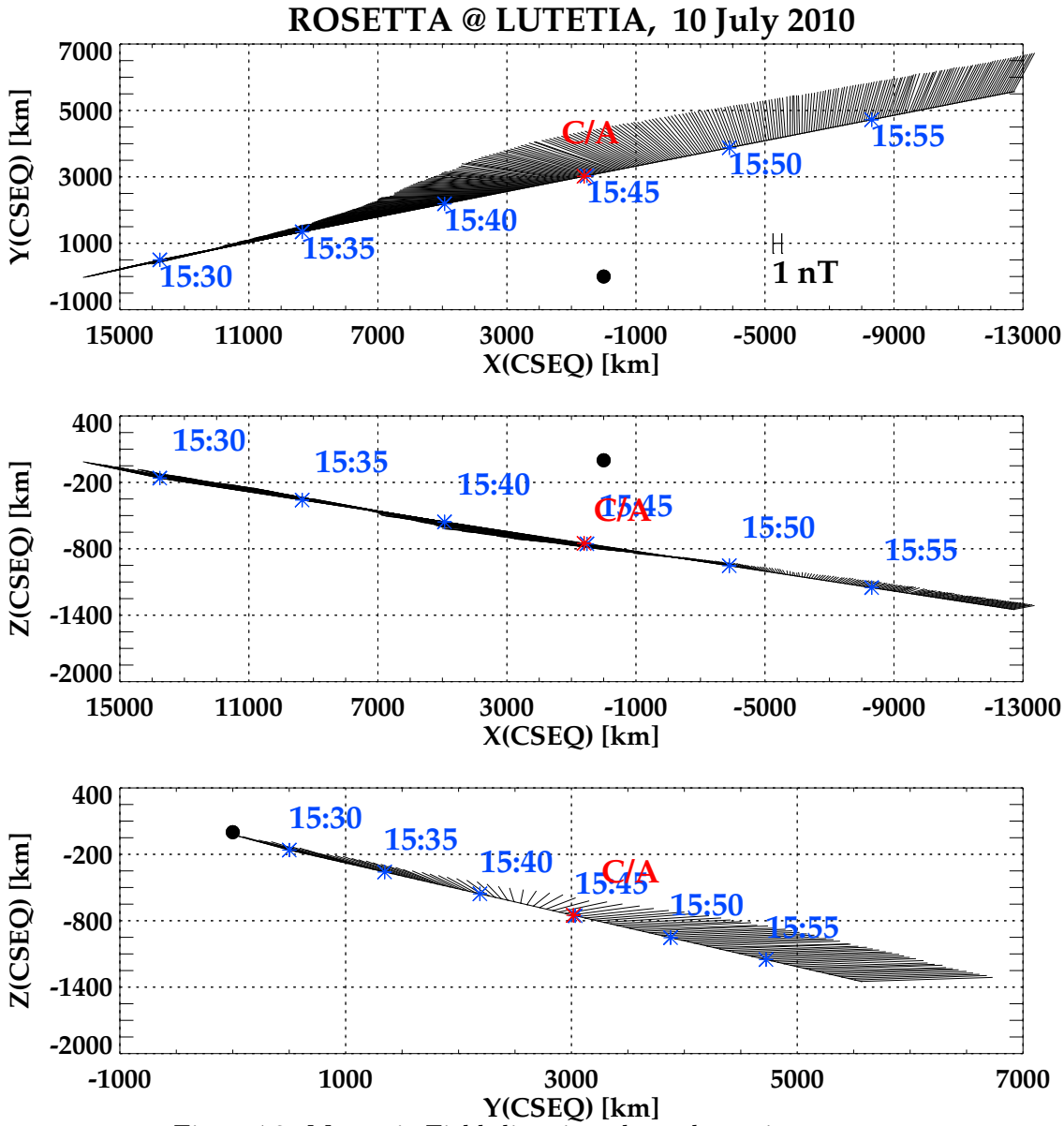

Figure 73: Magnetic Field direction along the trajectory.

Another feature seen in the OB data of Figure 69 is the slow variation of the components which could be a draping of the magnetic field around the asteroid. To study this in detail Figure 73 has been created, showing the magnetic field directions during the flyby. From the Flyby geometry shown in Figure 4 one would expect a Bx-component which changes its sign between inbound and outbound leg, keeps the sign of the By-component constant and keeps finally the Bz-component almost constant. Figure 73, however, exhibits a complete different picture: the Bx-component changes its sign, the sign of By remains constant and Bz varies slightly. These features do not fit into the classical draping picture.
As a result it can be stated that no draping happens at the comet. The change of the mag-

netic field direction is again caused by s/c effects or by the transient solarwind structure passing by.

Although no magnetic signature of LUTETIA greater than 1 nT can be seen in the data, we will try to estimate some upper limits for the magnetic properties of LUTETIA.

Let's assume that we could see the formation of a magnetosphere. For a stand off distance in the order of ≈1000 km - like the closest flyby distance- a magnetic dipole moment of $\approx 10^{18}$ Am^2 would be required. This has been calculated by simulation of Simon et al. 2004 ,2006. As we did not measure any magnetospheric stucture, the dipole moment of LUTETIA must definitely by less than this value.

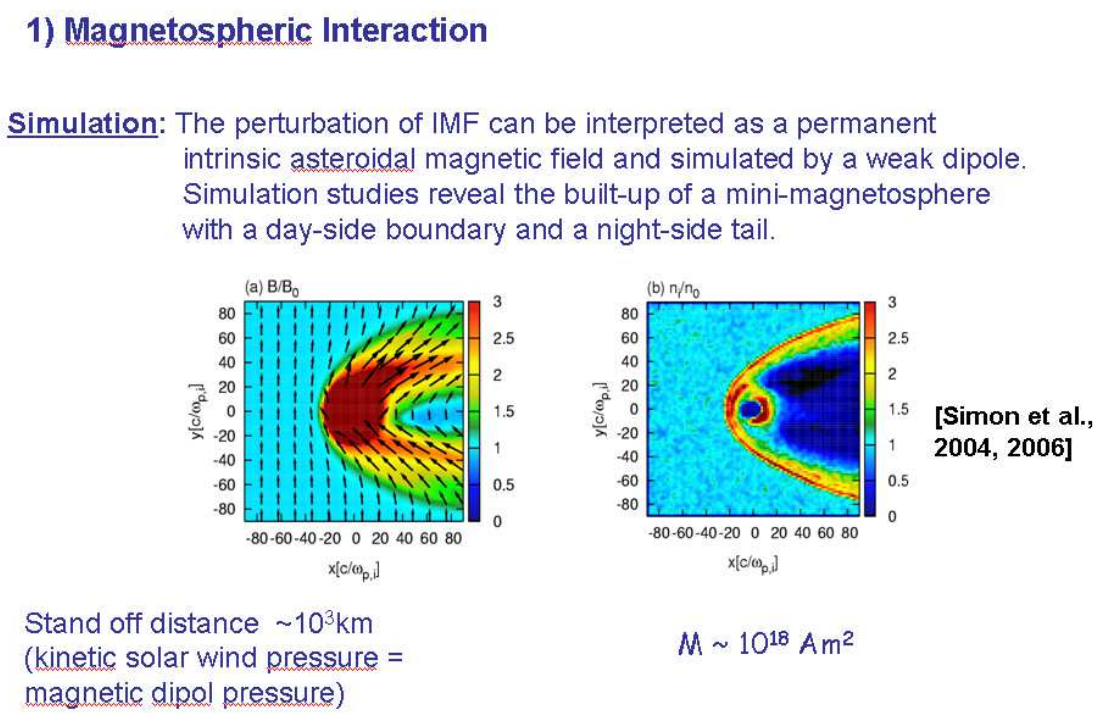

Figure 74: Theoretical aspects for the formation of an asteroidal magnetosphere.

As a second scenario at least the occurrence of upstream waves might possible. Following the assessment of Baumgaertel et al. 1997 a wave activity in the distance of ≈1000 km requires a magnetic dipole moment of at least 10^{12} Am^2. Again, as no wave activity could be recognized, the moment of LUTETIA must be less.

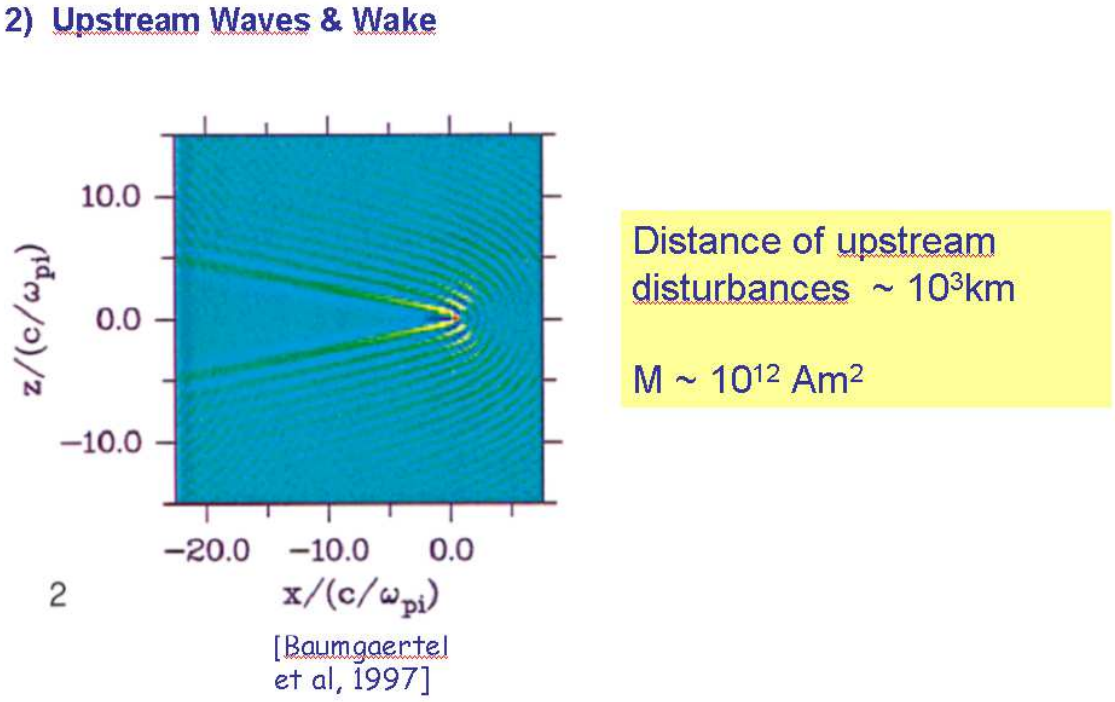

Figure 75: Theoretical aspects for the formation of upstream waves.

As a summary a maximum magnetic dipole moment of LUTETIA in the order of $1 \cdot 10^{12}$ Am^2 can be calculated as an upper limit from these theoretical considerations. Related to the volume this leads to an upper limit of the magnetization of 0.0022 A/m. Related to the mass, a maximum specific moment of $3.9 \cdot 10^{-7}$ Am^2/kg can be calculated.

The following table show the result for the LUTETIA flyby in a wider frame by comparing its properties with various asteroids which have been visited by space missions and investigated using magnetic field measurements. As a main feature the table splits up in two parts: one group (GASPRA & BRAILLE) seems to be magnetic, characterized by a max. magnetization of about 100 A/m. The second group (LUTETIA, EROS, STEINS) seems to be non magnetic.

	LUTETIA	Eros	Gaspra	STEINS	Braille
					
	← 130 km →	← 30 km →	← 25 km →	← 6 km →	← 3 km →
Dimension [km]	132 x 101 x 76	33 x 13 x 13	18.2 x 10.4 x 9.4	6.7 x 5.8 x 4.5	2,2 x 1 x 1
Equivalent Radius [km]	48	9	8.0	3	0.78
Volume [km^3]	460357	2500	2145	113	2
Density [kg/m^3]	5500	2650	3900	3200	3900
Material	Carbon. Chond.,Metal	Chondrites	Metal,Olivine,Pyrox.	Enstatite	Pyroxene,Olivine
Spectral Class	C/M-Type	S-Type	S-Type	E-Type	Q-Type
Mass [kg]	2.53E+18	6.63E+15	8.36E+15	3.62E+14	7.75E+12
Shape	Lump	Banana	Potato	Diamond	Peanut
Periheldistance [AU]	2.03	1.13	1.82	2.02	1.33
Apheldistance [AU]	2.83	1.78	2.59	2.71	3.36
Orbital Period [year]	3.80	1.76	3.29	3.63	3.58
Rotational Period [d]	0.34	0.22	0.29	0.25	9.4
Encounter	ROSETTA 10.7.2010	NEAR: 12.2.2001	Galileo: 29.10.1991	ROSETTA: 5.9.2008	DS1: 29.07.1999
Encounter Distance R [km]	3120	Landing	1600	800	28
Magnetic Field [nT] @ R	1	5	Draping	1	2
Max. Dipole Moment [Am^2]	1.0E+12	1.3E+10	2.0E+14	1.0E+12	2.2E+11
Max. Magnetization [A/m]	0.0022	0.005	93	9	110
Spec. Moment [A m^2/kg]	3.9E-07	1.9E-06	0.024	0.003	0.028

Figure 76: Properties of various asteroids visited by space mission

11 Conclusions

- RPCMAG itself worked as expected.
- Reaction Wheel influence and the disturbance of of the LAP instrument can be seen whilst RPCMAG is operating in Burst mode.
- The comparison between IB and OB data showed that the measurements are very sensitive to specific temperature changes at the single sensors
- Ater proper calibration OB and IB depict a reasonable agreement during the AST2 phase.
- A transient solar wind feature travelling from Earth to the location of LUTETIA could be detected with OB,IB and WIND.
- The flyby data are disturbed most of the time. Disturbances occur in various time scales. The origin of all the disturbance can not clearly be identified. However, COSAC and PTOLEMY generate signatures in the order of 2 nT which can clearly be seen.
- Rotation of the solar array and movement cannot be seen in the magnetic field data.
- Last but not least: The magnetic impact of LUTETIA is less than 1 nT at the flyby distance of 3120 km. This leads to a maximum magnetic dipole moment of LUTETIA in the order of $1 \cdot 10^{12}$ Am^2. Related to the volume this leads to a maximum magnetization of 0.0022 A/m. Related to the mass, a maximum specific moment of $3.9 \cdot 10^{-7}$ Am^2/kg results.